AN EXPLORATION OF FITNESS LANDSCAPES: THEORY AND EXPERIMENTS

A Dissertation Presented to

the Faculty of the Department of Biology & Biochemistry

University of Houston

In Partial Fulfillment

of the Requirements for the Degree

Doctor of Philosophy

By

Kedar Karkare

August 2018

AN EXPLORATION OF FITNESS LANDSCAPES:
THEORY AND EXPERIMENTS

Kedar Karkare

APPROVED:

Dr. Ricardo Azevedo, Chairman

Dr. Timothy Cooper
Massey University

Dr. Rebecca Zufall

Dr. Richard Meisel

Dr. Christina Burch
University of North Carolina at Chapel Hill

Dr. Thomas Bataillon
Aarhus University

Dean, College of Natural Sciences and Mathematics

Acknowledgements

My fascination with evolution began, through books, in high school. I thank my parents for encouraging me to read relentlessly and always follow my interests.

Thank you to Dr. Christina Burch, for inspiring me to conduct research in evolutionary biology as an undergraduate, and for the opportunity to start my research in her laboratory.

Thank you to the University of Houston department of Biology and Biochemistry for allowing me to pursue my passion for evolutionary biology.

Special thanks to my advisors, Dr. Tim Cooper and Dr. Ricardo Azevedo, without whom I would not be the scientist, or espresso drinker, that I am today.

I'd also like to thank the other members of my dissertation committee, Dr. Thomas Bataillon, Dr. Rebecca Zufall, and Dr. Richard Meisel, for their genuine interest in, feedback on, and criticism of my work.

I'd like to thank my colleagues for their constructive criticism and camaraderie. Azevedo Lab: Dr. Ata Kalirad, Dr. Bingjun Zhang, Grimaldo Elias Ureña, Hao Zhang, Logan Chipkin, and Saul Acevedo. Cooper Lab: Dr. Andrea Wünsche, Dr. Fen Peng, Dr. Yinhua Wang, Kelly Phillips, Rachel Staples, Scott Widmann, Kristina Duan, Stephanie Nguyen.

Lastly, this thesis would not have been possible without the unconditional love and support from my fiancée, Elizabeth Raines, over the past 4 years.

AN EXPLORATION OF FITNESS LANDSCAPES: THEORY AND EXPERIMENTS

An Abstract of a Dissertation

Presented to

the Faculty of the Department of Biology & Biochemistry

University of Houston

In Partial Fulfillment

of the Requirements for the Degree

Doctor of Philosophy

By

Kedar Karkare

August 2018

ABSTRACT

Genotypes, phenotypes, and fitness are the ultimate determinants of evolution. The relationship between these three components is collectively referred to as the fitness landscape. Evolutionary biologists have been working to understand the mechanisms and processes governing the fitness landscape since the early 20th century. However, it has proved difficult to unravel due to the tremendous combinatorics of genotypes, and the complex relationships between all components of the landscape. Here I study evolution on the fitness landscape through a combination of modeling and experiments. I identify a paradox within Fisher's Geometric Model of Adaptation, and relax the model's assumptions in an effort to solve this problem. I find that restricting the level of pleiotropy and restricting the number of maladapted traits simultaneously solves the paradox, and maintains fits to other experimental data. To complement this modeling, I spend the second two results chapters discussing experimental results. I focus on a case study of genetic divergence in the *E. coli lac* operon repressor (*lacI*), and aim to understand the underlying processes and mechanisms that cause divergence. Divergence at this site is due to the historical contingency of mutation fitness effect on epistatic interactions with other substitutions. I then examine the underlying mechanism of change in *lacI* mutation fitness effects. I find that the cost of *lac* expression has decreased in evolved strains, due to an increase in translational capacity. The major benefit of *lacI* mutations is rendered obsolete, by other mutations that provide a similar growth benefit, and they do not fix.

Contents

Chapter 1

Evolution on the Fitness Landscape

1.1 The Genotype-Phenotype-Fitness Map

The genotype-phenotype-fitness (g-p-f) map is a key determinant of evolution [68, 188,199,234]. For example, the complex relationship between genotype and phenotype has constrained evolution of the vertebrate glucocorticoid receptor specificity over the past 40 million years [37]. Evolutionary biologists aim to understand the evolutionary causes and consequences of the g-p-f map [68, 172, 232, 312]. It plays a role in many theories of evolution, from reproductive isolation and speciation [111, 144, 270] to genetic robustness [126, 186] and evolvability [68, 111, 232]. At a fundamental level, the relationship is direct: an organism's genes contribute to its phenotypes, and those phenotypes contribute to evolutionary success. However, as I will discuss, elucidating the g-p-f map has proved to be a complicated endeavor.

1.1.1 Fitness Landscape Metaphor

Part of what makes the g-p-f map difficult to unravel is its tremendous complexity. One-hundred genes, each with 2 alleles, represent 2^{100} (1.3×10^{30}) possible combinations. Each of these combinations maps to a vast array of phenotypes, which all contribute to fitness (Fig. 1.1). Given the difficulty of capturing the relationship between all three components simultaneously, evolutionary biologists typically focus on one aspect of the g-p-f map. Here I break the map down into three distinct relationships, genotype-fitness, genotype-phenotype, and phenotype-fitness, and explain each using a brief case study.

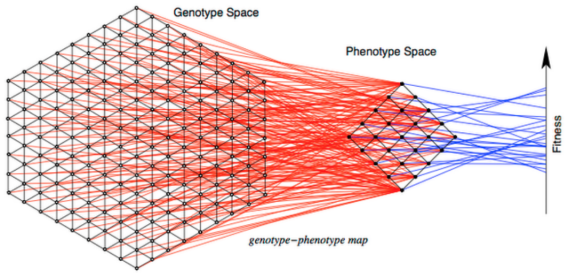

FIGURE 1.1: **Example of genotype-phenotype-fitness map.**The large matrix represents genotype space, and the smaller phenotype space. Red lines connect genotypes to the phenotypes they produce. Blue lines connect phenotypes to fitness values. Redrawn after [286].

Genotype-Fitness. First introduced by Sewall Wright in 1932, the genotype-fitness landscape is a simple visualization of the high-dimensional genotype-fitness space [333]. Wright's iconic figure shows three dimensions: an x-y plane where genotypes are distributed, and a z dimension that represents fitness. Mutations

move the genotypes on the landscape, and when combined with effective selection, populations adapt to progressively higher fitness genotypes. Wright hypothesized that the relationship between genes and fitness is very complex, due to epistasis (see Section 1.5) [333]. Despite its appeal, the relationship between genotype and fitness proved difficult to test until the development of modern genetic methods. Recently, many local mutation landscapes have been constructed [1, 36–38, 49, 57, 63, 72, 103, 128, 154, 179, 182, 189, 202, 214, 297, 319, 323]. Indeed, as Wright suspected, epistasis is common.

Genotype-Phenotype. The relationship between genotype and phenotype can be even more complex, as it relies on cellular biophysical and biochemical properties. RNA folding is one case where significant progress has been made to map genotypes to phenotypes. RNA folding has been extensively studied at the chemical and physical level [58, 97, 290, 293, 296]. This system contains a close link between genotype and phenotype, as the RNA structure is dictated by thermodynamics. Using the thermodynamic information, computer models can directly predict the secondary structure of a given nucleotide sequence. One emergent property from this work is that small movements in genotypic space need not correspond to similarly small movements in phenotypic space [293]. Such biologically realistic genotype-phenotype maps have great utility for testing evolutionary theory [144].

Phenotype-Fitness. Experiments testing phenotype-fitness relationships often focus on functional pathways where the relationship between genotype and phenotype is known. Perfeito et al. (2014) mapped expression of the *lac* operon to

fitness effects. The *lac* operon is well-described and the phenotypes of each gene in the system have been tested [4,74,137,159,160,212,269,291,327,337]. Using this metabolic network, they found a nonlinear relationship between fitness and expression [229]. Because the entire metabolic system is subject to selection as a unit, the results can be applied to other similar pathways [336]. Models focusing on this relationship often assume that genotypes contribute additively to phenotypes [99], in order to isolate the relationship between phenotypes and fitness. They range from models of specific biological systems [5,302] to more abstract approaches like Fisher's Geometric Model of Adaptation [99].

Because populations adapt in complex g-p-f space, fitness landscapes serve as a useful metaphor to explore my two questions of interest here:

1. What are the underlying biological processes that govern adaptation?

2. To what extent is evolution repeatable, and what are the mechanisms that cause divergence?

1.2 The Utility of Experimental Evolution

Lineages of natural populations are only one realization of all evolutionary possibilities from an ancestor. Stephen J. Gould famously hypothesized that replaying the 'tape of life' would yield different results, than what actually occurred, due to the inherent contingency and stochasticity of evolution [124]. Experimental evolution allows us to infer principles of evolution by replaying the tape many times. The essence of experimental evolution is relatively straightforward. A group of

replicate populations is allowed to evolve in a novel environment for many generations. The new environment may be changed in any number of ways, however usually only a small number of variables are altered to keep the experiment as simple as possible. The new selective conditions reward novel adaptations. After some number of generations, these evolved populations can be compared to one another or to the common ancestor (if possible).

The strengths of experimental evolution lies in its replication and control. It is often used to examine characteristics of mutations, such as spectrum, fitness effects, and interactions [18, 94, 194]. It also provides a mechanism for studying genetic and environmental interactions ($G \times E$) [314], social interactions [220], the evolution of multicellularity [240], and the evolution and persistence of sexual reproduction [8, 118, 130, 152, 227, 249].

Within experimental evolution, there are multiple methodologies that are utilized depending on the question of interest. For those investigators interested in the role of de novo genetic variation (mutations) in adaptation, long-term evolution experiments with microbes are most common. *Escherichia coli* and *Saccharomyces cerevisiae* are common choices for such work [120, 154, 174, 240, 338], as they can be maintained at large populations sizes, have short generations times, and have extensive genetic manipulation toolkits. Experimental evolution allows the freedom for evolutionary response across all levels of biological organization. However, there are some drawbacks to this approach. It is difficult to conduct experimental evolution outside the laboratory due to the difficulty of control and

replication in nature (but see [104, 242, 243]). Additionally, laboratory environments lack the complexity of natural environments. This limits the ability to make robust inferences about environmental effects. Nonetheless, experimental evolution allows us to "isolate and analyze the adaptive response to specific environmental factors" [110]. In my work, I employ the bacterium *Escherichia coli* to address questions about evolution driven by *de novo* mutations.

1.3 Mechanisms of Adaptation

"Natural Selection is the only means known to biology by which complex adaptations of structure to function can be brought about" – R.A. Fisher (1930)

Evolution can be defined as a change in allele frequency across generations. We say that adaptation has occurred when a population's "intrinsic rate of natural increase" [282] improves as a result of changes in allele frequencies. This adaptation can be measured through the phenotype of fitness. Fitness is a combination of many biological components of the life cycle. For example, in bacteria the three stages of growth: lag phase, exponential phase, stationary phase. In practice, and in this thesis, fitness is often estimated through "a biological contest between genotypes" [282]. The ratio of rates of reproduction is an effective measure of fitness difference between two competitors [13, 99, 114, 257]. To further understand the factors contributing to evolution, it is useful to explore the scenario in which fitness does not change over time. G.H. Hardy and Wilhelm Weinberg (1908) did

this exactly [129]. Their equilibrium principle, for diploid sexually reproducing organisms, contains 5 critical assumptions: no mutation, no selection, no gene flow, random mating, large population size.

Here I study only the case of a single haploid asexual population. As such, the assumptions about gene flow and random mating are not pertinent to this situation. In my work (both theory and experiment) I employ population sizes greater than 10^5. While genetic drift certainly plays a role, I assume here that 10^5 is reasonably high to minimize its in these experiments. Remaining are mutation and selection - the core processes of adaptation. I now describe selection and mutation in some detail, so as to provide context for my theoretical work on these processes.

1.3.1 Selection

As Darwin first explained in *On the Origin of Species*, some individuals are more successful at surviving and reproducing than others – and this success is not random with respect to genotype [66]. Natural selection in novel environments is in involved in various phenomena, from the evolution of drug resistance to the radiation of mammals after the Cretaceous-Paleogene extinction event. One of the most best studied examples of natural selection is Darwin's Finches. Fourteen species of Finches evolved on the Galapagos Islands, all sharing a common ancestor from Central or South America over 2 million years ago [256]. These species, primarily characterized by their beak size and shape, diverged due to type of food available on the different islands [125].

Natural selection acts on both new and existing variation. Here I am interested in the impact of new variation on evolution, and only further discuss selection on *de novo* mutations. Broadly, there are three types of selective forces on phenotypes: directional, disruptive, and stabilizing.

Directional Selection. The situation in which selection favors one extreme of a phenotypic distribution such that a population's phenotypic distribution changes in a consistent pattern until the peak (or plateau) is reached. An example of directional selection is laboratory selection in a single sugar medium [257].

Disruptive Selection. The situation in which selection favors two extremes of a phenotypic distribution, such that the proportion of intermediates decreases. For example, three-spined Stickleback morphology diverges more in lakes with balanced amounts of prey-type [32].

Stabilizing Selection. The situation in which selection favors the mean of the phenotypic distribution, such that the population's phenotypic variance decreases over time. A classic example of stabilizing selection is birth weight in humans. Both high and low birth weights, compared to the mean, are correlated with higher mortality for both males and females [145].

In many environments there are likely multiple solutions to achieve high fitness [67,162,192]. Depending on where a population is on the fitness landscape, it may experience different selective pressures. For example, if there are two nearby fitness peaks the population would experience disruptive selection towards those two fitness maxima. Alternatively, if the population has reached a local fitness peak, it would experience stabilizing selection. Directional selection would occur

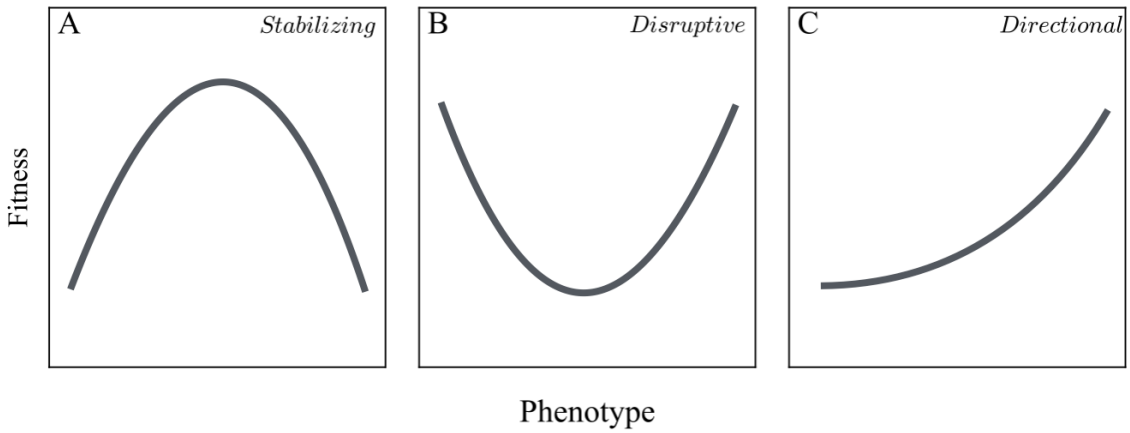

FIGURE 1.2: **Types of Selection.** The fitness function across an arbitrary phenotype for A) Stabilizing Selection B) Disruptive Selection C) Directional Selection

if there was only one nearby fitness peak. Here I study the situation in which organisms are maladapted in a single-niche environment. As such, I model populations adapting to a single fitness peak under directional selection.

1.3.2 Mutation

In the absence of genetic variation, natural selection will not modify population phenotypes. Mutations are the ultimate source of all genetic variation. However, mutation are a rare occurrence, arising on the order of 10^{-10} to 10^{-9} per nucleotide per generation in unicellular eukaryotes and bacteria [184]. Furthermore, there are restrictions, imposed by the biological system in question, on phenotypes that can be produced via mutation. As H.J. Muller noted, "the organism cannot be considered as infinitely plastic ... as the effects of mutations are, of course, conditioned by the entire developmental and physiological system resulting from the action of

all other genes already present" [207]. At face value, it may seem that mutations occur so infrequently and sporadically (at most loci) that mutations are too rare to have an effect on population fitness.

Darwin explored the effect of phenotypic changes on the evolution of complex traits in *On the Origin of Species* [66], with regards to the vertebrate eye. He theorized that such complex adaptations must be due to a series of successive beneficial changes (mutations) from a simpler ancestral structure. This specific hypothesis is indeed supported by more recent studies [210, 211]. More broadly, we now know that mutations are the driving force behind evolution when paired with natural selection in large populations. There are many efforts to understand the characteristics of mutations [18, 94, 194]. Here I focus on two mutation characteristics that are particularly important for evolutionary dynamics: fitness effect size and pleiotropy.

Fitness Effect Size. Fisher proposed that the adaptation of complex structures (e.g., the vertebrate eye) occurred as a result of movements in multi-dimensional space. He studied changes in mutation fitness effect size during adaptation [99]. He concluded that adaptation likely proceeds through many very small beneficial mutations because mutations with smaller effect sizes have a greater probability of being beneficial in his model. However, Kimura (1983) noticed that Fisher neglected an important factor in this calculation – the fixation probability of beneficial mutations [156]. Each arising mutation has some probability of reaching a frequency of 100% in the population. For deleterious and neutral mutations,

this probability is very small in large populations, while fixation is driven by genetic drift in small populations. For beneficial mutations, Haldane derived that the probability of fixation for a beneficial mutation is $\sim 2s$ (for large population size), where s is the fitness effect [127]. Kimura showed that mutations of intermediate size likely contribute most to adaptation, as they strike a balance between high probability of being beneficial and fixation probability [156]. Orr further extended this work to show that the effect size of mutations is expected to be exponentially distributed along successive adaptive mutational steps. That is, the mean size of a fixed beneficial mutation tends to decrease over time [216]. The fitness effects of all occurring mutations dictate the distribution of fixed effects studied by Fisher, Kimura, and Orr. This distribution of fitness effects (DFE, Fig. 1.3) is a key determinant of evolution [19,20,51,87,93,94,233], and a focus of this thesis.

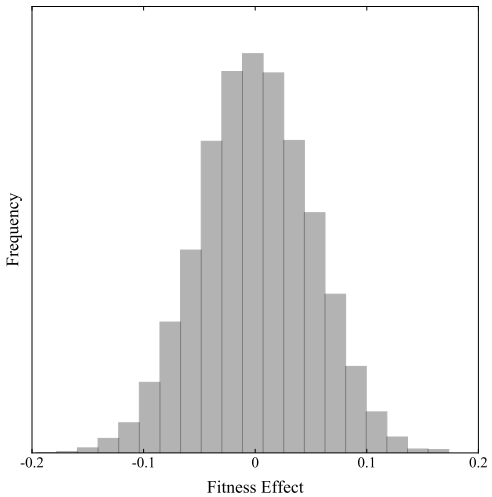

FIGURE 1.3: **Sample Distribution of Fitness Effects (DFE).**

Pleiotropy. This is the phenomenon of a single mutation (or gene) affecting multiple phenotypes. Pleiotropy is implicated in many fields of biology, including evolution [99, 110, 218, 221, 305, 317], development [42, 136], aging [176, 247, 324], and human disease [27, 28, 245]. A mutation to a single gene in humans causes the disease phenylketonuria (PKU), which has effects across multiple seemingly unrelated phenotypes — mental acuity, hair, and skin pigment. Antagonistic pleiotropy, where a mutation/gene has beneficial effects on some trait(s) and deleterious effects on other trait(s), is implicated in theories of aging and senescence [326]. For example, genes in the mTOR (mammalian target of rapamycin) pathway are critical for early development, but also contribute to age-related diseases such as neurodegeneration and cancer [27, 28, 245].

1.4 Models as a Tool to Study Evolutionary Processes

Models play a significant role in the study of evolution. They can be used to develop hypotheses and testable predictions, offer a way to further explore biological patterns, and serve as a method to test verbal arguments mathematically [272]. Since the emergence of adaptive landscape theory [99, 333], biologists have employed models in an attempt to better characterized g-p-f map properties relevant to underlying principles of adaptive processes (e.g., selection and mutation).

1.4.1 Types of Models

There are many types of adaptive landscape models, which vary in their underlying biological reality. I've outlined a few categories below to provide perspective for my work with Fisher's Geometric Model of Adaptation (FGM).

Random Field Models. This approach creates fitness landscapes through a random probabilistic process that assigns fitness values to genotypes [285]. These models often employ tunable epistasis, which allows one to test the impact of epistasis strength on landscape characteristics. The simplest version of a random field model is the House-of-Cards (HOC) model, which assigns fitness independently from a fixed probability distribution [146]. A more sophisticated model is the NK model, created by Kauffman and Weinberger [147]. In this model, each of L loci interacts with K other loci, where K can be any value be between 0 and $L-1$. This allows the model to be modified from additive ($K=0$) to maximally epistatic ($K=L-1$, i.e., HOC). The identity of a locus' interaction partners creates varying genotypic architectures.

Sequence-Structure Maps. These models employ an explicit genotype-phenotype map, which must be known a priori. Perhaps the most commonly used case is the RNA secondary structure map. Here the genotype-phenotype map, the secondary structure of RNA, can be predicted directly from the thermodynamic properties of base-pairing. These structures are then mapped to a fitness landscape defined by RNA structure [58, 97, 290, 293, 296]. Similar models can be used for protein structure [169]. Complex proteins are reduced to a model where each amino acid is a

vertex of a lattice [175, 335]. This limits the number of potential folding configurations and allows for computationally feasible simulations [62].

Phenotype-Fitness Maps. I use FGM in this work, as it has shown remarkable fits to complex bacterial evolution data [194, 229, 289]. FGM is based on a continuous multidimensional landscape, much as Wright initially imagined. However Fisher instead defined this space as phenotypic space, as opposed to genotypic. Despite its simplicity, with just a few parameters, FGM is a full model of selection, mutation, pleiotropy and epistatic interactions. An organism is a set of phenotypic traits, each represented by an axis in n-dimensional Euclidean space. A genotype creates a single phenotype, which is a point in this multidimensional space. Mutations displace phenotypes in this space and selection moves the population closer to the phenotypic optimum. R.A. Fisher made some simplifying assumptions, about nature of mutation and selection, which have continued to be used when modeling with FGM. However, these assumptions lead to inconsistencies with empirical data. In this work I modify mutation and selection in FGM to improve fits with empirical data.

1.4.2 Evolutionary Repeatability and Historical Contingency

Evolution proceeds through a combination of deterministic (selection) and stochastic (mutation) processes. This tension between genotypic and phenotypic evolutionary repeatability underlies some of the debate regarding whether evolution is predictable. Stephen J. Gould argued that evolution is dominated by specific contingencies, such that replaying the 'tape of life' would result in a different world

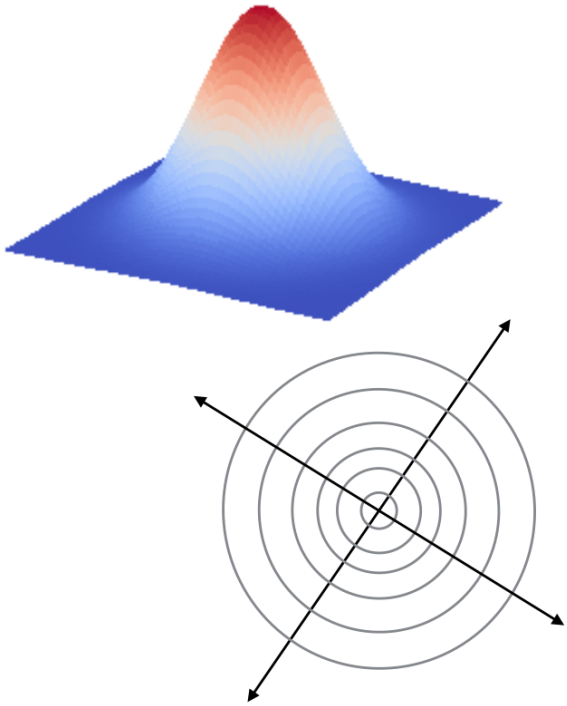

FIGURE 1.4: **Fisher's Geometric Model with 2 Dimensions**. The 2-D landscape is depicted underneath, with concentric circles showing fitness decline as distance from the optimum increases. Fitness can be visualized a mountain with the peak at the phenotypic optimum. On top, warmer colors indicate higher fitness.

than that which exists today [124]. He used the Burgess Shale, a rich deposit of fossils from the Cambrian explosion 500 million years ago, as an example. Despite the tremendous diversity of animal phyla evident in the Burgess Shale fossil record, very few of those species left modern descendants. Gould hypothesized that the evolutionary fate of populations is contingent on chance historical occurrences (e.g., environmental changes, rare mutations). Simon Conway Morris

disputed Gould's claim, suggesting that environmental pressures (natural selection) would cause populations to converge to the same (or few) outcome(s) each time [203]. An example of this is *thylacine*, or Tasmanian wolf, which was morphologically and behaviorally similar to the ancestral North American wolf, despite no recent shared ancestry. Morris' hypothesis requires historical contingency to be minimal, such that evolution will arrive at similar phenotypic outcomes, even if by different genetic paths. Testing these hypotheses is not possible on the scale that Morris and Gould considered, however experimental evolution in the laboratory allow us to test these hypotheses.

1.4.3 Evidence for Historical Contingency

Evidence for historical contingency has been found across multiple organisms and time scales. Bedhomme et al. (2013) evolved 60 lineages of *Tobacco etch potyvirus*, each with a different evolutionary history, to the host *Nicotiana tabacum* for 15 rounds of transfer. They found that the different evolutionary history had a strong influence on evolved genotype. In a similar experiment, Dickinson et al. (2013) evolved T7 RNA polymerase genes to different environments for 200 generations, then evolved all genes in a common environment. Initial adaptation to alternate environments created strong contingencies during adaptation to the common environment. This path dependence, at the protein level, resulted in unique phenotypic outcomes [78]. In an experiment with *E. coli*, only $1/12$ replicate populations evolved the ability to utilize citrate after $31,500$ generations [31]. Blount et al. (2008) found that a prior mutation, of marginal benefit, was required for the

subsequent citrate metabolism mutation to be beneficial [30, 239]. Bridgham et al. (2009) tested for contingency in the ancestral protein of the vertebrate glucocorticoid receptor [37]. The ancestral receptor is five, specificity-optimizing, steps away from the evolved protein. They reverted the substitutions and tested the effect on protein and fitness. Reverting any single substitution to its ancestral state yields a non-functional protein because each substitution is contingent on prior adaptations for its benefit [37].

1.4.4 Long-Term Evolution

Bacterial long-term evolution (LTE) has proven particularly useful to test the hypotheses of Gould and Morris. Bacteria have long been used to study the evolutionary processes of mutation and selection [7, 183]. Large population sizes and short generation times allow experimenters to observe adaptation over just a few months (hundreds) or years (thousands) of generations. Furthermore, bacteria can be stored in a non-evolving state and revived. This allows experimenters to 'travel back in time' to conduct experiments with population samples from different time steps in evolution.

Bacterial long-term evolution experiments typically consist of replicate populations that are founded from a common ancestral clone and propagated for many generations in a laboratory environment. The common ancestor ensures that all replicate populations begin from the same genotypic and phenotypic location on the fitness landscape. Populations can then be tracked in a variety of ways, including fitness (phenotype) and mutations (genotype). Richard Lenski identified that

even simple environments can lead to different outcomes [173,174]. Replicate populations can adapt to the same phenotypic fitness peak, with similar or different genotypes [164]. Alternatively, populations may adapt to different fitness peaks due to a rugged fitness landscape [67,192,251].

LTE, which was initially performed with *E. coli* in a minimal glucose environment, has now been carried out with multiple organisms and in many different environments [148]. It has yielded insights into evolutionary parallelism [54,173,332], pleiotropy [56, 201, 299], evolvability [174], causes of aging [247], reproductive isolation [276, 277], the evolution of mutation rates [71, 279]. Multiple experiments have found that replicate populations do indeed adapt to multiple fitness peaks [67,192,251]. This is in part due to a phenomenon known as epistasis.

1.5 Epistasis

Genes interact in a complex, non-additive manner to produce phenotypes – a phenomenon known as epistasis. Bateson first described epistasis as the effect of a modifier allele on an allele at another locus [21]. In an evolutionary context, Fisher's later definition is used more frequently [99]. He defined epistasis as a statistical deviation from the expected effects of genotypes on phenotypes. These expected effects are often calculated from an additive or multiplicative (used here) model [141]. Epistasis is implicated in many aspects of evolution, including organismal robustness [69], speciation [76,113,237], dominance [9,98] and adaptive

landscape ruggedness [39, 167, 251]. Using this definition, epistasis can be categorized in a variety of ways. I focus here on a few that are useful for understanding the work to follow.

No Epistasis. An interaction between mutations that matches the fitness expected under the null model (Fig. 1.5).

Positive. An interaction between mutations that results in a higher fitness than expected under the null model. Positive epistasis between two beneficial mutations causes a greater benefit than expected (Fig. 1.5).

Negative. An interaction between mutations that results in lower fitness than expected under the null model. Negative epistasis between two beneficial mutations causes a lower benefit than expected (Fig. 1.5).

Sign. An interaction between two mutations where the effect of one (or both) mutation(s) switches sign in the presence of the other. Sign epistasis may cause a mutation that is beneficial in one background to be costly in another (Fig. 1.5). When both mutations in a pairwise interaction have this relationship, it is called *reciprocal sign epistasis*.

Epistasis can also be separated, based on their interaction-locale, into two categories: local and global.

Local. These are interactions which depend on a specific genetic background. For example, a mutation which enabled citrate metabolism in *Escherichia coli* became beneficial only after a previous mutation increased the activity of the citrate synthase enzyme [30, 31, 239]. Local interactions are instrumental in evolutionary

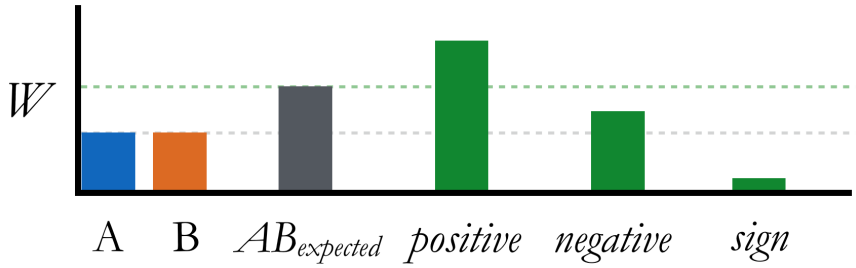

FIGURE 1.5: **Types of Epistasis.** Independent fitness effects of arbitrary mutations A and B are shown in blue and orange respectively. The expected fitness, shown as an additive model (for visual simplicity) ,is in grey. Example effects of A and B together (AB) are shown from left to right as: positive epistasis, negative epistasis, and sign epistasis (here sign is also reciprocal sign).

genetics [34, 198, 288, 303, 319], however recent work suggests that global interactions also play a key role [159, 164].

Global. Global interactions are those that depend on general characteristics of the background, such as fitness. Kryazhimskiy et al. (2014) evolved 64 closely related genotypes of *Saccharomyces cerevisiae* for 500 generations [164]. They found that the initial fitness, not genotype, of strains determined subsequent fitness improvements. Sequence evolution was also not contingent on the initial genotype. Reconstructed mutational combinations showed a trend of diminishing returns epistasis; the fitness of mutation combinations decreased as background fitness increased, regardless of the genetic background. Although specific epistatic interactions certainly exist, it is striking that knowledge of interaction mechanisms is not always necessary for predicting the fitness trajectory of evolving populations [330]. This diminishing returns has been observed in a number of other studies as well [49, 154, 319]. Kryazhimskiy et al. (2014) suggest that this phenomenon

may be due to a global mechanism that creates indirect interactions between mutations, regardless of their specific biological effect [164].

Local epistatic interactions are likely to be idiosyncratic, reflecting specific biological mechanisms within genome modules [48, 271]. In contrast, global epistasis may be mediated by common cell-wide physiological processes. Kacser and Burns, in a foundational paper of systems biology, note that "in principle, variation anywhere in the genome affects every character" [142]. Although this may not be entirely true [2,153,331], they intuit that all genes must draw from a common pool of cellular resources, such as ribosomes, nucleotides, or polymerases. Any mutations which modify gene expression affect this resource pool, and thus indirectly affect other genes [222]. One candidate for a global epistasis mechanism is translational capacity [269]. All gene expression requires the translation of RNA into proteins. As such, limitation to a cell's translational capacity would directly impact gene expression throughout the genome. This may, in turn, modify the fitness effect of any expression-changing mutant.

1.5.1 Epistasis Experiments

Recent experiments have attempted to quantify epistasis between beneficial mutations in evolving populations. Both Khan et al. (2011) and Chou et al. (2011) explored the interactions between the first few substitutions in evolved bacterial populations [49, 154]. They each constructed the full set of possible mutation combinations in order to determine the effect of background genotype on mutation fitness effect. Both studies found primarily negative epistasis between

beneficial mutations. This decreases the rate of adaptation observed in LTE experiments [49, 261, 330]. Khan et al. showed that the effects of most mutations were consistent with the diminishing returns hypothesis. Interestingly, the finding of negative epistasis in bacterial adaptation (*E. coli* [154] and *Methylobacterium extorquens* [49]), is in contrast with patterns of interactions between mutations in single proteins, which show a high proportion of sign epistasis [37,319]. For example, Weinreich et al. found that only 18 out of 120 (15%) possible adaptive paths were accessible in the antibiotic resistance gene β-lactamase [319] (75% accessible in Khan et al. (2011) [154]).

There has been an increased effort in recent years to decipher the impact of epistasis on fitness landscapes and adaptation. Constructions are starting to become feasible at larger scales. A recent experiment tested $> 45,000$ interactions between 87 mutation-pairs in yeast tRNA [82]. Another study synthesized 4^{10} DNA oligomers and tested for affinity to one protein [248]. However, it remains technically challenging to study interactions between genes. As such, it is important to continue analysis of inter-gene fitness landscapes on a case-study basis. I present one such case study in this thesis.

1.6 Structure and Principal Findings

In this thesis I study the fitness landscape through both theory and experiment. In Chapter 2, I use Fisher's Geometric Model of Adaptation to investigate the

core evolutionary processes of mutation and selection. I identify a statistical inconsistency in the original FGM and explore model variants that relax Fisher's assumptions about mutation and selection. I find that FGM supports experimental evidence for restricted mutational pleiotropy, but only in the case of restricted maladaptation. In Chapter 3, I test the role of historical contingency in divergent evolution using a case study of genetic divergence in the *E. coli lac* operon. I find that the evolutionary fate of the *lac* repressor is contingent on other occurring substitutions, through negative epistatic interactions. In Chapter 4, I explore the basis of changes in the effect of a *lac* repressor mutation. I find that the effect decreased over time in some populations because those populations likely fixed phenotypic alternatives.

Chapter 2

The Realism of Fisher's Geometric Model

2.1 Introduction

Mutations provide the ultimate source of all evolution. The distribution of fitness effects of mutations (DFE) plays a crucial role in many evolutionary processes, including the rate of adaptation [3,114], the accumulation of deleterious mutations [41,108,123,185], the maintenance of genetic [44] and trait variation [135], and the evolution of sex and recombination [122,131,226,227]. Traditionally, the DFE has been modeled using standard probability distributions, such as the exponential [246] and gamma [150]. These distributions describe the DFE but provide little insight into its causes.

Fisher [99] proposed a model of the fitness landscape that, when coupled with additional assumptions, provides a theoretical framework for studying the DFE

[193]. Fisher's geometric model (FGM) considers n quantitative traits under stabilizing selection, each with a single optimum. The phenotype of an organism corresponds to a single point in the n-dimensional trait space, and its fitness decreases with the distance to the optimum. Mutations are represented by vectors that displace the phenotype, and every mutation affects all traits simultaneously (universal pleiotropy).

Some predictions from FGM have received empirical support. FGM predicts that mutations of larger beneficial effects are more likely to occur in genotypes of lower fitness—i.e., at a greater distance from the optimum [216]. This prediction has been confirmed experimentally in *Escherichia coli* [229, 281] and *Arabidopsis* [289]. A variant of FGM, modified to incorporate arbitrary phenotypic correlations, provided good fits to DFE data from mutation accumulation experiments on multiple organisms [193]. The same model also accurately predicted the distribution of pairwise epistasis in *E. coli* and an RNA virus [194].

Despite these successes, FGM has been criticized for its unrealistic assumptions about mutation and selection [50, 193, 215, 218]. The assumption that mutations are universally pleiotropic has been challenged by experimental evidence that each mutation can only affect a subset of all possible traits [2, 52, 153, 200, 292, 310, 315, 340], and that these subsets form distinct modules [310–312]. Two ways of incorporating restricted pleiotropy into FGM have been proposed: one implements *non–modular* pleiotropy where mutations affect random subsets of traits [178], whereas the other implements *modular* pleiotropy where mutations affect fixed subsets of traits [321].

Two additional problematic assumptions of FGM are that both mutation and selection operate equally and independently on all phenotypes. These assumptions have been relaxed through the incorporation of mutational [193] and selective correlations [193, 321]. Lastly, the assumptions that there is a single, stationary optimum are unlikely to be met in natural environments, which are both spatially and temporally heterogeneous. These concerns have been addressed by incorporating a moving optimum [51, 121, 196], genotype-by-environment interactions [51], and multiple optima [195] into the FGM framework. Although it is clear that the FGM can be extended to make it more realistic in specific ways, the extent to which any particular FGM variant is broadly realistic remains an open question.

Here I explore variants of FGM to determine the extent to which relaxing Fisher's simplifying assumptions about mutation and selection can make both the DFE and the rate of adaptation more realistic. I find that the original version of FGM cannot simultaneously generate a realistic DFE and realistic rate of adaptation. I go on to show that restricting both pleiotropy and the proportion of maladapted traits simultaneously improves FGM realism in both regards.

2.2 Methods

2.2.1 Model

Selection: I consider a generalized version of FGM introduced in earlier studies [298]. I model an organism as a set of n quantitative phenotypes, represented as continuous orthogonal axes in n-dimensional space. The dimensionality, n, is

also known as the complexity. The phenotype of an individual is described by a vector $z = \{z_1, z_2, \ldots, z_n\}$. Organisms experience stabilizing selection with a single optimal phenotype z_{opt}. The fitness of an individual with phenotype z is given by [298]

$$W(z) = e^{-\alpha D(z)^{\epsilon}} \tag{2.1}$$

where, α and ϵ are robustness and epistasis parameters, respectively, and

$$D(z) = \sqrt{(z - z_{\text{opt}})^{\text{T}}\, \mathbf{S}^{-1}\, (z - z_{\text{opt}})} \tag{2.2}$$

is the Mahalanobis distance to the optimum, where T indicates the transpose, and $\mathbf{S}$ is a $n \times n$ variance-covariance matrix, whose diagonal elements S_{ii} are proportional to the strength of selection on phenotype i, and off-diagonal elements $S_{ij} = S_{ji}$ represent the selective interaction (covariance) between phenotypes i and j $(i, j = 1, 2, \ldots, n)$ [193,316,318]. Following Martin and Lenormand [193], I assume S to be positive semidefinite.

Mutation: Mutation changes an organism's phenotype. I model a mutation as a vector u such that the phenotype of an organism changes from z to $z' = z + u$. I draw mutation vectors from a multivariate normal distribution with mean 0 and variance-covariance matrix M, whose diagonal elements M_{ii} represent the variance of mutational effects on phenotype i, and off-diagonal elements $M_{ij} = M_{ji}$ represent the covariance between the effects of mutations on phenotypes i and j $(i, j = 1, 2, \ldots n)$ [193]. Like S, I assume that M is positive semidefinite [193].

2.2.2 Model Variants

Isotropic selection: Selection acts independently and equally strongly on each phenotype: $S = \beta I$, where I is the identity matrix and $\beta > 0$. $D(z)/\sqrt{\beta}$ is the Euclidean distance to the optimum.

Isotropic mutation: Mutation acts independently and equally strongly on each phenotype: $M = (\sigma^2/n)\, I$, where σ^2/n is the variance of mutational effects on each trait. Dividing by n gives an approximately constant mean mutational displacement across dimensions for a given value of σ^2. This is a standard normalization in FGM studies [196, 216, 218, 321, 329]. When the level of pleiotropy b is altered, I divide σ^2/b such that mean mutational displacement is constant across levels of pleiotropy.

Universal pleiotropy: Every mutation can potentially affect every one of the n phenotypes. Isotropic mutation is a special case of universal pleiotropy.

Original model: This assumes $\alpha = 1/2$, $\epsilon = 2$, isotropic selection with $\beta = 1$, and isotropic mutation with parameters σ and n [218, 321].

Random matrices: To evaluate the effect of changes to the M and S variance-covariance matrices, I generated random Wishart matrices [193] of the form XX^{T}, where X is a $n \times m$ matrix with elements drawn independently from a normal distribution with mean 0 and variance λ [193]. Correlation strength (c) can then be expressed as $\approx 1/\sqrt{m}$. Following Martin and Lenormand (2006), I slightly modify

our fitness function under this model, such that it is calculated using S, instead of S^{-1}.

Fitness ridge: Sign epistasis can create narrow ridges in a fitness landscape that restrict the paths along which populations adapt. Here I implement a fitness ridge, such that the fitness corresponding to a given phenotypic value for one trait depends on the values for other traits. For simplicity, all covariance (i.e., off-diagonal) values in the selection matrix S are set to a single value, p. This ensures that each phenotype correlates with all others to the same degree. The original model has $p = 0$. As p increases the ridge becomes narrower. Mutation occurs in the same fashion as in the original isotropic model.

Restricted pleiotropy: Every mutation affects a subset, b, of the total n phenotypes. This is implemented in one of two ways:
Non-modular pleiotropy: The b traits affected by a given mutation are selected at random; all traits have equal probability of being picked. Also known as *partial* pleiotropy [178].
Modular pleiotropy: The n traits are initially placed into n/b modules, each with b traits. Each mutation is selected to affect a single module, chosen at random. Also known as *parcellated* pleiotropy [321].

Maladaptation: I define n_{mal} as the number of traits that are not at the optimum (i.e., for which $z_i \neq 0$). Typically, I assume that any genotype with fitness $W < 1$ has $n_{\text{mal}} = n$, and that it is equally maladapted in all phenotypes. I also consider

cases where $1 \leq n_{\text{mal}} < n$. Note, however, that mutations can affect initially well-adapted phenotypes.

2.2.3 Distribution of fitness effects (DFE)

I estimate the probability density function (pdf), $f(s)$, of the effect of a mutation, s, on a genotype with fitness W, using numerical simulations.

I consider two summary statistics of the DFE. First, the mean effect of a mutation:

$$\bar{s} = \int_{-W}^{1-W} s\, f(s)\, ds \quad , \tag{2.3}$$

where $-W$ and $1 - W$ are the largest possible deleterious and beneficial effects of mutations, respectively. Note that this mean effect is expressed with respect to absolute fitness, W. Typically, I express it in terms of relative fitness: $\bar{s}/W$.

Second, the proportion of beneficial mutations:

$$P_b = \int_{0}^{1-W} f(s)\, ds \quad . \tag{2.4}$$

2.2.4 Evolutionary simulations

I simulate evolution under FGM using an individual-based Wright-Fisher model, a model with constant, finite population size N, and discrete, non-overlapping generations. I assume that individuals reproduce asexually. Mutations are drawn from the multivariate normal distribution with variance-covariance matrix M, and occur with a genome-wide rate of $U = 7 \times 10^{-4}$ per generation [171,325].

2.2.5 Realism

DFE: I evaluate the realism of a DFE in relation to empirical estimates of mutational parameters in *E. coli*. The mean effect of all mutations, $\bar{s}$, is slightly deleterious, ranging from –3% to –1.2% (based on four independent estimates [88, 155, 177, 301]). The mutation rate is $U \approx 7 \times 10^{-4}$ per genome per cell division (average of two independent estimates [171, 325]). The beneficial mutation rate, U_b, has been estimated to range from 4×10^{-9} to 4.5×10^{-5} (based on five studies [134, 140, 228, 281, 339]). Thus, I estimate that the proportion of beneficial mutations, $P_b = U_b/U$, ranges from 5.7×10^{-6} to 0.064. Hereafter, I classify the DFE as realistic if its summary statistics fall within these ranges.

Author	Rate	Method
Lee et al. (2012)	10^{-3}	Mutation Accumulation
Wielgoss et al. (2011)	4.1×10^{-4}	Adaptive Evolution
Long et al. (2018)	1.1×10^{-3}	Mutation Accumulation
Observed Range	4.1×10^{-4} , 1.1×10^{-3}	N/A

TABLE 2.1: **Mutation rate per genome per generation estimates for E. coli.**

For all analyses to follow, I adjust σ such that $\bar{s}$ is realistic ($-0.03 \leq \bar{s} \leq -0.025$), and plot P_b only. This allows a simple visualization in which a realistic P_b indicates a realistic DFE.

Author	Rate	Method
Perfeito et al. (2007)	2.0×10^{-5}	Adaptive Evolution
Hegreness et al. (2006)	$1 \times 10^{-5} * *$	Marker divergence
Sousa, Magalhães, & Gordo (2012)	$4.5 \times 10^{-5} *$	Marker divergence
de Sousa et al. (2017)	$6.8 \times 10^{-6} *$	Adaptive Evolution
Wünsche et al. (2017)	1.9×10^{-5}***	Marker divergence
Woods et al. (2011)	1.8×10^{-8}****	Marker divergence
Observed Range	1.8×10^{-8} to 4.5×10^{-5}	

TABLE 2.2: **Beneficial mutation rate estimates for *E. coli*.** We calculate an estimate of the upper bound for P_b as 0.064 by dividing the observed range of beneficial mutation rate by the mean of the genomic mutation rate (Table 2.1). * = average of 2 estimates given. ** = mean estimate assuming an exponential distribution of mutation effects. *** = mean estimate based on 16 replicates (8 at high effective population size, and 8 at low). **** = estimated based on Woods et al. (2011) Fig. 2C.

Author	$\bar{s}$	Method
Trindade, Perfeito, & Gordo (2010)	-0.030	Mutation Accumulation
Elena & Lenski (1997)	-0.028	Adaptive Evolution
Kibota & Lynch (1996)	-0.012	Mutation Accumulation
Loewe, Textor, & Scherer (2003)	-0.030	Mutation Accumulation
Observed Range	-0.030 to -0.012	

TABLE 2.3: **Mean effect of mutations estimates for *E. coli*.**

Marker Divergence: To investigate the evolutionary consequences of a particular DFE, I simulate neutral marker divergence experiments (Fig. 2.1). These experiments consist of an asexual population that initially contains a neutral marker at 50% frequency The marker will either fix by hitchhiking with a beneficial mutation, or be lost if an unlinked beneficial mutation sweeps to fixation. This method is often used to estimate evolutionary parameters of experimental populations [13, 43, 134, 250]. Here I use the time to fixation or loss, T_{fix}, as a proxy for rate of adaptation, as it depends critically on both P_b and the effect sizes of beneficial mutations. I consider a marker to be fixed or lost when it reaches 90% or 10% of the population, respectively.

Eleven populations of *E. coli* were evolved for up to 1,000 generations in a minimal glucose environment. These populations contained a neutral GFP marker at 50% frequency initially. Effective population size was $N_e = 3.8 \times 10^5$. The proportion of fluorescent cells was measured each day ($\sim$7.64 generations) until sensitivity was lost (entire sample was fluorescent or not, due to fixation or loss). I use these experimental times to fixation as a benchmark for comparing simulation data (Fig. 2.1) [334].

For a given variant and parameter combination, I simulated 10^3 replicate populations and recorded the values of T_{fix} for each run. I then used the T_{fix} histogram and a Voronoi parition function to calculate the model likelihood for each experimental data point. The total $\ln L$ of the model is the product of those individual likelihoods.

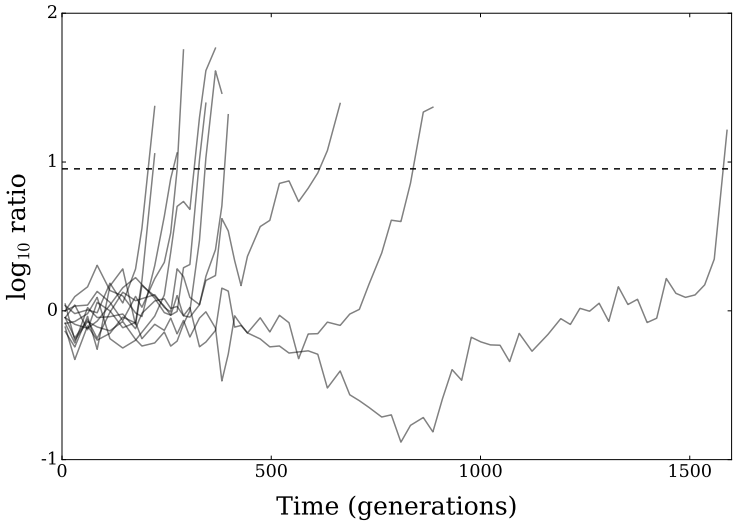

FIGURE 2.1: **Experimental marker divergence trajectories for *E. coli*.** Black lines show the $\log_{10}$ marker ratio over time. Once a marker reaches $\geq$ 90% of the population (dashed line) I deem it to be fixed.

2.2.6 Measures of Epistasis

A unique strength of FGM is its ability to capture non-additive genetic interactions (epistasis) [194], with complex underlying mechanisms, despite making few explicit assumptions. After exploring model variants for realism, I use multiple measures of epistasis to confirm that realistic model variants (for DFE and rate of adaptation) also maintains fits to empirical epistasis data.

Epistasis Coefficients: Epistasis can occur at multiple levels of interaction. The lowest, and most commonly measured, is a pairwise interaction between two mutations. However, epistasis is also present in higher order interactions as well. I

calculate coefficients of epistasis for each order of interaction in a 5-mutation adaptive landscape [320]. This method, which uses a Walsh Transform of the fitness landscape, is described in detail by Weinreich et al. (2013).

Proportion Accessible Paths: The proportion of accessible adaptive paths is a measure of landscape ruggedness (epistasis). I recreate all potential adaptive paths for the original 5-mutation adaptive walk ($2^5 = 120$) and calculate the fitness of each mutation-combination along each path. Those paths that increase monotonically from ancestor to the 5-mutant are considered accessible as they do not have to traverse any fitness valleys.

Roughness to Slope: The ratio of landscape roughness to slope measures how closely the data fit to an additive landscape. I fit *E. coli* data and simulation results to a multidimensional linear model (no epistasis), using least-squares fitting [295]. A higher ratio indicates a worse fit to the linear model, and thus a more rough landscape. Rougher landscapes, by definition, contain more epistasis. This method is described in detail by Szendro et al. (2013).

Proportion of Epistasis: The proportion of epistasis types provides information about the shape of the fitness landscape. Here I define epistasis multiplicatively, as

$$\epsilon = W_{12} - W_1 W_2 \tag{2.5}$$

where fitness is calculated relative to the ancestor (no mutations, $W = 1$), W_{12} is the fitness of mutations 1 and 2 together, and W_1 and W_2 are the fitness of mutations 1 and 2 independently. Using this epistasis definition, positive epistasis is $\epsilon > 0$, negative is $\epsilon < 0$ and no epistasis is $\epsilon = 0$. Sign epistasis is the scenario in which a mutation is beneficial independently ($W_1 - 1 > 0$), yet deleterious in combination with the other mutation ($W_{12} < W_2$). Reciprocal sign epistasis occurs when both mutations are beneficial independently ($W_1 - 1 > 0$ and $W_2 - 1 > 0$), yet deleterious together ($W_{12} - 1 < 0$). These five measures of epistasis provide a comprehensive view of interaction types on the landscape.

2.2.7 Epistasis Fits

I compare model epistasis statistics to empirical data from an *E. coli* landscape [154]. Measures of epistasis will inherently contain correlations if they are calculated from the same set of mutations in the same environment. I use principal components analysis (PCA) on the correlation matrix to convert 17 epistasis statistics into a set of uncorrelated variables. This allows us to visualize how the simulation data cluster, with respect to the experimental data, on orthogonal axes.

2.3 Results

2.3.1 Conditions for a Realistic DFE

The DFE in the original FGM is defined by the dimensionality, n, the fitness of the genotype, W, and the mutational variance, σ^2/n. Figure 2.2 shows P_b, for a realistic $\bar{s}$, across n (Fig. 2.2A) and W (Fig. 2.2B) in the original FGM. At $W = 0.5$, a realistic DFE only occurs if dimensionality is high ($n \gtrsim 250$, Fig. 2.2A). If the dimensionality is lower, say $n = 100$, only genotypes with higher fitness can show a realistic DFE ($W \gtrsim 0.75$, Fig. 2.2B).

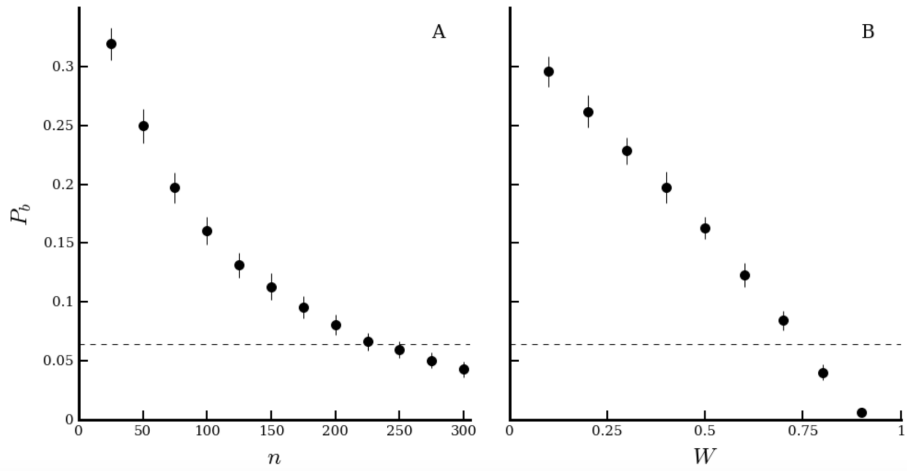

FIGURE 2.2: **A) Increasing dimensionality makes the DFE more realistic under the original FGM.** Proportion of beneficial mutations and model dimensions in the original FGM, for genotypes with $W = 0.5$, $\alpha = 1/2$, $\epsilon = 2$, and a σ that gives realistic $\bar{s}$ ($-0.03 \leq \bar{s} \leq -0.025$). **B) Increasing fitness makes the DFE more realistic under the original FGM.** Proportion of beneficial mutations and fitness in the original FGM, for genotypes with $n = 100$, $\alpha = 1/2$, $\epsilon = 2$, and a σ that gives realistic $\bar{s}$ ($-0.03 \leq \bar{s} \leq -0.025$). For both panels, each point is the mean of 100 simulations of 1,000 mutations, with one standard deviation shown. The dashed line is the upper bound for realistic P_b.

When 12 populations derived from a single genotype of *E. coli* were subjected to $50,000$ generations of evolution in a simple, constant environment, their mean fitness increased by $\sim 70\%$ [330]. If the evolved genotypes have reached the optimum $(W = 1)$, the ancestral genotype must have had a fitness of $W \approx 0.59$. If, as seems more likely, the populations have not yet reached the optimum, the ancestor must have had $W < 0.59$. Under this restriction, FGM can only generate a realistic DFE when n is high (Fig. 2.2)

The original FGM makes specific assumptions about the shape of the fitness landscape through its robustness (α) and epistasis (ϵ) parameters. Changing the robustness parameter, α, has no effect on the shape of the curves in Figures 2.2A and 2.2B, regardless of the value of ϵ. For any value of α, setting $\sigma = \tilde{\sigma}/(2\alpha)^{1/\epsilon}$ will yield the same DFE as the original FGM with $\sigma = \tilde{\sigma}$ (Fig. 2.3). Modifying the epistasis parameter, ϵ, however, can change the DFE. Figure 2.4 shows that a genotype with a fitness of $W = 0.5$ and a dimensionality of $n = 100$ can show a realistic DFE if $\epsilon \lesssim 0.75$. A value of $\epsilon < 1$ corresponds to positive epistasis among mutations. However, a detailed study of the first five adaptive mutations fixed during the evolution of an *E. coli* population revealed diminishing-returns epistasis—i.e., *negative* epistasis—between them [154]. With poorly adapted genotypes ($W < 0.59$), and negative epistasis between beneficial mutations ($\epsilon > 1$), an isotropic FGM can only generate a realistic DFE when dimensionality is high (Fig. 2.2).

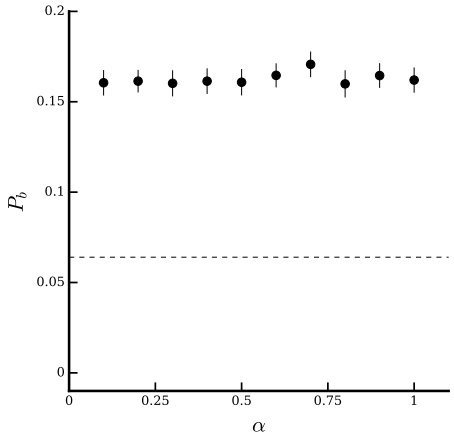

FIGURE 2.3: **Constant P_b across α in isotropic FGM.** Proportion of beneficial mutations and α in isotropic FGM for $n = 100$, with $W = 0.5$, $\epsilon = 2$, and a σ that gives realistic $\bar{s}$ ($-0.03 \leq \bar{s} \leq -0.025$). Each point is the mean of 100 simulations of $1,000$ mutations, with one standard deviation shown. The dashed line is the upper bound for realistic P_b. The isotropic case is $\alpha = 0.5$.

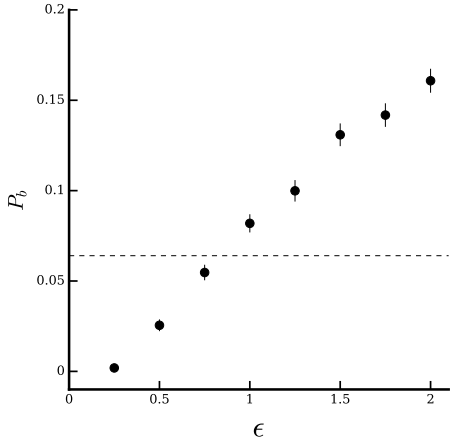

FIGURE 2.4: **Decreasing P_b across ϵ in isotropic FGM.** Proportion of beneficial mutations and ϵ in isotropic FGM for $n = 100$, with $W = 0.5$, $\alpha = 2$, and a σ that gives realistic $\bar{s}$ ($-0.03 \leq \bar{s} \leq -0.025$). Each point is the mean of 100 simulations of $1,000$ mutations, with one standard deviation shown. The dashed line is the upper bound for realistic P_b. The isotropic case is $\epsilon = 2$.

2.3.2 The Isotropy Paradox

In the previous section, I showed that an isotropic FGM can only generate a realistic DFE when complexity is high. Given this result, I now explore whether this DFE will lead to a realistic rate of adaptation. The rate of adaptation is expected to be influenced by other properties of the DFE [19], such as the mean and variance in beneficial effects.

To measure the rate of adaptation, I compare simulations to neutral marker divergence experiments in *E. coli* (Fig. 2.1). Time to fixation (T_{fix}) of a neutral marker (via hitchhiking) serves as a proxy for the rate of adaptation as it depends on both P_b and $\bar{s}$. Specifically, the rate of adaptation should be proportional to $1/T_{\text{fix}}$. I simulated populations in FGM across n, with realistic $\bar{s}$ ($-0.03 \leq \bar{s} \leq -0.025$) for ease of comparison, and then calculated log-likelihood given the *E. coli* data. The minimum dimensionality ($n = 250$) that can generate a realistic DFE (Fig. 2.2) under the original FGM has a log-likelihood of $\ln L = -84.9$ given the *E. coli* data. A dimensionality of $n = 150$ leads to a dramatic increase in log-likelihood of $\Delta \ln L = 9.6$. Approximating the relationship between $\ln L$ and n by a polynomial leads to a maximum likelihood estimate of $n = 150.2$ (95% CI: 107.9 to 192.7). However, recall that $n = 150$ produces a DFE that lies outside of the realistic range (Fig. 2.2).

Herein lies the isotropy paradox. Increasing organismal complexity (n) improves DFE realism, however it reduces the likelihood of rate of adaptation [218]. High complexity ($n = 250$), with a realistic DFE (Fig. 2.2A), causes populations

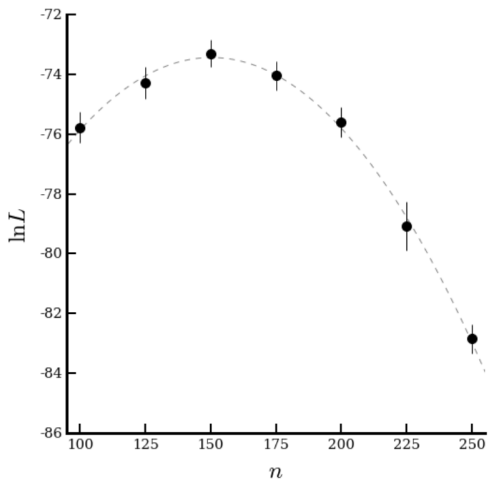

FIGURE 2.5: **Maximum likelihood of marker divergence simulations occurs at $n = 150$.** Each point represents the maximum likelihood of *E. coli* marker divergence data given a distribution of fixation times generated from 1,000 individual-based simulations in FGM. The dashed line is a best-fit polynomial whose maximum occurs is $n \sim 150$ (95% CI: 107.9 to 192.7).

to adapt slower than experimental observations [218] (Fig. 2.6B). At a complexity ($n = 150$) where populations can realistically adapt to their environment (Fig. 2.1A), there is an unrealistic DFE (Fig. 2.2A). This pattern for n is not affected by other parameters in the original version of FGM.

2.3.3 Analyzing Variants

FGM makes two major, simplifying assumptions: spherical symmetry and universal pleiotropy. I now explore conditions for a realistic FGM by analyzing model variants that relax these assumptions. Given the isotropy paradox, there are two approaches to analyze the realism of FGM variants. First, use the model with a realistic DFE ($n = 250$) and relax model assumptions in an effort to improve the rate

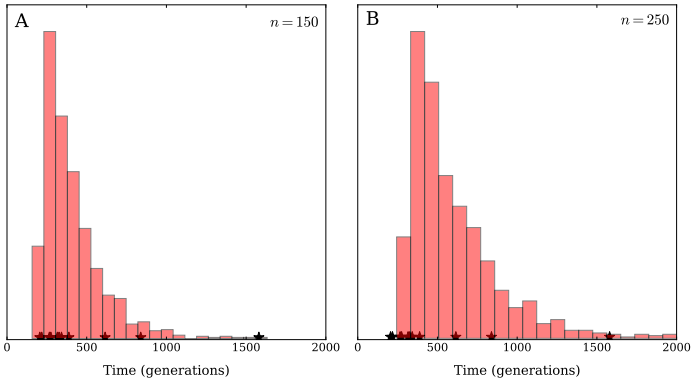

FIGURE 2.6: **Histograms of T_{fix} for simulations under the isotropic FGM.** Shown are 1,000 replicate simulations for $n = 150$ (A) and $n = 250$ (B), with an initial fitness of $W = 0.5$, $\alpha = 1/2$, $\epsilon = 2$, and a σ that gives realistic $\bar{s}$ ($-0.03 \leq \bar{s} \leq -0.025$). The log-likelihoods of these distributions are -75.3 and -84.9 for $n = 150$ and $n = 250$ respectively. Black stars on the x-axis show fixation times calculated for experimental marker divergence data (Fig. 2.1).

of adaptation likelihood ($\ln L$). Second, use the model with highest $\ln L$ ($n = 150$) and relax assumptions in an effort to improve the DFE. I present both of these approaches for all model variants tested.

2.3.4 Random Phenotypic Correlations

One major assumption of FGM is spherical symmetry. The original model assumes that traits are affected equally (strength) and independently (no covariance) by both mutation and selection. Such spherical symmetry seems unlikely to be true in nature, as empirical studies support the existence of asymmetry in both selection [157] and mutation [92, 139].

Given this evidence, a model variant that relaxes its symmetry may be more realistic and applicable [193]. Martin and Lenormand (2006) incorporated selection (S) and mutation (M) matrices to account for covariance and non-uniform strength of selection and mutation on phenotypes. Using random matrix theory, they showed that FGM fits DFE data from mutation accumulation (MA) experiments. Note that MA experiments have limited power to detect beneficial mutations, and thus Martin and Lenormand did not consider P_b in their analysis. Here I use their framework to examine if random M and S matrices can fit a realistic DFE (as defined by P_b and $\bar{s}$).

The DFE becomes less realistic when trait correlations are introduced for both mutation and selection (Fig. 2.7). Increasing correlation strength ($1/\sqrt{m}$) further worsens DFE realism. This result is due to a decrease in effective dimensionality (n_e) [193]. Random matrices in FGM create trait heterogeneity, which can be dissolved by reducing the model to a set of n_e isotropic orthogonal axes [318]. This n_e is the value of n at which the isotropic model produces the same DFE as the random correlations model. As $1/\sqrt{m}$ increases, the model can be reduced to a lower n_e, and thus creates a less realistic DFE. This explains why P_b quickly converges to a similar trajectory for both $n = 150$ and $n = 250$; both complexities are reduced to similar n_e as $1/\sqrt{m}$ increases. Independently, random mutational (M) or selective (S) correlations increase P_b to a lesser degree. However, the realism of the DFE still declines as $1/\sqrt{m}$ increases. Because random correlations do not create a realistic DFE, for either $n = 150$ or $n = 250$, I do not evaluate the likelihood of adaptation.

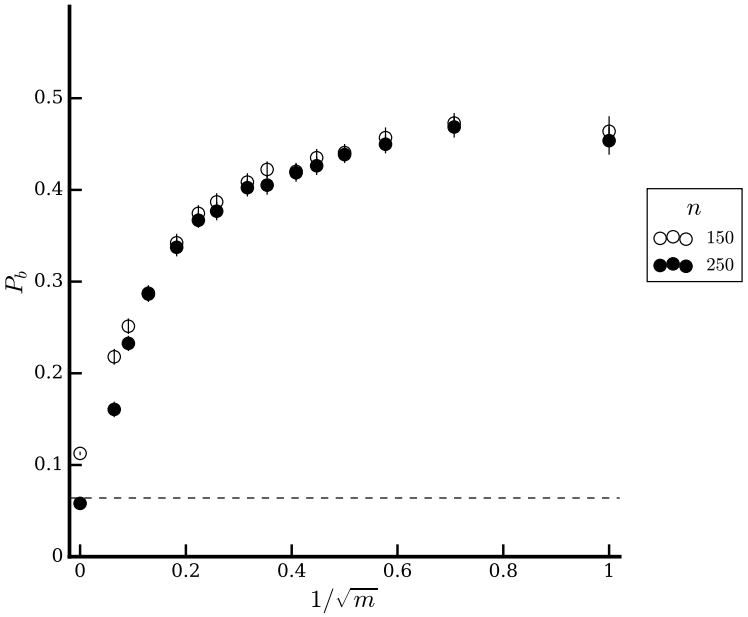

FIGURE 2.7: **Increasing correlation strength decreases DFE realism for random M and S matrices**. Proportion of beneficial mutations and correlation strength ($1/\sqrt{m}$) in the original FGM for $n = 150$ (open circles) and $n = 250$ (closed circles), with $W = 0.5$, $\alpha = 1/2$, $\epsilon = 2$, and a σ that gives realistic $\bar{s}$ ($-0.03 \leq \bar{s} \leq -0.025$). Each point is the mean of 100 simulations of 1,000 mutations, with one standard deviation shown. The dashed line indicates the upper bound for realistic P_b.

2.3.5 Fitness Ridge

Recent empirical studies have shown genotypic fitness landscapes to be rugged, due to the prevalence of epistatic interactions [101, 154, 295]. Sign epistasis, when an allele is beneficial in one genetic background and costly in another, creates fitness ridges in genotypic space [112]. Given support for genotypic fitness ridges [319], I posit that phenotypic fitness ridges, where the fitness of a trait depends on the state of another trait, exist as well [181, 322]. Rugged fitness landscapes are likely to have multiple paths to the optimum [208, 262, 319], and may even contain

multiple peaks [67,192,263]. However here I aim to test if adaptation along a ridge is realistic, which is independent of the number of fitness ridges in the landscape. As such, I test the realism of the DFE and adaptation along a single phenotypic fitness ridge towards the optimum.

Low pairwise correlations are necessary to create a ridge at high dimensions. A fitness ridge with $p \gtrsim 0.01$ produces a realistic DFE for $n = 150$ (Fig. 2.8A). For $n = 250$, the DFE remains realistic, with a lower P_b, as p increases. As the ridge becomes steeper (higher p), more mutations become deleterious (P_b decreases) and the DFE becomes more realistic. Despite a realistic DFE, populations adapt unrealistically on fitness ridges (Fig. 2.8B). The likelihood of adaptation, given the *E. coli* marker divergence data, drops drastically when $p > 0$. For $n = 150$, when $p = 0.005$ (realistic DFE), $\Delta \ln L = -13.7$ from the isotropic model. For $n = 250$ the decrease in likelihood from isotropy is even greater ($\Delta \ln L = -30.0$). Mutations must be of very small magnitude in order to maintain a realistic $\bar{s}$ and P_b on a fitness ridge. This causes longer fixation times for neutral markers (Fig. 2.9). Despite empirical motivation [101, 112, 154, 295, 319], the fitness ridge variant fails to produce both a realistic DFE and rate of adaptation.

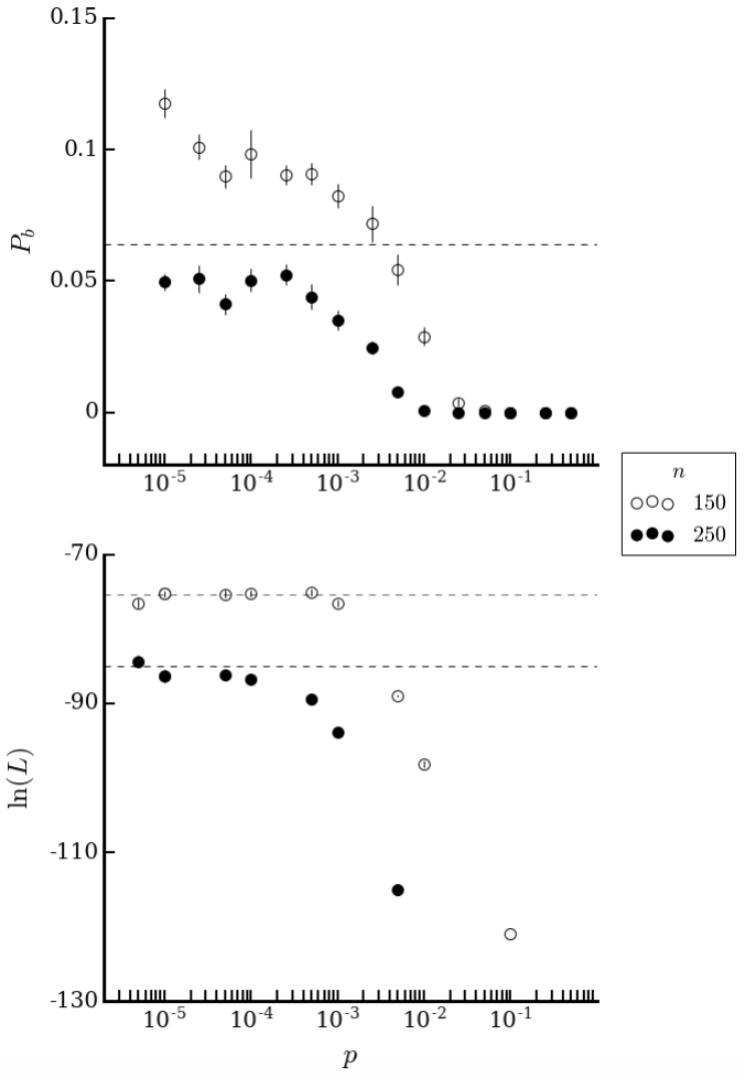

FIGURE 2.8: **Steeper fitness ridges create a more realistic DFE but decrease the likelihood of rate of adaptation.** Both panels show $n = 150$ (open circles) and $n = 250$ (closed circles), with $W = 0.5$, $\alpha = 1/2$, $\epsilon = 2$, and a σ that gives realistic $\bar{s}$ ($-0.03 \leq \bar{s} \leq -0.025$). A) Proportion of beneficial mutations and p. Each point is the mean of 100 simulations of $1,000$ mutations, with one standard deviation shown. The dashed line indicates the upper bound for realistic P_b. B) $\ln L$ and p. Each point is the mean for $1,000$ calculations, each bootstrapped from the distribution of T_{fix} for $1,000$ simulations. The dashed lines show the isotropic $\ln L$ for $n = 150$ (grey) and $n = 250$ (black) for comparison.

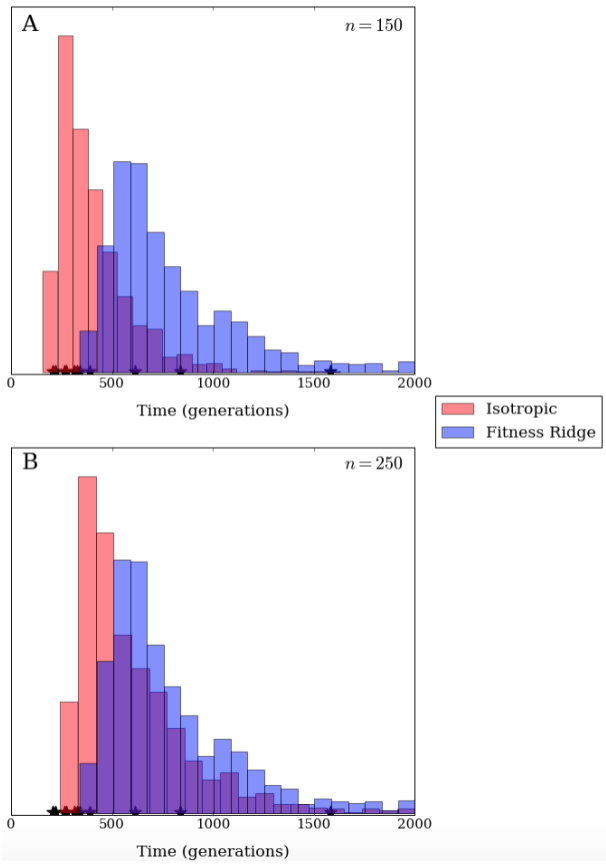

FIGURE 2.9: **Fitness ridges result in longer fixation times for neutral markers.** T_{fix} for 1,000 marker divergence simulations for $n = 150$ (A) and $n = 250$ (B) with $p = 0$ (red) or $p = 0.01$ (blue), and $W = 0.5$, $\alpha = 1/2$, $\epsilon = 2$, and a σ that gives realistic $\bar{s}$ ($-0.03 \leq \bar{s} \leq -0.025$).

2.3.6 Restricted Pleiotropy

The other major simplifying assumption of FGM is universal pleiotropy — every mutation is expected to affect every trait equally. This assumption is biologically unrealistic, as empirical work shows that mutations affect a limited subset of traits [2,200,278,292,310,315,340]. Here I explore whether restricted pleiotropy, in

modular [225, 311, 321] or *non—modular* [47, 178] form, can produce a realistic DFE and rate of adaptation. Decreasing the level of *nonmodular* pleiotropy (b) worsens realism of the DFE (Figure 2.10). P_b increases for a given $\bar{s}$ because mutations only affect $b < n$ traits, and thus the chance that $D(z + z\text{-}) < D(z)$ is higher. This result holds for *modular* pleiotropy as well. Because restricted pleiotropy does not create a realistic DFE, for either $n = 150$ or $n = 250$, I do not evaluate the rate of adaptation.

2.3.7 Restricted Pleiotropy and Restricted Maladaptation

Despite empirical evidence for low levels of mutational pleiotropy [2, 200, 278, 292, 310, 315, 340], implementing it in FGM decreases the realism of the DFE (Figure 2.10). It is important to recognize that these results are under the assumption that all traits are equally maladapted ($z[1] = z[2] ... = z[n]$). This is not the scenario in which pleiotropy is expected to evolve [46, 309]. Restricted pleiotropy is advantageous when some traits are maladapted and others are well adapted because it allows adaptation to proceed without undoing previous adaptation [309, 321]. I tested the realism of restricted pleiotropy variants in these conditions by modifying the number of maladapted traits (n_{mal}) in the ancestor. Low levels of pleiotropy combined with few traits maladapted produces a realistic DFE for $n = 150$ and improves DFE realism for $n = 250$ (Fig. 2.11). Unlike the previous restricted pleiotropy variant, here P_b does not increase as b decreases. Due to low n_{mal}, mutations are less likely to improve the maladapted phenotypes. As such, most mutations are deleterious, resulting in a realistic P_b. This is robust to our scaling of σ,

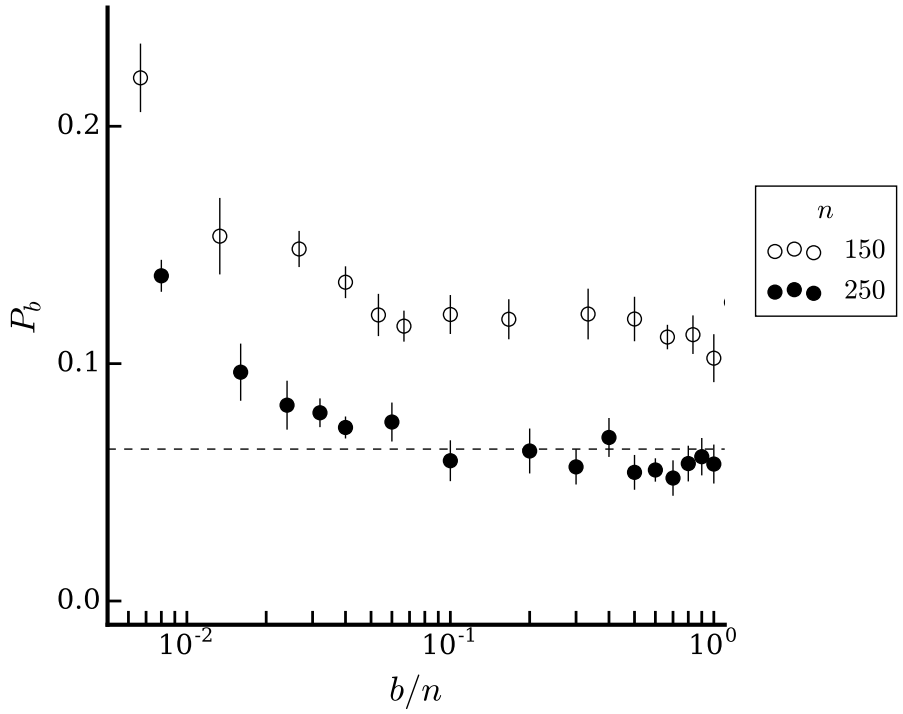

FIGURE 2.10: **Decreasing pleiotropy worsens DFE realism.** Proportion of beneficial mutations and pleiotropy (as a proportion of total traits, b/n) in the original FGM for $n = 150$ (open circles) and $n = 250$ (closed circles), with $W = 0.5$, $\alpha = 1/2$, $\epsilon = 2$, and a σ that gives realistic $\bar{s}$ ($-0.03 \leq \bar{s} \leq -0.025$). Each point is the mean of 100 simulations of 1,000 mutations, with one standard deviation shown. The dashed line indicates the upper bound for realistic P_b.

and reliably results in a realistic DFE when both b/n and n_{mal}/n are small.

Given a realistic DFE, I simulated adaptation to test if restricted pleiotropy ($b < n$) with restricted maladapatation ($n_{\text{mal}} < n$) improves the likelihood of adaptation. The likelihood of $n = 150$ is unchanged for most combinations of b and n_{mal}, but decreases at values where the DFE becomes realistic (low b, low n_{mal}) (Fig. 2.12). The likelihood decreases because low values of b and n_{mal} result

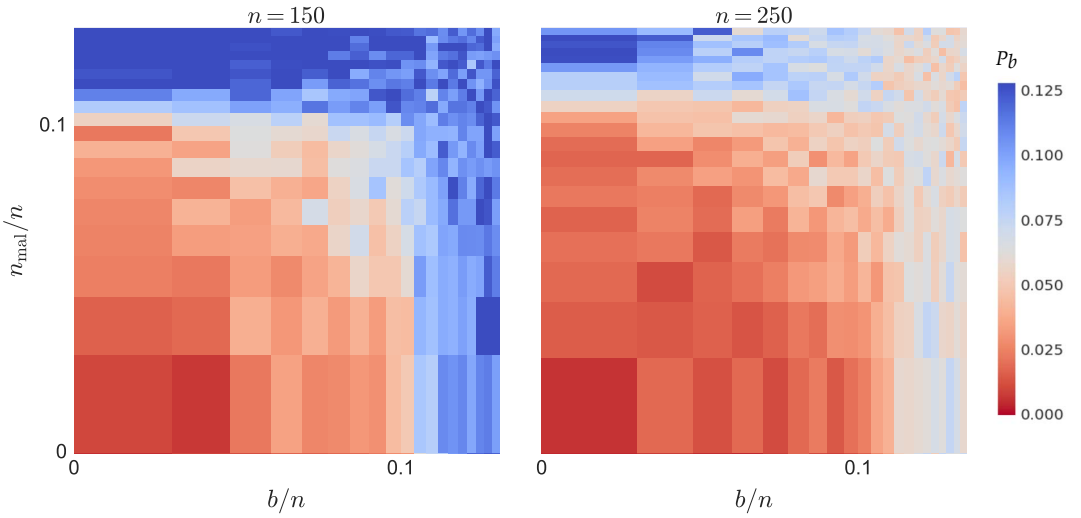

FIGURE 2.11: **DFE realism increases for $n = 150$ and $n = 250$ as b/n and n_{mal}/n decrease.** Each square shows P_b for 100 replicate simulations testing 1,000 mutations each. Red indicates DFE realism ($P_b < 0.064$) and blue shows an unrealistic DFE ($P_b > 0.064$).

in faster fixation times (Fig. 2.6), and cause the model to miss high experimental T_{fix} observations (Fig. 2.13). The $n = 250$ isotropic model had low $\ln L$ due to long fixation times (Fig. 2.13). Low b and n_{mal} create faster T_{fix} and make the $n = 250$ model more likely, given experimental data. The highest likelihood here occurs at $b/n = 0.2$ and $n_{\text{mal}}/n = 0.1$ ($\ln L = -75.3$). It is $\Delta \ln L = +9.6$ greater than the likelihood of isotropic $n = 250$ and has the same likelihood as the best isotropic model ($n = 150$). The DFE of the realistic restricted model is narrower than that of the highest likelihood isotropic model, and is realistic due to fewer beneficial mutations (Fig. 2.14) This model variant - with high complexity, low pleiotropy and low maladaptation - results in a realistic DFE and lnL. The fitness effects of

mutations are subject to high n, yet adaptation proceeds in a low dimension subset of phenotypic space (n_{mal}).

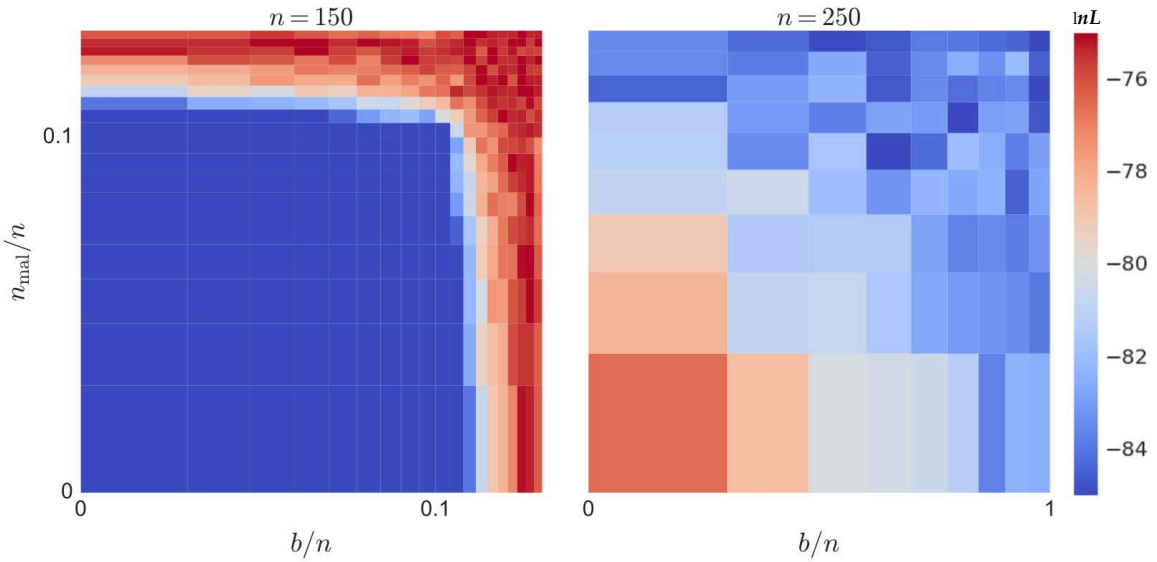

FIGURE 2.12: **Rate of adaptation realism (**ln L**) decreases for** $n = 150$ **and increases for** $n = 250$ **as** b/n **and** n_{mal}/n **decrease.** Each square shows ln L calculated using 1,000 replicate simulations, given *E. coli* experimental marker divergence data. Warmer colors indicate a more realistic ln L while cooler colors show a less realistic ln L.

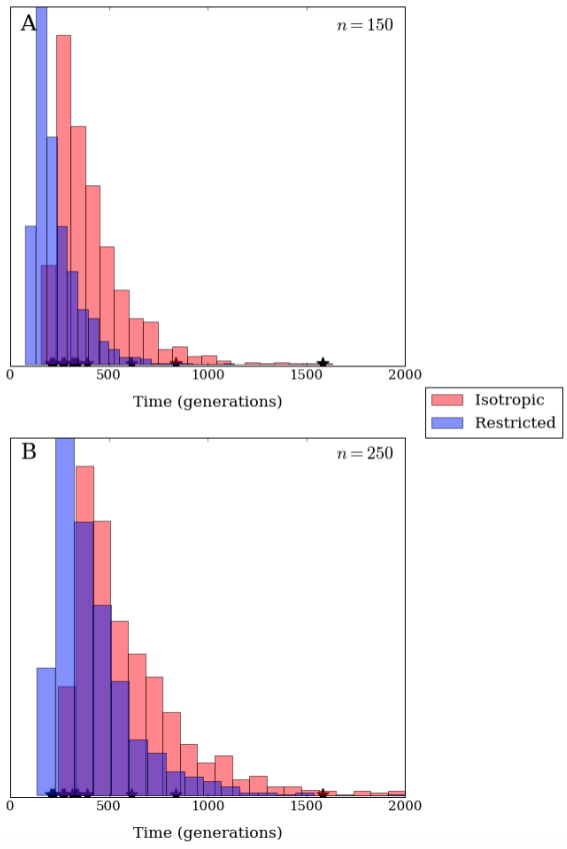

FIGURE 2.13: **Histograms of T_{fix} for simulations under FGM with restricted pleiotropy and restricted maladaptation.** Shown are 1,000 replicate simulations for $n = 150$ (A) and $n = 250$ (B), with an initial fitness of $W = 0.5$, $\alpha = 1/2$, $\epsilon = 2$, and a σ that gives realistic $\bar{s}$ ($-0.03 \leq \bar{s} \leq -0.025$). Black stars on the x-axis show fixation times calculated for experimental marker divergence data (Fig. 2.1). Red shows the isotropic model. Blue shows the restricted model with $n_{\text{mal}}/n = 0.1$ and $b/n = 0.1$.

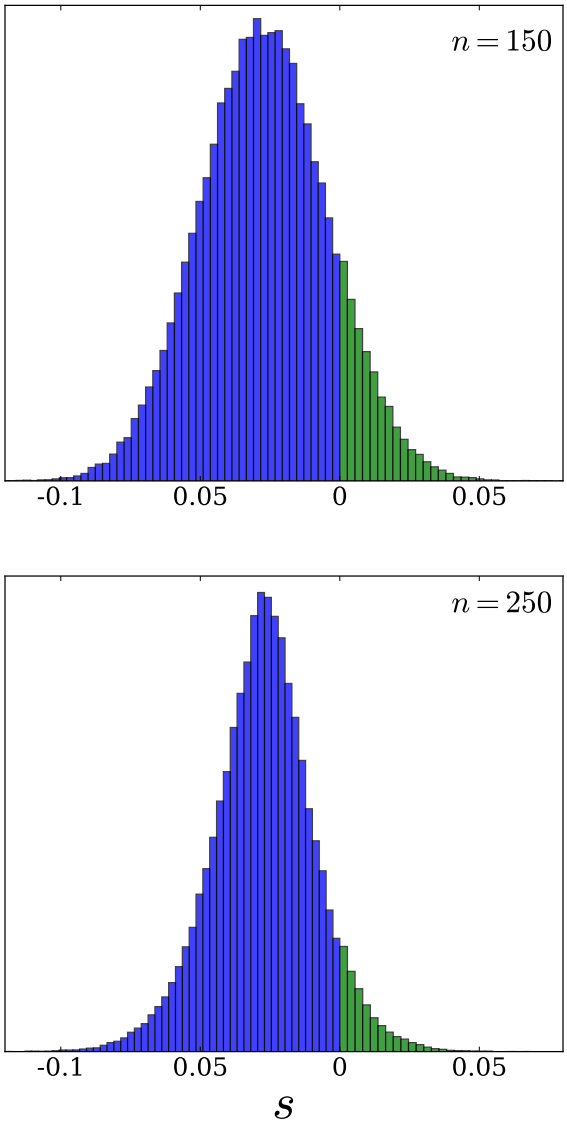

FIGURE 2.14: **DFE for the isotropic and restricted models.** Shown are histograms for the fitness effects of $1,000,000$ sampled mutations for isotropic $n = 150$ and restricted $n = 250$ ($b/n = 0.2$, $n_{\text{mal}} = 0.1$). Blue indicates deleterious mutations ($s < 0$) and green indicates beneficial mutations ($s > 0$). These simulations were done with $W = 0.5$, $\alpha = 1/2$, $\epsilon = 2$, and a σ that gives realistic $\bar{s}$ ($-0.03 \leq \bar{s} \leq -0.025$).

2.4 Discussion

Fisher's Geometric Model of Adaptation (FGM) is commonly used to fit empirical data on experimental evolution and epistatic gene interactions [39, 194, 229], and draw insights about the underlying fitness landscape. I identified a mismatch between model fits to the distribution of mutation fitness effects (DFE) and the rate of adaptation. The isotropic model with the highest likelihood ($n = 150$, Fig. 2.5), given *E. coli* marker divergence data, generates an unrealistically high proportion of beneficial mutations (P_b) (Fig. 2.2A). Yet, when the DFE is realistic in the isotropic model ($n \gtrsim 250$), adaptation proceeds slowly in comparison to empirical findings (Fig. 2.13) and lnL decreases (Fig. 2.5). Lacking information on the genetic basis of adaptation, Fisher made two simplifying assumptions in his model: spherical symmetry and universal pleiotropy. Others have since created new model variants by relaxing these assumptions [178, 193, 318, 321]. Here I examined if relaxing Fisher's assumptions about selection and mutation improve the fit both the DFE and rate of adaptation.

I first tested if relaxing spherical symmetry improved the DFE and likelihood of adaptation. Random correlations in mutation and selection create trait heterogeneity, which reduces the effective dimensionality (n_e) of the model and makes the DFE less realistic. I next tested if a fitness ridge, a specific case of selective correlations, could satisfy a realistic DFE. This exploration was motivated by empirical evidence for sign epistatic interactions which create fitness ridges in genotypic space [101, 112, 154, 295, 319]. This variant produces a realistic DFE as p increases.

However, this resulted in a decreased rate of adaptation and low model likelihood, given marker divergence data (Fig. 2.8).

Fisher's other major assumption was universal pleiotropy. Understanding and modeling pleiotropy is key for comparing mutation-selection models with empirical data [141]. Universal pleiotropy assumes a single genotype network where all nodes are connected. This concept stems from cellular architecture; every gene uses the same metabolic pool of ribosomes, nucleotides, and polymerase, and any mutation that affects gene activity may affect the competition for those molecules [142]. Critics of universal pleiotropy argue that the fitness effects of a metabolite pool may be minimal and biologically meaningless [222], and that pleiotropy is restricted and highly structured [311].

Both theoretical and experimental work support the existence and evolution of restricted pleiotropy. Early support came from Gibson, who used a statistical thermodynamic model of transcriptional regulation to show that inevitable trade-offs during evolution naturally lead to pleiotropic effects [115]. Using the NK model, which accounts for both epistasis and pleiotropy, Østman et al. (2009) showed that populations of asexual haploids reach the highest fitness with intermediate levels of pleiotropy [219]. Another locus-based model found high levels of sign epistasis, an indicator of adaptive gene modules [225].

Experimental evidence for restricted pleiotropy is rapidly accumulating. A systematic study of pleiotropic effects in yeast, worms (*C. elegans*), and mice, found a low proportion of genes to affect multiple traits, with an average of 6.8% (95% CI: 5.1% to 8.5%) [315]. Other such studies have found similarly low levels of

pleiotropy [292, 340]. A QTL analysis mapped 70 skeletal traits in mice and found an average pleiotropic effect of 7.8, with a maximum of 30 [153]. A similar study in sticklebacks also supports low levels of pleiotropy [2]. Recent work using $> 11,000$ gene expression traits in MA experiments with *Drosophila serrata* found that only mutations affect 2.1% of variable traits measured [200]. Comparing these studies proves difficult because both the organisms and number of traits measured vary. This makes interpreting the 'level' of pleiotropy non-trivial. Nonetheless, the empirical literature across multiple organisms supports an 'L-shaped' distribution of pleiotropic effects, with most genes affecting few phenotypes and few genes affecting many [222].

Our work with FGM corroborates previous theoretical and empirical studies of pleiotropy [2, 200, 278, 292, 310, 315, 340]. I find that restricted pleiotropy variants, with a low percentage of maladapted traits, satisfy a realistic DFE (Fig. 2.11) while simultaneously producing a realistic rate of adaptation (Fig. 2.12). The results of these variants makes sense if I consider the situation where restricted pleiotropy is favorable [309, 321]. It provides a benefit when some traits are maladapted but others are not because it allows improvements to parts that require adaptation without disrupting the entire system [16].

Beyond fitting the DFE and rate of adaptation, FGM has proven to be a useful model for capturing the fitness of complex mutation interactions (epistasis) [194]. I compared epistasis fits of our realistic variant (restricted pleiotropy and restricted maladaptation) to the original isotropic model, using multiple measures of epistasis (2.2.6).

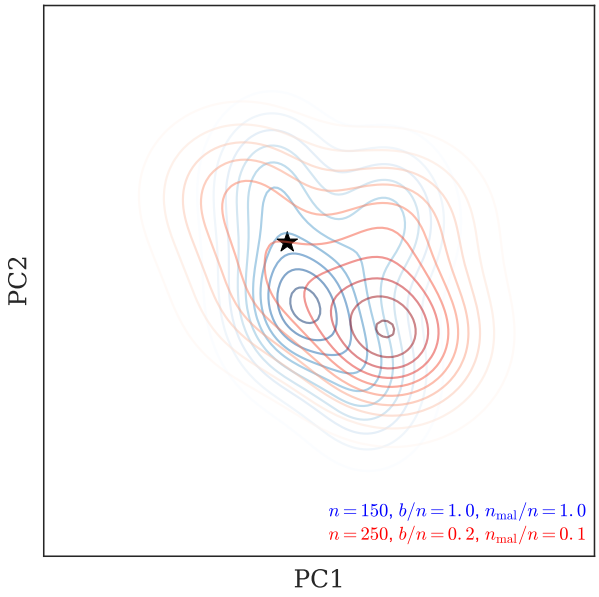

FIGURE 2.15: **Isotropic and Restricted FGM produce similar fits to epistasis data.**f Shown are kernel density estimates (*kde*) of principal components analysis for 25 5-mutation landscape constructions in FGM (red and blue) and the experimental data (black star). Isotropic $n = 150$ is in blue, and restricted $n = 250$ with $b/n = 0.2$ and $n_{\text{mal}} = 0.1$ is in red.

Given that the original FGM has repeatedly produced good fits to epistasis data [194], it is not surprising that simulations under the isotropic model ($n = 150$) cluster near the Khan et al. (2011) data (Fig. 2.15). The most realistic restricted variant **(**$n = 250$**,** $b/n = 0.2$**,** $n_{\text{mal}} = 0.1$**)** produces a similar fit to the experimental data (Fig 2.15). Here principal components 1 and 2 explain 61.4% of the data, providing assurance that the models are indeed similar across the statistics. Not only does restricted pleiotropy and restricted maladaptation improve the DFE and likelihood of adaptation, it also maintains fits to epistasis data.

FGM is not applicable to all experimental data. For example, some organisms

have a substantial proportion of lethal mutations [45, 77, 253]. Due to the fitness function, lethal mutations are not possible in FGM. More broadly, recent work suggests that the DFEs of some organisms may be multi-modal [163]. Many systems also show strong genetic incompatibilities [15], a phenomenon that does not occur in the original FGM (but see [102]). FGM is particularly useful for fitting evolutionary trajectories [229], epistasis data [193], and uni-modal DFEs. However, it is certainly not a universal framework for modeling experimental data.

Overall, I take our results to be encouraging support for restricted pleiotropy, particularly because I did not intend to test it directly. I aimed to alleviate a paradox between the DFE and likelihood of adaptation, and ultimately found the most realistic model to contain a mutational regime with ample support in the literature. Our results presented here depend critically on the estimates of realistic P_b and $\bar{s}$. Some work suggests that P_b may be higher than 0.064 for populations with low fitness [128]. In FGM, increasing the upper bound for realistic P_b increases the parameter space of n_{mal} and b in which the DFE is realistic. Future experimental work may test how n_{mal} correlates with P_b using a knockdown gene expression framework.

Chapter 3

The Role of Historical Contingency in Divergent Evolution

A case study in the *Escherichia coli lac* operon

3.1 Introduction

The relationship between genotypes and fitness often deviates from expectations based on independent effects - a phenomenon known as epistasis (1.5). These epistatic interactions can cause evolutionary trajectories to be contingent upon prior adaptations (1.4.2). For example, in a ligand-binding protein, the evolutionary fate of a newly arising mutation depends on epistasis with the genotype in which it occurs [275]. Such contingencies may alter the set of potential evolutionary outcomes (1.4.3), resulting in divergent evolution from a common ancestor [53, 174]. This chapter examines the role of historical contingency in a case study of divergent evolution in the *E. coli lac* operon.

Experimental evolution offers a method with which to test the role of historical contingency in divergent evolution. However, it has yielded mixed findings to date. One experiment showed that historical contingency plays a large role in the adaptation of pathogens to antibiotics [264, 265]. Reducing the use of antibiotics had been proposed as a measure to curb antibiotic resistance. However, when the antibiotic is removed, fitness of evolving populations increases quickly via compensatory mutations, such that resistance is maintained when antibiotic is added back [264, 265]. These compensatory mutations are contingent on the cost of the resistance mutation for their benefit. In another evolution experiment, the adaptation of multiple *E. coli* phenotypes was dependent on prior evolutionary history (across four environments) [235]. These examples show that evolution can be contingent on prior adaptations. However, some recent experiments suggest that not all epistatic interactions rely on specific contingencies (1.5). In fact, in *E. coli* and *M. extorquens* beneficial mutation effects can be predicted based on background fitness alone [49, 154]. Other work shows similar trends of convergent phenotypic evolution [13, 229, 330], even when genotypes diverge [23, 164].

Here I focus on a case study of divergent evolution in the *E. coli lac* operon. For populations evolved in a lactose-containing environment, less regulation of the *lac* operon is beneficial. In particular, a mutation to the *lac* operon repressor (*lacI*) increases fitness in the common ancestor [238]. In the absence of lactose, the functional ancestral repressor (*lacI+*) produces the LacI protein, which binds to the *lac* operon operator to inhibit transcription by RNA polymerase. In the presence of lactose, allolactose binds to LacI and the operon is transcribed at high levels.

Most mutations to *lacI* result in a non-functional repressor (*lacI–*) that does not produce the LacI protein [259, 260]. As a result, transcription is independent of lactose availability and the *lac* operon is constitutively expressed.

The *lac* operon is a useful model for testing the influence of historical contingency on adaptation for a few reasons. First, the *lac* operon has been shown to be under selective pressure across multiple experiments [74, 238]. Second, fitness effects of mutations to the *lac* operon depend on the environment [238]. This allows an analysis of the effect of environment on contingency. Lastly, underlying mechanisms of contingency can be elucidated as the regulatory and molecular components of the *lac* operon are well-understood [4,74,137,159,160,212,269,291,327,337].

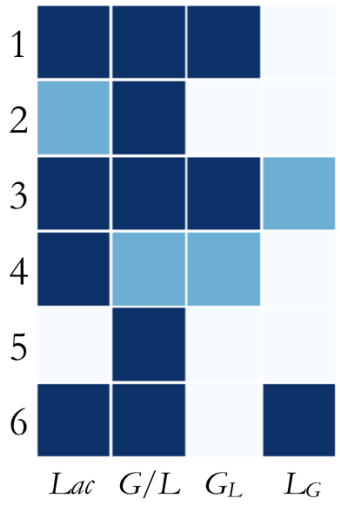

FIGURE 3.1: ***lacI* status in 8,000-generation evolved populations.** Squares represent populations for 6 populations each of four evolution environments (*Lac*, G/L, G_L, L_G). Dark blue indicates fixation, white indicates absence, and light blue indicates a mixed population with *lacI–* still segregating.

Despite a large fitness benefit in the ancestor [238], only 50% (12/24) of populations evolved in selective environments containing lactose fixed a *lacI*– mutation after 8,000-generations of evolution (Fig. 3.1). Here I first confirm the fitness benefit of *lacI*– mutations in the ancestor. I then use simulation to show that observed experimental divergence in the *lacI* gene cannot be attributed to stochasticity. Mutation rates have also not changed in most evolved populations. I find that fitness effects of *lacI*– deviate from the ancestor in most populations, suggesting that the observed divergent evolution is driven by negative epistasis with previous substitutions. Lastly, I identify a candidate epistatic interaction for an evolved population that had a dramatic decrease in fitness within the first 500-generations of adaptation. In total, my results demonstrate that divergent adaptation in the *lac* operon is due to historical contingency on previous adaptations.

3.2 Materials and Methods

3.2.1 Bacterial Strains and Growth Conditions

Bacterial clones used for this experiment were selected from populations in a long-term evolution experiment in 7 environments (4/7 used here) [53]. Strains that fixed a *lacI*- mutation are denoted as *lacI*–$_{\text{ev}}$ and those that maintained the ancestral allele are *lacI*+$_{\text{ev}}$. Evolution environments comprised a simple base medium (Davis Minimal) supplemented with: Lactose only (*Lac*), daily alternating between glucose and lactose (G/L), or 2,000-generation alternating starting with glucose (G_L)

or starting with lactose (L_G). Sugars were added to the DM medium in concentrations as follows: glucose = 175 μM/mL, lactose = 210 μM/mL. These concentrations support approximately equal concentrations of stationary phase bacteria (3.5×10^8 cfu/mL) [53]. Lysogeny broth (LB) was used for non-selective culturing, while the respective evolution environment of each clone was used for fitness assays and growth measurements.

Populations were propagated in 1 mL in 96-well blocks for 8,000 generations, using a daily 1:100 serial transfer. Each population was initially homogeneous, such that *de novo* mutation was the only source of genetic variation. Samples were frozen at –80°C, with glycerol as a cryoprotectant, every 500 generations. Six replicate populations were evolved in each environment, with three from each ancestor (REL606,REL607). These ancestors are isogenic with the exception of a neutral marker (*ara*+/-) which indicates ability to utilize the sugar arabinose [174]. The *ara* marker can be differentiated by plating on tetrazolium-arabinose (TA) plates, on which *ara*+ strains form white colonies and *ara*– are red. Arabinose is not used as growth media in my experiments, and thus does not affect fitness measurements.

3.2.2 Identification of *lac* operon mutations

To determine fixation or absence of a *lacI* mutation, I plated 8,000-generation population samples (1,000 to 3,000 cells) on TGX indicator medium. This medium consists of agar plates with 0.5% glucose and 30 mg/ml of the lacZ substrate 5-bromo-4-chloro-3-indolyl-beta-D-galactopyranoside (X-gal). Colony color on this medium indicates the level of lacZ activity, and thus distinguishes between the

ancestral *lacI*+ allele (no expression, white) and *lacI*– mutations (constitutive expression, dark blue). Any populations that showed a mix of blue and white were not used here, as I am interested in divergent adaptive paths; if a *lacI* mutation is currently segregating then the adaptive path has not yet been chosen.

For this work I did not use mutations which occurred in the *lacI* repressor binding site of the *lac* promoter (*lacO1*). Previous work has shown that *lacO1* mutations reduce binding efficiency of *lacI*, and thus increase expression via reduced repression (intermediate expression, light blue) [26, 95, 190, 204, 238]. I did not consider these mutations, as the aim was to evaluate epistatic interactions with a single parallel evolved mutant gene.

3.2.3 Strain Constructions

***lacI*–$_{ev}$:** I replaced evolved *lacI*– alleles with ancestral *lacI*+ using the suicide plasmid pDS132 [231, 238]. This vector contained the the ancestral *lacI* gene (+), along with chloramphenicol resistance (Cm^R) and *sacB*, which confers susceptibility to sucrose. The plasmid was conjugated into recipient cells and Cm^R cells (formed by chromosomal integration of the plasmid) were selected. Resistant clones were streaked onto LB + sucrose agar to select cells which lost the plasmid. These cells were then screened for *lacI*+ using X-gal agar and phenyl-β-D-galactoside (P-gal) agar. White color on X-gal indicates no *lacZ* activity (*lacI*+, full repression). To confirm this, I screened white colonies on P-gal agar to ensure they could not grow. P-gal is a substrate for β-galactosidase (*lacZ* product) but does not induce the *lac* operon. Therefore only cells that express the *lac* operon without

induction (*lacI*–) can survive on P-gal. After white color on X-gal and no growth on P-gal, I sequenced these cells to ensure that the *lacI* gene was identical to the ancestor.

***lacI*+$_{ev}$:** Mutants (*lacI*–) of *lacI*+$_{ev}$ were selected by plating a population sample, grown in a non-selective medium (here LB), onto P-Gal plates. Only constitutive mutants can grow on P-Gal. Colonies were re-streaked onto fresh P-Gal plates 2–3 times to ensure *lac* constitutive expression. I then used PCR and sequenced the *lacI* gene and used only those mutants with the same mutation that was present in evolved clones (4 base-pair insertion or deletion).

3.2.4 Mutation Rate Estimates

The rate of mutation to the constitutive *lac* expression phenotype, most of which reflect *lacI* mutations [259, 260], was estimated using a fluctuation test [183] for *lacI*+ populations, to determine whether *lacI*– mutations were absent due to a lower evolved mutation rate. For each clone, the freezer stock was grown overnight at 37°C in LB and diluted 1:1000 independently into 10 fresh LB cultures (1 mL each). After overnight growth, 100μL sample from each replicate population was plated onto DM agar supplemented with X-gal and P-gal. A diluted sample was also plated onto LB agar plates to estimate total cell density in the culture. After 48-hr incubation at 37°C I counted blue colonies on the X-gal/P-gal plates (*lacI*– mutants) and colonies on the LB plates.

Plating Efficiency: Here, the plating efficiency of a given strain represents the ability to accurately identify *lacI*– mutants in a culture. This was measured by combining a known number of *lacI*– mutants with a *lac* operon deletion strain and plating on P-Gal. The deletion strain is not capable of acquiring a *lacI*– mutation, since the entire operon is deleted. The plating efficiency can then be calculated as

$$p_{\text{eff}} = \frac{m_c}{m_e} \tag{3.1}$$

where m_c is the number of mutants counted when plated in combination with the deletion strain, and m_e is the number of mutants counted when plated alone. Colony counts were multiplied by $(1/p_{\text{eff}})$ to obtain corrected mutation counts.

Calculation: Mutation rate analysis was carried out using the bz-rates estimator (http://www.lcqb.upmc.fr/bzrates) [116].

3.2.5 Individual Based Simulations

The frequency of substitution (f_s) for a *lacI*– mutant is a function of mutation rate, population size, and mutation dynamics. These dynamics, such as clonal interference and hitchhiking, can cause significantly faster or slower fixation times. To estimate the expected fixation time (T_{fix}) for *lacI*– mutants in the long-term evolution experiment, I conducted individual based simulations.

These simulations were done under a Wright-Fisher regime with a genome-wide mutation rate of $U = 7 \times 10^{-4}$ (estimated in Chapter 2) and *lacI* mutation rate

of 1.72×10^{-7} (measured in the ancestor). Background mutations were subdivided into 6 classes (3 deleterious, 3 beneficial), each comprising a different proportion of occurring mutations (Table 3.1). This maintains a realistic DFE (as defined in 2.2.5). Mutations to *lacI* contributed the measured benefit (8.31% in Lac, 4.05% in G/L) The effective population size ($N = 3.3 \times 10^7$) [287] is too large to reasonably simulate. As such, I simulated population sizes from 1×10^1 to 1×10^5, and use f_s for $N = 1 \times 10^5$ as a conservative estimate for $N = 3.3 \times 10^7$.

Effect	Proportion
-10%	4.75%
-5%	23.5%
-2.5%	70%
$+2.5\%$	1%
$+5\%$	0.5%
$+10\%$	0.25%

TABLE 3.1: **The Distribution of Fitness Effects (DFE) for simulations.** Background mutations were segmented into 6 classes, with fitness effects from -10% to $+10\%$ (Table 3.1). Proportions for each class satisfy the realistic mean effect ($\bar{s}$) and proportion of beneficial mutations (P_{ben}) defined in 2.2.5. Background mutations occur at a genome-wide rate of 7×10^{-4} (Table 2.1). Mutations to *lacI* occur at a rate of 1.72×10^{-7} (Fig 3.4).

Here I classify a mutation as fixed when it is present in 95% of the population. Populations were allowed to evolve until a *lacI* mutation fixed, or they reached 8,000 generations. For each population I simulated 100 replicate populations and recorded the proportion of populations that fixed a *lacI* mutation. I then bootstrapped the simulation results $1,000$ times to estimate the 95% confidence interval

for f_s. For the 2,000-generation fluctuating environment, I simulated only 2,000 generations of evolution in lactose, and calculated f_s as

$$f_s = f_{2k} + f_{2k}(1 - f_{2k}) \tag{3.2}$$

where f_{2k} is the frequency of substitution for 2,000-generations of evolution. The second term represents the number of remaining populations that have not fixed *lacI*– after 2,000-generations $(1 - f_{2k})$ multiplied by the proportion of those populations expected to fix *lacI*– in the second bout of lactose evolution (f_{2k}).

3.2.6 Fitness Assays

The relative fitness of a given strain was assayed relative to its opposite marker construct (e.g., *lacI*+ vs *lacI*–). Fitness assays were carried out in identical conditions to the strain's evolution environment. Prior to each assay, the two strains were independently preconditioned to the competition environment. Preconditioning and competitions lasted for 1 day, except for the G/L environment, which lasted 2 days. For the G/L environment, the growth medium was switched from glucose to lactose for day 2 (for both precondition and competition). Following preconditioning, strains were mixed at a 1:1 volume ratio (200-fold dilution) and immediately plated on the indicator agar (TGX or TA). Competition proceeded for 1 or 2 days, with a transfer to fresh media (100-fold dilution) between days. Samples were again plated on the indicator agar at the end of the competition.

Absolute fitness of a given strain a is calculated as

$$W_a = \ln\left(100^d \times \frac{N_a(f)}{N_a(i)}\right) \tag{3.3}$$

where d is the number of competition days, and N is the number of colony forming units at the initial (i) and final (f) time points. Fitness of a relative to strain b is then $W_{\frac{a}{b}} = W_a/W_b$, and the selective advantage of a over b is $s_a = W_{\frac{a}{b}} - 1$.

3.2.7 Sequencing

lacI: Constructed $lacI+$ strains (from *lacI*– evolved clones) were confirmed via their inability to grow on P-gal agar. It is more difficult to select *lacI*– mutants, as any *lac* operon mutant that increases expression may grow on P-gal agar [238]. Following the selection of blue colonies (constitutive lac expression) on P-gal, I confirmed the identity of mutants through PCR and sequencing. Beyond confirming the presence of a *lacI* mutant, I chose only 4 base-pair deletions or insertions for my work. The reasoning is as follows:

1. 8/12 $lacI{-}_{\text{ev}}$ evolved populations contain a 4 base-pair insertion or deletion
2. 4 base-pair insertions and deletions make up 70% of *lacI* mutants [259, 260] and thus provide an accurate representation of *lacI* mutant effects.

Whole Genome: Genomic DNA was isolated and purified using the Wizard Genomic DNA Purification Kit (Promega) following the protocol for Gram negative bacteria at one-third volume. Double stranded DNA was then quantified

using SYBR Green I Nucleic Acid Stain (Invitrogen) in a SpectraMax M5 Fluorescence Microplate Reader (Molecular Devices). Libraries were created following the Nextera XT DNA Library Prep Kit protocol, at one-quarter volume, with Nextera XT Index Kit v2 adapters (Illumina). Libraries were individually quantified using the Qubit dsDNA High Sensitivity Assay with a Qubit 2.0 Flourometer (ThermoFisher). DNA fragment size was confirmed using the Agilent 2100 BioAnalyzer with a High Sensitivity DNA Analysis Kits (Agilent). Libraries were pooled and sequenced using a 300 cycle mid-output run on an Illumina NextSeq, producing 150 base-pair, paired-end reads (at the University of Houston Seq-N-Edit Core]. Breseq, a computational pipeline, was used to align reads to the reference sequence and identify mutations [73]. The whole genome sequencing was carried out by Rachel Staples, a fellow PhD candidate in the Cooper lab.

3.3 Results

3.3.1 Mutations to *lacI* are beneficial in the ancestor

Mutations to *lacI* in the ancestor (REL606) increase relative fitness by 8.31% in lactose (95% CI: 6.50% to 10.1%, 2-tailed t-test: $p < 0.001$). The same mutation is costly in the absence of lactose, as the operon is unnecessarily expressed; there is a -3.83% effect in glucose (95% CI: -6.05% to -1.61%, 2-tailed t-test: $p = 0.07$). In the daily switching evolution environment (G/L), *lacI*– increases relative fitness by 4.05% over two days (95% CI: 2.54% to 5.55%, 2-tailed t-test: $p < 0.01$). These fitness results are similar to previous work in the same strain [238].

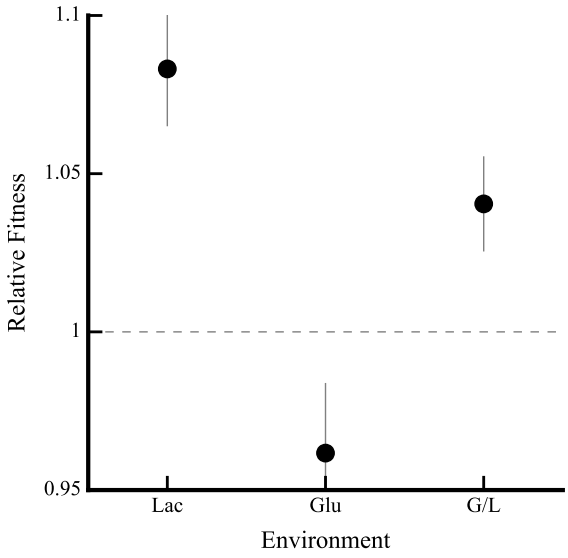

FIGURE 3.2: **Effect of *lacI* mutations on fitness in the ancestor.** Fitness of ancestor *lacI*- mutants in the three evolution environments. Competitions were performed for *lacI*– versus the ancestor (*lacI*+). As a control, I tested the ancestor versus itself (data not shown). The dashed line indicates a relative fitness of 1 (no fitness difference). 95% confidence intervals are shown for each competition ($n \geq 3$).

3.3.2 Simulations predict more *lacI*– substitutions than observed

The frequency of *lacI*– substitution depends not only on its benefit (Fig. 3.2), but also on dynamics with other occurring mutations. Clonal interference and hitchhiking, along with the stochasticity of mutation occurrence makes *lacI*– fixation difficult to predict analytically. Furthermore, it is computationally infeasible to simulate populations at the experimental size ($N_e = 3.3 \times 10^7$). To test the frequency of *lacI*– substitution (f_s) in populations in which other mutations are occurring, I simulated populations at various sizes between $N = 10$ and $N = 1 \times 10^5$, and used f_s at $N = 1 \times 10^5$ as a conservative estimate for $N = 3.3 \times 10^7$. Simulations

predict that 95.1% of populations in *Lac* are expected to fix a *lacI*– mutation. In experimentally *Lac*-evolved populations, only 4/6 (67%) populations fixed *lacI*– (Binomial test: $p = 0.03$). For 2,000-generation fluctuating environments, $f_s = 0.879$. In this environmental regime, 3/12 (25%) populations fixed *lacI*– (Binomial test: $p < 1 \times 10^{-6}$). I did not simulate G/L, as this would require data for the effects of all occurring mutations in both glucose and lactose. If the effect of *lacI*– lies in the right tail of the distribution for G/L, as it does for *Lac*, I expect f_s to be similar between G/L and *Lac*. Five out of six (83%) experimental G/L populations fixed *lacI*– (Binomial test using simulated f_s for *Lac*: $p = 0.26$). This is indeed more similar to *Lac* than to the 2000-generation fluctuating environments. In total, simulations predict *lacI*– to fix in most populations (91.5% overall). However, only 12/24 fixed *lacI*– in the evolution experiment (Binomial test: $p < 1 \times 10^{-6}$).

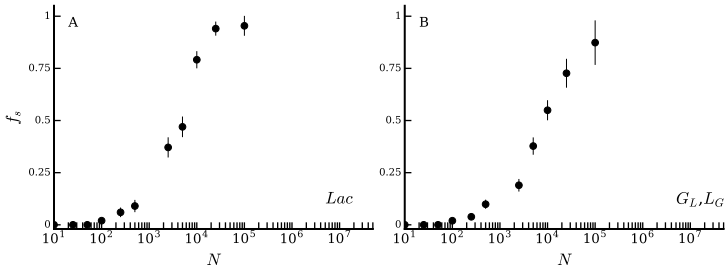

FIGURE 3.3: **Simulated frequency of substitution (f_s) for *lacI*–** in Lactose (A) and 2,000-generation fluctuating environments (B). Points represent the proportion of replicate simulations ($n = 100$) in which *lacI*– fixed. Error bars are one standard deviation. Means and errors were calculated using 1,000 boot-strapped samples. For *Lac* (A), populations were simulated for 8,000 generations. For 2,000-generation fluctuating environments, populations were simulated for 2,000 generations and f_s shown was calculated using Eq. 3.2.

3.3.3 Evolved clones have similar mutation rates to ancestor

The ancestor has a mutation rate of 1.72×10^{-7} (95% CI: 1.01 to 2.43×10^{-7}). This is very similar to foundational *lacI* work by Schaaper and Dunn, which found a rate of 2×10^{-7} (1-sample two-tailed *t*-test: $p = 0.39$) [259]. Note that the per-site rate for *lacI* (1.56×10^{-10}) is near the upper bound of estimated per-site mutation rate for this strain (1.6×10^{-10}) [14]. This is because the *lacI* gene contains a known mutational hot-spot [96].

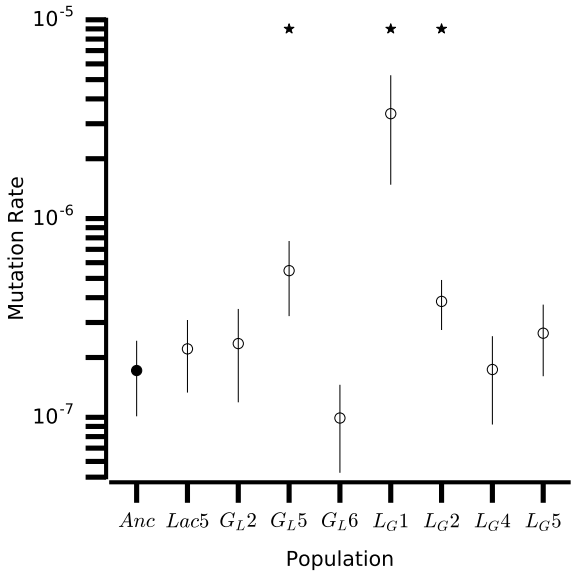

FIGURE 3.4: **Constitutive mutation rate to *lacI* for $8,000$-generation *lacI*+$_{\text{ev}}$ populations.** Open circles are evolved populations and the filled in circle is the mutation rate in the ancestor. Mean per locus mutation rates are calculated from $n >= 10$ replicates, and errors are the 95% confidence interval ($n \geq 10$). Stars are those populations with a significantly different *lacI* constitutive mutation rate, based on a two-tailed *t*-test.

Mutations to *lacI* are expected to have fixed in all populations, given the ancestral mutation rate (Fig. 3.3). If *lacI*+$_{\text{ev}}$ populations evolved lower mutation rates, this could explain the lack of *lacI*–. However, most populations have similar *lacI*– mutation rates compared to the ancestor (5/8). Three out of eight *lacI*+ populations have a significantly different *lacI* mutation rate than the ancestor (Fig. 3.4). All three have an elevated mutation rate, making the fixation of *lacI* more likely. L_G1 is the only population with a >10-fold difference from the ancestral mutation rate. This clone is a known hypermutator, which is the likely cause of the high *lacI* mutation rate observed here. In total, most populations have similar *lacI* mutation rates to the ancestor while a few have higher rates.

3.3.4 Fitness effect of *lacI*– is lower in *lacI*+$_{\text{ev}}$ populations

Epistatic interactions, which create historical contingency, can either increase or decrease the fitness effects of newly occurring mutations, and potentially cause populations to diverge. I measured the fitness effect of *lacI* mutations in 8,000-generation evolved populations. Deviations in fitness effect from the ancestor indicate the existence of epistatic interactions. Given that *lacI*– is beneficial in the ancestor (Fig. 3.2), I hypothesized that *lacI*– mutations exhibit negative epistasis with previous adaptations, lowering the fitness effect and decreasing probability of fixation.

I compared the fitness of *lacI*+ constructs to *lacI*–$_{\text{ev}}$ clones to test the fitness effect of *lacI*– in *lacI*–$_{\text{ev}}$ populations. The fitness benefit of *lacI*– remains beneficial after 8,000-generations in all 12 populations where it fixed (*lacI*–$_{\text{ev}}$). For populations

where fitness was measured in lactose (evolution environments = Lac, G_L, L_G), the grand mean fitness effect of *lacI*– (9.66%) is not significantly different from the effect in the ancestor (8.31%, two-tailed t-test: $p = 0.53$). However, 4/12 populations are themselves significantly different, three of which are higher ($Lac6$,$G/L6$,G_L3) and one is lower ($Lac1$). The only environment that showed a significantly higher *lacI*– fitness than the ancestor was G/L (8.50% vs 4.05%, two-tailed t-test: $p = 0.02$). This increase in fitness effect may be due to the compensation of *lacI*– costs of expression in glucose. The fitness benefit of *lacI*– has decreased in all 8 *lacI*+$_{\text{ev}}$ populations after 8,000-generations (Fig. 3.5). The grand mean fitness of *lacI*– (0.93) is 0.15 lower than *lacI*– in the ancestor (two-tailed t-test: $p < 0.001$). This indicates negative epistatic interactions between *lacI*- and the $8,000$-generation *lacI*+)ev genetic backgrounds. The genetic divergence at *lacI* is contingent on other adaptations, as the fitness effect of *lacI*– becomes costly in *lacI*+$_{\text{ev}}$ populations and remains beneficial in *lacI*+$_{\text{ev}}$ populations.

3.3.5 Long-term environmental fluctuation promotes divergence

Natural environments are unlikely to be constant, but rather change at some frequency [24,53]. Here, fluctuating between glucose and lactose mimics natural environmental changes. I compared the impact of environmental fluctuation (G/L,G_L,L_G) on *lacI* fixation and fitness effect. Briefly, environmental change appears to drive historical contingency by exposing or increasing mutational costs. However, this rate of change must be slow enough to select for adaptations which interact negatively with beneficial mutations in another environment.

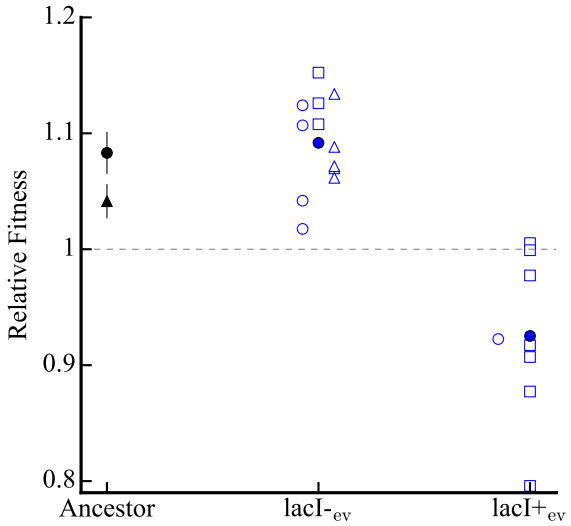

FIGURE 3.5: **Fitness of *lacI*– in 8,000-evolved populations.** Ancestral fitness is in black for *Lac* (circle) and *G*/*L* (triangle). Errors shown are 95% confidence intervals. Blue points are the grand mean for each population subgroup (*lacI*+$_{ev}$ and *lacI*–$_{ev}$) and open shapes are individual populations. Circles represent populations evolved in *Lac*, squares represent populations evolved in G_L or L_G, and triangles are populations evolved in *G*/*L*.

In the long-term fluctuating environment (every 2,000-generations), a *lacI*– mutation was absent in 7 out of 12 populations, and fixed in 3. The ratio of absence to fixation (7/3) is substantially higher than the other two environmental conditions (see below). If *lacI*– did fix (3/12), its fitness effect increased in comparison to the ancestor (mean = 1.13, 2-sample two-tailed *t*-test: $p = 0.03$). Alternatively, for populations in which *lacI*– did not fix (7/12), its fitness effect is significantly lower than the ancestor (mean = 0.93, 1-sample two-tailed *t*-test: p = 0.02). In the daily switching environment (*G*/*L*), populations are exposed to the benefits and costs of *lacI*– in rapid succession. In this environmental regime, *lacI*– fixed in 5 populations

and was absent in none. For the 5 populations that fixed *lacI*–, mean fitness of *lacI*– (1.085) increased compared to the ancestor (2-sample two-tailed *t*-test: p = 0.03).

In the constant lactose environment (*Lac*), cells reap the benefits of constitutive expression without interruption. Mean fitness effect of *lacI*– (1.073) is not significantly different from the ancestor (2-sample two-tailed *t*-test: p = 0.71). This is because fitness effect increased in two populations (*Lac*4, *Lac*6) and decreased in the other two (*Lac*1, *Lac*3). Interestingly, one population entirely lacked *lacI*– individuals. This is surprising given that this environment never exposes costs of constitutive expression. The fitness effect of *lacI*– in this population (*Lac*5) decreased to -0.01% (SD: 0.02) within the first 500 generations of evolution (Fig. 3.6).

3.3.6 Identifying a candidate negative epistatic interaction

In the only $8,000$-generation lactose-evolved *lacI*+$_{\text{ev}}$ population (*Lac*5), the effect of *lacI*– rapidly declined within the first 500 generations (Fig 3.6). I sequenced 4 clones from this *lacI*+$_{\text{ev}}$ population to elucidate the nature of this negative epistatic interaction. All four clones shared the same mutation, while 3/4 were mutated at another common site (Table. 3.2). All four selected clones contained a 3 base-pair insertion in the intergenic region ($\leftarrow$ *I* $\rightarrow$) between *yhiO* and *uspA*, which is a universal stress global response regulator. Previous work in this strain found a similar mutation at this site [304]. Three out of four clones have a large deletion of the *rbs* operon, which confers the ability to catabolize ribose. A *rbs* deletion also occurred in long-term evolved *E. coli* in glucose only medium [55, 154].

Gene	Clone 1	Clone 2	Clone 3	Clone 4
$yhiO \leftarrow I \rightarrow uspA$	$+3bp$	$+3bp$	$+3bp$	$+3bp$
Δrbs		$\Delta 5,943bp$	$\Delta 7,590bp$	$\Delta 7,590bp$

TABLE 3.2: **Shared mutations in** 500**-generation clones of the** *Lac*5 **population.**

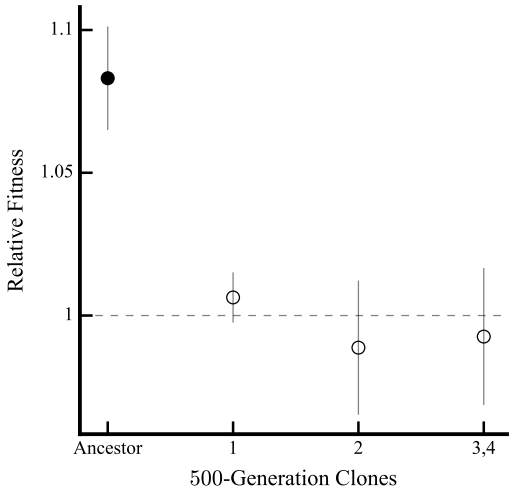

FIGURE 3.6: **Fitness effect of *lacI*– in sequenced** 500**-generation** *Lac*5 **clones.** The black point is effect in the ancestor, and blue points are the effect in evolved clones. The dashed line shows a relative fitness of 1. All unique genotypes have a significantly lower *lacI*– effect.

Both of these mutations are indeed present in 4,000- and 8,000-generation clones (previously sequenced [334]), indicating that sequenced clones are representative of the long-term evolutionary path of this population. However, $yhiO \leftarrow I \rightarrow uspA$ is present only in $lacI{+}_{\text{ev}}$ *Lac*-evolved populations (*Lac*2 = mixed, *Lac*5 = $lacI{+}_{\text{ev}}$), one of which is the population of interest here. In contrast, Δrbs is present in all six evolved populations, including both $lacI{+}_{\text{ev}}$ and $lacI{-}_{\text{ev}}$. As such, $yhiO \leftarrow I \rightarrow uspA$ is a candidate mutation for the negative epistatic interaction with *lacI*. Future

work will test this relationship directly through genetic constructions.

3.4 Discussion

Epistasis can cause the fitness effects of arising mutations to be contingent on prior substitutions. These historical contingencies can change available fitness peaks and thus result in divergent evolution. The degree to which epistasis and contingency shape evolution remain unclear. Large scale landscape reconstructions are ideal for understanding the principles governing adaptation on the fitness landscape. Some recent studies have constructed large numbers of constructs for single genes [82,248]. However, large inter-gene constructions remain technically infeasible (32,768 constructions required for 15 mutations), thus case studies are our best path forward.

In the ancestor of a long-term evolution experiment with *E. coli*, mutations to the *lac* operon repressor, *lacI*, causing constitutive expression, increase fitness. Evolutionary simulations predict that $\sim 90\%$ of 8,000-generation evolved populations are expected to have fixed a *lacI*– mutation. Yet, only 50% of evolved populations are *lacI*-$_{\text{ev}}$, suggesting the presence of historical contingency. To test the null expectation of fixation probability I used individual based simulations. Even a significantly lower population size (1×10^5) than the true effective population size (3.3×10^7) resulted in nearly all replicates (95.1%) fixing a *lacI*- mutation. Given this finding, I then tested the if evolved populations lacked *lacI*- due to a lower

evolved mutation rates to *lacI*. Most populations did not have a significantly different mutation rate than the ancestor after 8,000-generations of evolution. In fact, there were a few populations with a higher mutation rate, which may cause even faster fixation of *lacI*-.

An alternative hypothesis is that the effect of *lacI*- on fitness has changed during evolution, due to other fixed mutations in the genetic background. I tested this hypothesis by creating *lacI*- mutants of the *lacI*+$_{\text{ev}}$ clones and conducting fitness competitions. I found that the fitness effect of *lacI*- mutations has become neutral or deleterious in all *lacI*-$_{\text{ev}}$ populations at 8,000-generations. This is strong evidence that negative epistasis with the genetic background prevented the fixation of *lacI*-. For one population in particular (*Lac*5), the fitness effect of *lacI*- decreased rapidly within the first 500 generations of evolution. I sequenced four clones from this population to identify a candidate negative epistatic interaction. There were only two mutated sites common among the clones. One of these sites was also mutated in most *lacI*-$_{\text{ev}}$ clones. As such, I hypothesized that the alternate mutation (*yhiO* $\leftarrow$ *I* $\rightarrow$ *uspA*) interacts negatively with *lacI*-. Future work will confirm this hypothesis.

This example of historical contingency is due to the stochastic occurrences of alternative adaptive mutations. It is important to note that the occurrence of such mutations is environmentally dependent. It is plausible that historical contingency may be dependent on the environmental regime. In fact, 2,000-generation switching environments in this experiment have the highest frequency of *lacI*+$_{\text{ev}}$ populations. This suggests that mutations that are adaptive in glucose may interact

negatively with the *lacI-* mutation, which is beneficial in lactose. Another interesting implication of this work is that it is evidence against the 'use it or lose it' theory of gene regulation control [258]. The theory states that regulatory systems controlling genes that are not needed should act as negative regulators. This is because the loss of regulation will provide a selective disadvantage (unnecessary gene expression). For example, *lacI* regulates *lac* operon expression. However, lactose is perhaps not often present in the *E. coli* natural environment. As such, it may be advantageous to negatively regulate, so that loss of regulation is selected against. If such an uncommonly used operon was positively regulated, the loss of regulation during absence of the inducer may go unnoticed. Yet, when the organism required the operon products it would not be able to positively induce. The loss of *lacI-* in an artificial, high demand environment is consistent with this idea. Here I observed such loss in only 50% of evolved populations. It is then interesting that there appears to be an alternative path to negative regulator loss. In Chapter 4, I further explore this study to determine if the maintenance of *lacI-* is indeed an 'equivalent alternative' adaptive path to loss of regulation.

Chapter 4

Alternate genotypic solutions cause divergent evolution in *E. coli*

4.1 Introduction

Interactions with the genetic background can alter mutation effects [187, 198, 237, 249]. For example, a mutation may be beneficial in one genetic background and costly in another. This epistasis, a statistical deviation from a null model (here multiplicative) in the fitness effects of genes, is implicated in many parts of evolutionary biology. For example, metabolic networks contain inherent negative epistasis due to the relationship between enzyme activity and fitness, which is linear at first but levels off as activity increases [17, 84, 142, 149, 151, 294]. Starting from low flux, the first mutation has a large effect, while a second mutation causing the same change in flux has a smaller fitness effect. At a larger scale, epistasis can lead to speciation. An allele that fixes in one population may interact negatively with an

allele at a different locus in a diverging population [81, 206]. These Dobzhansky-Muller Incompatibilities (DMIs) have been found in both theoretical models [144] and laboratory experiments [168, 205, 313]. Despite the complicated physiological nature of epistasis, recent studies point to general trends that may help predict mutation fitness effects [49, 154, 164].

One useful categorization of epistasis is the distinction between local and global interactions [164]. Local interactions are those that depend on specific genetic background. For example, a mutation which enabled citrate metabolism in *E. coli* became beneficial only after a previous mutation increased the activity of the citrate synthase enzyme [30, 31, 239]. Local interactions certainly play a role in evolution [37, 319], however recent work suggests that global interactions also play a key role [164]. Global interactions are those that depend on general characteristics of the background, such as fitness. Several studies have found a significant portion of the variation in the effect of mutations on fitness can be explained by the fitness of the background [49, 154, 164, 319]. This effect, known as diminishing returns epistasis, where mutations confer less benefit as background fitness increases, also explains the trajectories of experimentally evolved populations [330].

Global epistasis may be mediated by common cell-wide physiological processes [164]. In principle "variation anywhere in the genome affects every character" [142]. While this is not completely true [2, 153, 331], all gene expression does draw from the same pool of cellular resources. Gene expression requires a significant amount of a cell's energy and nutrients [35] and occupies shared cellular machineries such as polymerases and ribosomes. As such, the efficiency of gene expression

is directly linked to growth rate and fitness [143].

Studies in *E. coli* have typically found that the cost of gene expression is primarily incurred during translation [4,89,191,268,269,306] (but see [85]). The availability of ribosomes (i.e., translational capacity), which translate mRNA to proteins, is a primary cause of this expression cost [54,255,306]. Ribosomes are a growth-limiting factor for rapidly growing bacteria [75,89,158,191,252,267,269,306]. The use of ribosomes in translating unnecessary proteins confers a cost by reducing the capacity to translate necessary proteins that do contribute to growth. For example, unnecessary expression of the *lac* operon, in the absence of lactose, can reduce cell growth [74,83,85,138,209,212,212,269] (Fig 4.4).

Here I investigate the basis of changes in the fitness effect of a constitutive expression mutant (*lacI-*) in the *lac* operon. After a long-term evolution experiment (8,000-generations), replicate populations of *E. coli* show divergence in the *lacI* gene. This divergence is due to epistasis with other substitutions, which caused *lacI-* to become neutral or costly in populations that did not fix a *lacI-* mutation (*lacI*+$_{ev}$) (Chapter 3).

In this chapter, I examine various global phenotypes to better understand the mechanism of epistasis. I find that *lacI-* mutations no longer provide the same growth benefit in *lacI*+$_{ev}$ strains as they do in the ancestor. This cannot be explained by a greater cost of *lac* expression, as costs have decreased in *lacI*+$_{ev}$ strains. To understand why cost of expression has decreased, despite higher maximum expression, I tested for a change in the translational capacity of *lacI*+$_{ev}$ strains. A selected *lacI*+$_{ev}$ strain has a higher translational capacity than the ancestor, likely

due to mutations in the *spoT* gene. The decrease in cost of expression indicates that the benefit of *lac* expression has also decreased, resulting in a net neutral or deleterious fitness effect (Chapter 3). The *lac* operon in *lacI*+$_{ev}$ populations is more sensitive to induction, indicating that these populations may be able to express *lac* proteins more quickly in lactose. This may cause the observed lack of *lacI*- growth curve benefit. I find that *lacI*+$_{ev}$ populations and *lacI*-$_{ev}$ populations have similar evolved fitness, which is consistent with the hypothesis that *lacI*+$_{ev}$ strains substituted an equivalent alternative to *lacI*-. In total, the decrease in fitness effect of *lacI*- mutations in *lacI*+$_{ev}$ populations appears to be a result of alternate mutations that provide a similar benefit and render the benefits of *lacI*- obsolete.

4.2 Materials and Methods

4.2.1 Bacterial Strains and Growth Conditions

Bacterial clones used for this experiment were selected from populations in a long-term evolution experiment in 7 environments (4/7 used here) [53]. Strains that fixed a *lacI*- mutation are denoted as *lacI*$-_{\text{ev}}$ and those that maintained the ancestral allele are *lacI*$+_{\text{ev}}$. Media used are identical to those described in Chapter 3 (details in 3.2.1). One addition is the use of glycerol as a growth medium. Here I use a DM + 0.2% glycerol environment to measure costs of expression.

4.2.2 Growth Curves

Measurement: For a given clone, growth curves were collected as follows. The clone was first inoculated from a freezer stock into 1 mL of LB media and grown overnight. The following day, cells were preconditioned to the desired growth media (DM supplemented with glycerol, lactose, or glucose) by transferring 1 μL into 1mL of said growth media and incubated at 37 °C for 24 hours. On day three, 2 μL of the preconditioned culture was transferred into 198 μL of the same media in a 96-well polystyrene plate. This plate was incubated in the microplate reader (VersaMax) and grown at 37 °C until cells reached stationary phase. The culture's optical density at 450nm (OD_{450}) was measured every 5 minutes during growth.

Analysis. Growth curves were analyzed using an extension of the standard logistic model, as presented by Baranyi and Roberts [10, 11, 241]. The model is

defined as the differential equation

$$\frac{dN}{dt} = r\alpha(t)N\left(1 - \left(\frac{N}{K}\right)^{v}\right) \tag{4.1}$$

where N is optical density, r is growth rate, t is time, K is the maximum density, v is the deceleration parameter, and $\alpha(t)$ is an adjustment function which determines lag phase time.

Parameter	Biological Meaning
N_0	Initial OD
K	Final OD
r	Growth Rate
q_0	Initial state of population
m	Rate of sugar accumulation in cell
v	Deceleration of growth

TABLE 4.1: **Parameters of the Growth Curve Model.**

The adjustment function

$$\alpha(t) = \frac{q_0}{q_0 + e^{-mt}} \tag{4.2}$$

accounts for the adjustment period of a population to new growth conditions after a transfer to new media. After 24 hours of preconditioning, cultures are in the stationary phase of the growth cycle and thus do not immediately begin growth when transferred to fresh media. This equation is useful as it is biologically derived [11, 241]. The variable q_0 denotes the starting amount of a given molecule (e.g., lactose) necessary for growth. The variable m is the rate of accumulation of

that molecule in the cell. Here I set $m = r$ in order to achieve more stable model fitting [10]. This simplification is biologically reasonable, as the growth rate is likely determined by the rate of nutrient accumulation in the cell.

The single-strain Baranyi-Roberts equation (Eq. 4.1) has a closed analytical solution

$$N(t) = \frac{K}{\left(1 - \left(1 - \left(\frac{K}{N_0}\right)^{v}\right) e^{-rvA(t)}\right)^{\frac{1}{v}}} \tag{4.3}$$

$$A(t) = \int_0^t \alpha(s)\, ds = t + \frac{1}{m} \ln \frac{e^{-mt} + q_0}{1 + q_0} \tag{4.4}$$

where A(t) is the adjustment equation.

4.2.3 Measuring Expression

The *lac* operon can be induced both naturally and artificially. Here I employ both methods, as noted in the text. Natural induction occurs in a lactose-containing media. The LacZ protein acts on lactose to produce the isomer allolactose, which binds to *lacI* and stops repression. Artificial induction can be used to regulate the level of expression. Here I use it primarily to measure the induction-response of the *lac* operon. Isopropyl-β-D-thiogalactoside (IPTG) is a molecular analog of allolactose, and thus induces the *lac* operon. However, IPTG is not hydrolyzable by LacZ and thus confers no fitness benefit and remains at a constant concentration throughout the experiment.

Promoter Activity. The use of promoter activity as a measure of expression is motivated by cell growth diluting effects on LacZ. The activity of LacZ is stable during exponential growth, such that changes in activity level are primarily due to the diluting effect of growth [165]. Fitter cells (faster growth) may then appear to have lower expression levels, if only the standard Miller assay is used, due to dilution of LacZ. Following Kuhlman et al. (2007), I calculate promoter activity (α) as

$$\alpha = MU \times d_t \tag{4.5}$$

where MU stands for Miller units (4.2.3) and d_t is the rate of cell-doubling (hr^{-1}). The units of α are thus MU/hr.

LacZ Measurement and Calculation. I measured the activity of LacZ (in Miller Units) by measuring the amount of β-galactosidase protein (*lacZ* product). This is done by using a lactose analog (ONPG), which creates a yellow color after cleavage by LacZ. The solution absorbance is then used to calculate β-galactosidase content. I used the same inoculation and precondition described in Section 4.2.2. Following preconditioning, 2 μL culture was added to 200 μL fresh DM + 0.2% glycerol, with a concentration of IPTG as noted in the text. Cells were grown in a spectrophotometer at 37°C until mid-log phase ($0.15 < OD_{450} < 0.2$, typically 3-5 hours). At this point, cells were lysed by adding 4 μL SDS (0.1%) followed by 8 μL chloroform. The plate was immediately shaken for 1-2 minutes as solutions for the next step were prepared (this minimizes the effect of the chloroform

on the polystyrene plate). Thirty μL of the sample was transferred to a new 96-well polystyrene plate and 120μL of Z-buffer was added. The solution was mixed using a pipette, and 30μL of o-nitrophenyl β-D-galactosidase (ONPG) (4 mg/mL) was added. The plate was shaken for 30 seconds, before placing in the spectrophotometer. Absorbance (A) was then measured at 405nm (A_{405}) and 490nm (A_{490}) every 45 seconds for 15 minutes. The activity of *lacZ* was then calculated as described below.

First, the background reading of control wells (those with only Z-buffer and ONPG) was subtracted from all experimental replicates for both A_{405} and A_{490}. Next, β-galactosidase content was calculated as

$$\frac{(A_{405} - r) \times A_{490}}{OD_{450} \times v} \tag{4.6}$$

where OD_{450} is the cell culture density measured directly prior to the assay and v is the volume of cell culture (in mL) used (here $v = 0.2$ for all assays). The ratio of cell absorbency (r) at 405nm to 490nm is $r = 0.8$ [273].

Cell-Doubling Rate. The LacZ activity assays described above were conducted during exponential growth. To determine the rate of growth, cells were monitored using a spectrophotometer until they grew exponentially. The doubling time was calculated using the OD_{450} from the 10 minutes of growth immediately prior to removing cells for the assay. Doubling time is then calculated as

$$d_t = \log_2 \left(\frac{OD2}{OD1} \right) / \left(\frac{10}{60} \right) \tag{4.7}$$

where $OD2$ is the OD_{450} at time of removal and $OD1$ is the OD_{450} from 10 minutes prior.

Model Fitting. I fit a modified Hill function to IPTG induction-response data data to quantify various features of promoter activity (Table 4.2) [165].

Parameter	Meaning
b (MU/hr)	Basal expression
f	Fold-change
c (μM)	Dissociation constant
m	Hill coefficient

TABLE 4.2: **Parameters and Meaning for the Hill function (Eq. 4.8)**.

$$\alpha = b \times \frac{1 + f\frac{[IPTG]}{c}^m}{1 + \frac{[IPTG]}{c}^m} \tag{4.8}$$

4.2.4 Costs of Expression

Virtual Competitions.

Costs of expression are measured in a 0.2% glycerol environment, such that expression does not confer any benefits. It is not possible to compete strains at different expression levels (i.e., different concentrations of IPTG) in a standard fitness assay due to the shared environment. Here I use simulated competitions to estimate relative costs of expression between different expression levels.

I implement a double-strain Baranyi-Roberts [11, 241] to simulate fitness competitions. I first measure growth curves under two different IPTG concentrations and fit those curves using the single-strain model (Eqs. 4.1, 4.3). These parameters

are then used in the double-strain model to conduct a virtual competition. The model is

$$\begin{aligned}
\frac{dN_1}{dt} &= r_1\alpha_1(t)N_1(1-(\frac{N_1}{K_1}^{v_1})-(\frac{N_2}{K_2}^{v_2})) \\
\frac{dN_2}{dt} &= r_2\alpha_2(t)N_2(1-(\frac{N_1}{K_1}^{v_1})-(\frac{N_2}{K_2}^{v_2})) \\
\alpha_i(t) &= \frac{q_{0,i}}{q_{0,i}+e^{(}-m_it)}
\end{aligned} \tag{4.9}$$

such that i denotes the parameter for a given strain. Critical assumptions of this model are that the strains occupy independent niches, and all competition occurs only through resource competition [241]. Costs of expression have previously been measured as change in maximum growth rate [74, 85]. However, this measure does not consider all phases of bacterial growth (lag, log, stationary). Moreover, costs can also change throughout the growth cycle [274]. Here I measure cost as a decrease in relative fitness (i.e., selection coefficient) over the entire growth cycle.

4.2.5 Translational Capacity

I calculate translational capacity (K_t) by measuring growth rate, and RNA and protein levels in environments with varying nutritional quality. This is similar to the approach used by Scott et al. (2010) [269]. I grow cells in multiple concentrations of lactose (70 μM, 140 μM, 210 μM, 280 μM). These concentrations result in multiple data points (r, λ), to which I use non-linear least-squares fitting to determine r_0 and K_t (Eq. 4.13). I use this approach to compare the translational capacity of an evolved clone to the ancestor.

RNA Extraction.

Following overnight growth in LB, cells were transferred to the desired media for a preconditioning period of 24 hours. On day three, the assay was done using 1 mL of exponentially growing culture (this same sample was used for protein extraction). I first added 2 mL of RNAprotect Bacteria Reagent into the sample, to ensure RNA stabilization prior to purification. The sample was then pelleted and resuspended with 20 μL Qiagen Proteinase K and 200 μL of TE buffer. Following 10 minutes of room temperature incubation, 350 μL of Buffer RLT and 250 μL of 100% ethanol were added to the tube and mixed by vortexing. I then followed the exact protocol from the RNeasy Mini Kit (Qiagen: 74104) and measured RNA amount using a NanoDrop spectrophotometer.

Protein Extraction.

Following overnight growth in LB, cells were transfered to the desired concentration of lactose media for a precondition period of 24 hours. On day three, the assay was done with 1mL of exponentially growing culture (from the same culture as used for RNA extraction). Total protein content was measured with the Total Protein Kit (Sigma, TP0300) using the micro Lowry method (Peterson's modification). Bovine serum albumin (BSA) was used to calculate the standard curve. Cell culture and standard tubes were diluted to 1 mL in micro-centrifuge tubes. 100 μl of deoxycholate (0.15%) and 100 μl trichloroacetic acid (TCA, 72%) were added to each tube. After incubating at room temperature for 10 minutes, the samples were centrifuged at maximum speed. Supernatant was removed such that only

the protein pellet remained in the tube. This pellet was resuspended in 1mL of 50% Lowry Reagent (in water). After a 20 minute room-temperature incubation, 0.5mL of Folin and Ciocalteu's Phenol Reagent was added. The blue color was allowed to develop for 30 minutes. The OD_{750} was measured in comparison to the blank using a standard cuvette spectrophotometer. The BSA standard curve was then used to calculate the amount of protein in each experimental sample.

4.3 Results

4.3.1 *lacI-* mutations lack growth curve benefits in *lacI+*$_{ev}$

The fitness effect of *lacI-* mutations became neutral or costly in all *lacI+*$_{ev}$ populations (Chapter 3). To determine the basis of this change in effect, I first compared the growth curves, in lactose, of *lacI+*$_{ev}$ clones to their *lacI-* mutants (Fig. 4.2). Previously fixed mutations in these strains may modify *lacI-* fitness effect through effects on growth dynamics.

I found a significant difference in final density, with the ancestor reaching a slightly higher OD_{450} (Table 4.3). This alone suggests that the ancestor has a higher fitness, however mixed culture competition between strains depends on additional factors (Fig. 4.1). Cells that constitutively express the *lac* operon are not hindered by expression regulation which occurs in the ancestor. The time required to adjust to new growth conditions (lag phase) strongly affects competition results. A slower growing strain with a shorter lag phase may out-compete a faster growing strain

with a longer lag phase. Here, the parameter q_0 characterizes the initial physiological state of the population. Because both the ancestor and its *lacI-* mutants were preconditioned in lactose media, I expected no difference in this parameter. However, *lacI-* mutants have $q_0 = 0.0088$, more than two-fold higher than the ancestor ($q_0 = 0.0038$). Mutations to *lacI-* in the ancestor also increase the growth rate (r), from 0.85 to 0.89. The lack of expression regulation likely contributes to both of these parameter differences. The only parameter with a non-significant difference between the ancestor and *lacI-* is growth deceleration (v). In total, *lacI-* mutations in the ancestor have a significant effect on growth dynamics, with the largest effect on q_0 and r/m.

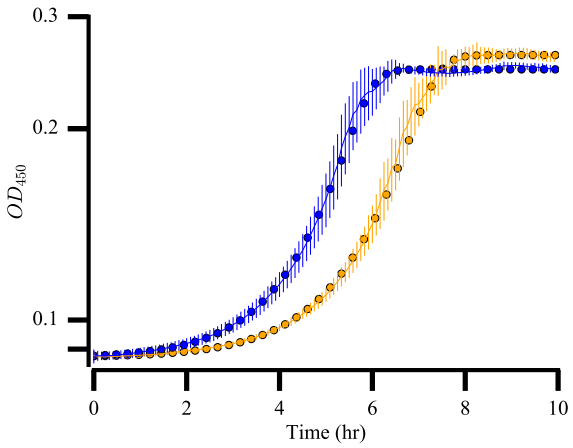

FIGURE 4.1: **Growth curves of the ancestor and *lacI-* mutant**. The ancestor is in orange and the *lacI-* mutant in blue. Mean OD_{450} is plotted as a line, with shaded region representing the 95% confidence interval. Points shown are model fits, whose parameters are in Table 4.3.

Previous work using these populations has found that mutations in the *lac* operon increase fitness by decreasing time in lag phase [238]. The adjustment

Parameter	Ancestor (*lacI*+)	Ancestor Mutant (*lacI*-)
$N0$	0.088 (0.00015)	0.088 (0.00005) *
K	0.26 (0.0002)	0.25 (0.0003) *
r	0.85 (0.008)	0.91 (0.02) *
q_0	0.0038 (0.0002)	0.0086 (0.0009) *
m	0.85 (0.008)	0.89 (0.0009) *
v	8.2 (0.86)	8.6 (1.8)

TABLE 4.3: **Fitted growth curve model parameters for ancestor and *lacI*- mutant.** Parameters were calculated by bootstrapping the data 1,000 times, and fitting Equation 4.3 using a non-linear least-squares approach. Shown are the mean bootstrapped fits with one standard deviation in parentheses. Stars indicate $p < 0.05$ under a two-tailed t-test. Parameters $N0$, K, r are all significantly different between the ancestor and *lacI*- mutant. Only v is not different.

function controls the acceleration of growth. I estimated when the acceleration of growth exceeds linear by solving

$$\frac{t}{24} = \frac{q_0}{q_0 + (e^{-m*t}])} \tag{4.10}$$

for t, using the fitted parameters q_0 and m. This approach is consistent with the expectation that lag time approaches zero as $1/m$ increases [241]. In lactose, the ancestor spends 4.98 hours in lag phase, while the *lacI*- mutants exit lag phase after only 3.23 hours. This decrease in lag time is due to a more 'ready' initial state (q_0) and a faster rate of lactose accumulation in the cell (m) (Table 4.3, Eq 4.10).

On average, *lacI*+$_{\text{ev}}$ clones grow at rate $r = 1.17$. In the ancestor, constitutive expression increases the growth rate. However, introducing *lacI*- into these evolved clones causes growth rate to decrease by -0.16 (SD: 0.09) to an average of $r = 1.01$.

Population	*lacI*+$_{ev}$	Mutants (*lacI*-)
*Lac*5	0.74 (0.02)	1.86 (0.01)*
G_L2	0.95 (0.01)	1.68 (0.21)*
G_L5	1.16 (0.02)	1.73 (0.02)*
G_L6	0.86 (0.01)	1.22 (0.02)*
L_G1	0.83 (0.01)	1.99 (0.02)*
L_G2	0.70 (0.01)	1.37 (0.02)*
L_G4	1.41 (0.02)	2.04 (0.01)*
L_G5	1.83 (0.02)	1.75 (0.02)*

TABLE 4.4: **Lag times (in hours) for *lacI*+$_{ev}$ and their *lacI*- mutants.** Calculated by bootstrapping data $1,000$ times and using Eq. 4.10 for model fits. Stars indicate $p < 0.05$ under a two-tailed *t*-test.

In this model, growth rate (r) and rate of cellular lactose accumulation (m) are equal. This implies that constitutive expression in *lacI*+$_{ev}$ clones cause lactose to be imported more slowly. *lacI*+$_{ev}$ clones have a more prepared physiological state ($q_0 = 0.012$) than the ancestor and its *lacI*- mutant. Mutations to *lacI* in *lacI*+$_{ev}$ clones cause little change in q_0; *lacI*- constructs have $q_0 = 0.013$ on average, which represents a 0.001 change (SD: 0.003) from the evolved clones. The primary benefit of *lacI*- in the ancestor is a shorter lag phase [238]. On average, *lacI*+$_{ev}$ clones exit lag phase after 1.06 hours. Selected *lacI*- mutants no longer provide the benefit of shorter lag time as seen in the ancestor (Fig. 4.2). In fact, *lacI*- mutants in *lacI*+$_{ev}$ populations have a longer lag time (mean: 1.70 hours). Constitutive expression causes lag time to increase by 0.64 hours on average (SD: 0.40 hours, Paired *t*-test: $p < 0.01$).

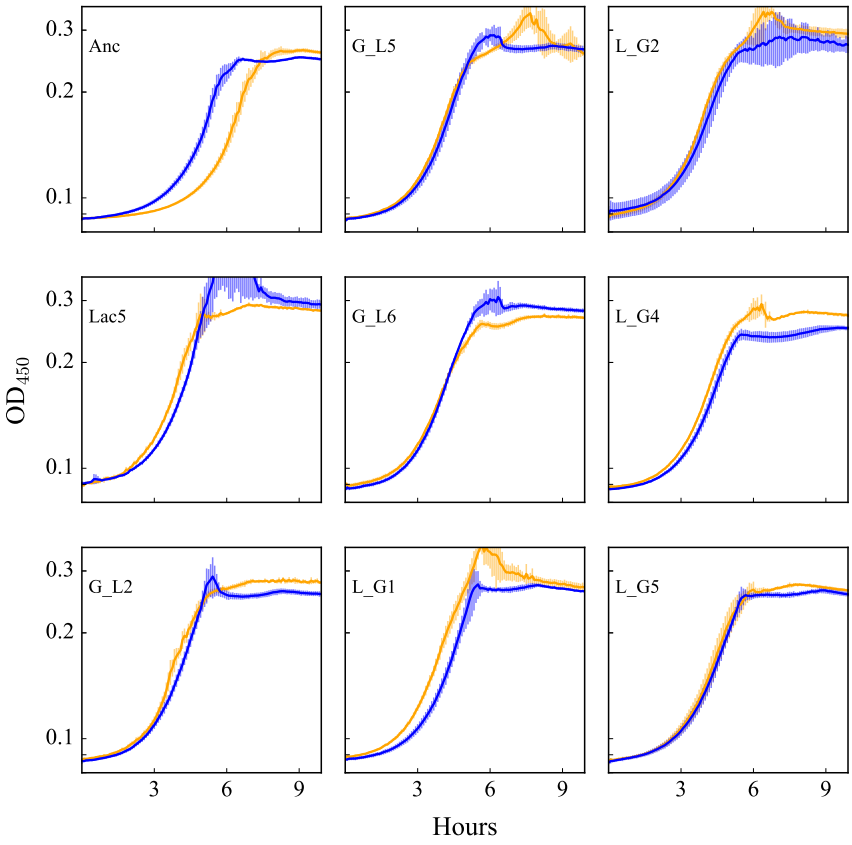

FIGURE 4.2: **Growth curves for *lacI*+$_{ev}$ clones and their *lacI*- mutants.** *lacI*+$_{ev}$ are shown in orange, with *lacI*- mutants in blue. Lines are the mean, with shaded regions as the 95% confidence interval.

4.3.2 The cost of expression is lower in *lacI*+$_{ev}$

Expression of the *lac* operon confers both a growth cost and a potential growth benefit. The benefit occurs only in the presence of lactose, as expressed *lac* proteins allow cells to metabolize lactose. The cost occurs from expression and activity of gene products [74, 85, 291], and is independent of lactose. Changes in cost, benefit, or both, may drive the observed changes in growth (Fig. 4.2) and fitness effect

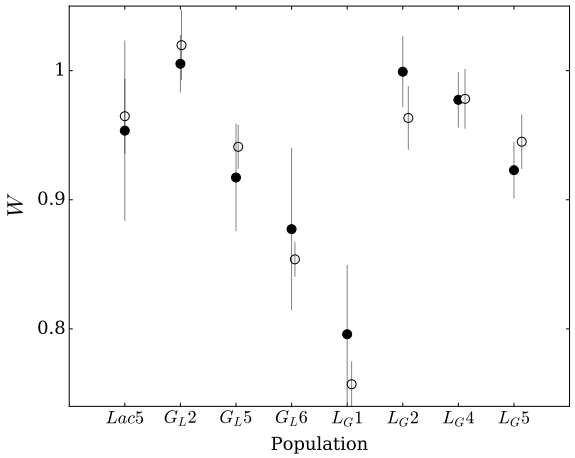

FIGURE 4.3: **Virtual competitions predict a similar *lacI-* fitness effect to measurements in lactose for *lacI*+$_{ev}$ strains.** Filled circles show experimental measured fitness effect of mutating *lacI*+$_{ev}$ strains to *lacI-*. Open circles show predicted fitness of *lacI-* vs *lacI*+$_{ev}$ based on independent growth curves in lactose. Errors are the 95% confidence intervals for both sets of points. Note that due to noise in the growth curve data, model fitting was unstable and some virtual competitions resulted in no growth (or even a decrease in OD) for one strain. I excluded such outliers from the virtual competition predictions.

(Chapter 3). I first tested if the relationship between *lac* expression and cost has changed from the ancestor to *lacI*+$_{ev}$ clones, using a virtual competition approach (Fig. 4.4) [11, 11, 241].

In the ancestor, the relative fitness cost of the *lac* operon increases with expression. Cost (C) increases quickly at first, and then more slowly as relative expression reaches a maximum ($L = 1$, Fig. 4.5). This relationship is in contrast to early work on the expression cost of the *lac* operon [74], but is consistent with a recent study that found the cost of *lac* expression to be the *lac* permease [85]. The relationship

between L and C can be fit using a logarithmic function of form

$$C = a \times \ln L + b \tag{4.11}$$

where a affects the curvature (lower a = faster plateau) and b the maximum (expression at $L = 1$) of the function respectively. For the ancestor, best fit parameters are $a = 0.13$ (SD: 0.01) and $b = 0.87$ (SD: 0.03). Measured over an entire growth cycle, maximum expression ($L = 1$) incurs a relative fitness cost of 0.95. This large cost is due to a later exit from lag phase and a slower growth rate (Fig. 4.4).

For most *lacI*+$_{\text{ev}}$ populations, the shape of the expression-cost curve is also well fit by the logarithmic function. However, compared to the ancestor, cost plateaus more rapidly on average ($a = 0.06$, 2-tailed Welch's t-test: $p < 1 \times 10^{-4}$) and reaches a lower maximum than in the ancestor ($b = 0.44$, 2-tailed Welch's t-test: $p < 0.005$). There is an average difference of 0.53 between the cost at $L = 1$ in the ancestor (0.95) and *lacI*+$_{\text{ev}}$ clones (0.42). Given that the fitness conferred by the *lacI*- mutation has decreased in *lacI*+$_{\text{ev}}$ populations (Chapter 3), it is somewhat surprising that the cost of expression has decreased in these clones. This decrease become more striking when expression is scaled to the ancestor maximum. Evolved populations not only have a lower cost of expression, but also have higher maximum expression capacity (Fig. 4.5).

There is one exception to the ln-relationship between expression and cost. This is the *Lac*5 population, where cost increases exponentially with expression. For this population, I find that the relationship fits a polynomial function proposed by

Dekel & Alon (2005)

$$C = n0 \times L + n0' \times L^2 \tag{4.12}$$

with parameters $n0 = 0.003$ and $n0' = 0.08$. This difference in the cost function is interesting, considering that this is also the only population that had a drastic decrease in *lacI-* effect within the first 500 generations of evolution (Chapter 3). In Chapter 3 I identified two candidate mutations for a negative interaction with *lacI-* in this population. Future work will determine if this change in the expression-cost curve may be due to the same interaction.

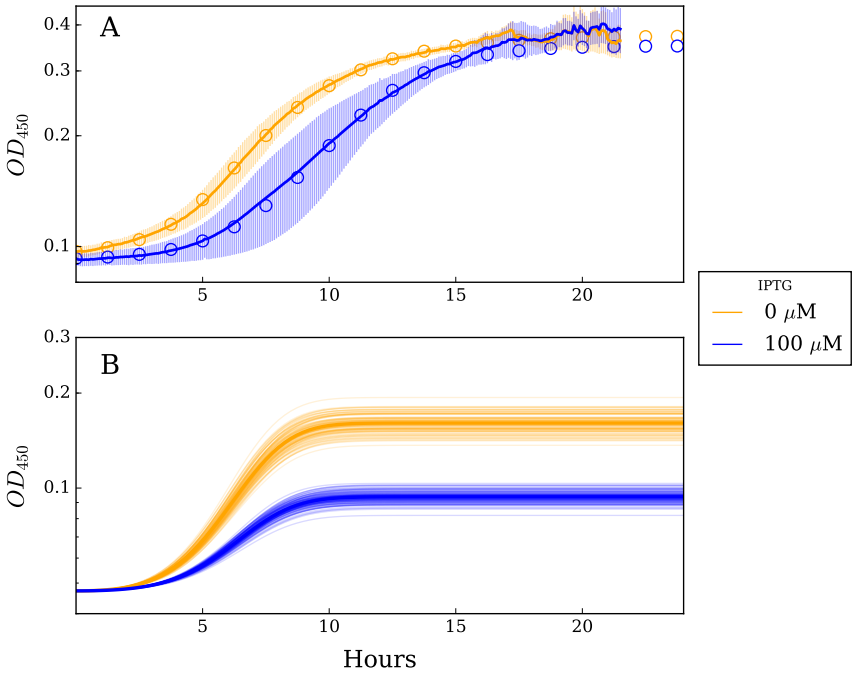

FIGURE 4.4: **Growth curves, model fit, and virtual competition for the ancestor in glycerol.** A) Growth curves for the ancestor with 0 μM (orange) and 100 μM IPTG (blue). Lines are the mean, with shaded regions as the standard deviation. Plotted points are model fits. B) One-hundred independent virtual competitions between each growth curve in panel A. Growth in competition is shown by orange (0 μM) and blue (100 μM) lines. Fitness is calculated using the same equation as experiments (3.2.6).

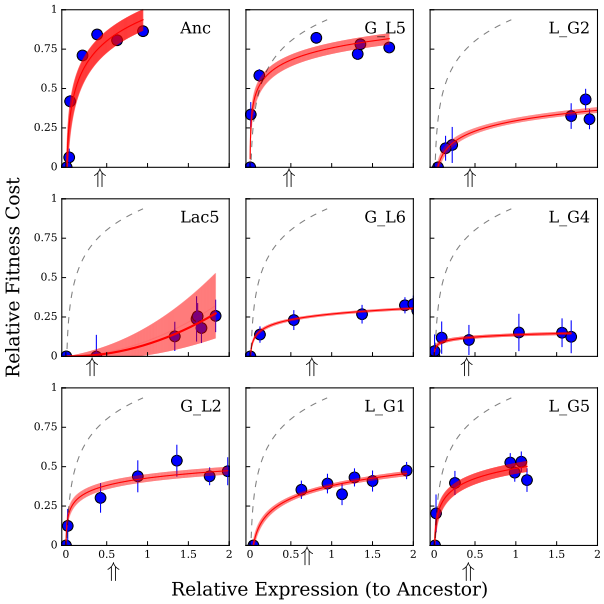

FIGURE 4.5: **Cost-expression curves for the ancestor and *lacI*+$_{ev}$ populations.** Blue points are calculated from independent growth curves and a virtual competition between model fits. Expression is scaled to the ancestor. Error bars are standard errors. The red line is the best fit logarithmic function, with shaded region representing the 95% confidence interval. For comparison, the ancestor best fit function is plotted as a grey dashed line on each panel. Arrows under the x-axis show the evolved expression level in *Lac* (Fig. 4.6)

4.3.3 *lacI*+$_{ev}$ *lac* expression is similar to the ancestor in evolution environments

Higher levels of maximum expression (Fig. 4.5) in *lacI*+$_{ev}$ strains may be a result of regulatory changes. I measured natural expression in *Lac* and *Glu* to test if *lacI*+$_{ev}$ clones have evolved different levels of expression in the evolution environments

Population	a	b
Ancestor	0.13	0.87
G_L2	0.05*	0.48*
G_L5	0.08*	0.82
G_L6	0.04*	0.30*
L_G1	0.08*	0.45*
L_G2	0.06*	0.36*
L_G4	0.02*	0.15*
L_G5	0.07*	0.54*
lacI+$_{\text{ev}}$ Average	0.06*	0.44*

TABLE 4.5: **Cost-expression model fit parameters for the ancestor and *lacI*+$_{\text{ev}}$ populations.** Parameters are calculated using expression normalized independently for each clone to its maximum. Stars represent a significant difference from the ancestor (1-sample 2-tailed Welch's t-test, $p < 0.05$).

Population	*Cost*
Ancestor	0.95
*Lac*5	0.30*
G_L2	0.48*
G_L5	0.82*
G_L6	0.30*
L_G1	0.45*
L_G2	0.36*
L_G4	0.15*
L_G5	0.54*
lacI+$_{\text{ev}}$ Avg	0.42 (SD: 0.20) *

TABLE 4.6: **Relative fitness costs of maximum expression ($L = 1$) for the ancestor and *lacI*+$_{\text{ev}}$ populations.** Stars represent a significant difference from the ancestor (2-tailed Welch's t-test, $p < 0.05$).

(Fig. 4.6). In *Glu*, where *lac* expression is unnecessary, expression is minimal in the ancestor (0.74 *MU*/*hr*, 95% CI: −0.34 to 1.82). In *Lac*, expression increases to 27.0 *MU*/*hr* (95% CI: 15.87 to 38.19). This is significantly below the 114 *MU*/*hr* expressed by the ancestor *lacI-* mutant in *Lac* (two-tailed *t*-test: p<0.001). However, this is consistent with work that finds that the benefit of *lac* expression plateaus at 30% of maximum expression (here 24%) [85,328]. Expression of the *lacI-* mutant is similar in both *Lac* and *Glu* (two-tailed *t*-test: p=0.08).

On average, *lacI*+$_{ev}$ populations have similar evolved *lac* expression to the ancestor in both *Lac* (26.9 vs 27.0 *MU*/*hr*, two-tailed *t*-test: p=0.99) and *Glu* (2.65 vs 0.74 *MU*/*hr*, two-tailed *t*-test: p=0.49). The *lacI-* mutants, of these *lacI*+$_{ev}$ clones, also show no significant difference with the *lacI-* ancestor mutant in *Lac* (104 vs 114 *MU*/*hr*, p=0.49) and *Glu* (63.3 vs 78.8 *MU*/*hr*, p=0.45). Evolved *lacI*+$_{ev}$ clones have higher maximum induced expression than the ancestor in glycerol (Fig. 4.5), but do not naturally express higher levels of *lac* than the ancestor in either of the evolution environments (Fig. 4.6).

4.3.4 Changes in cost of expression are not explained by background fitness

There is not a significant change in mean expression of *lacI*+$_{ev}$ in the evolution environments. Yet, the costs of that expression have decreased. To explore the cause of decreased cost, I tested the relationship between *lac* expression and the fitness of *lacI*+$_{ev}$ populations (Fig. 4.7). Changes in cost of expression may result

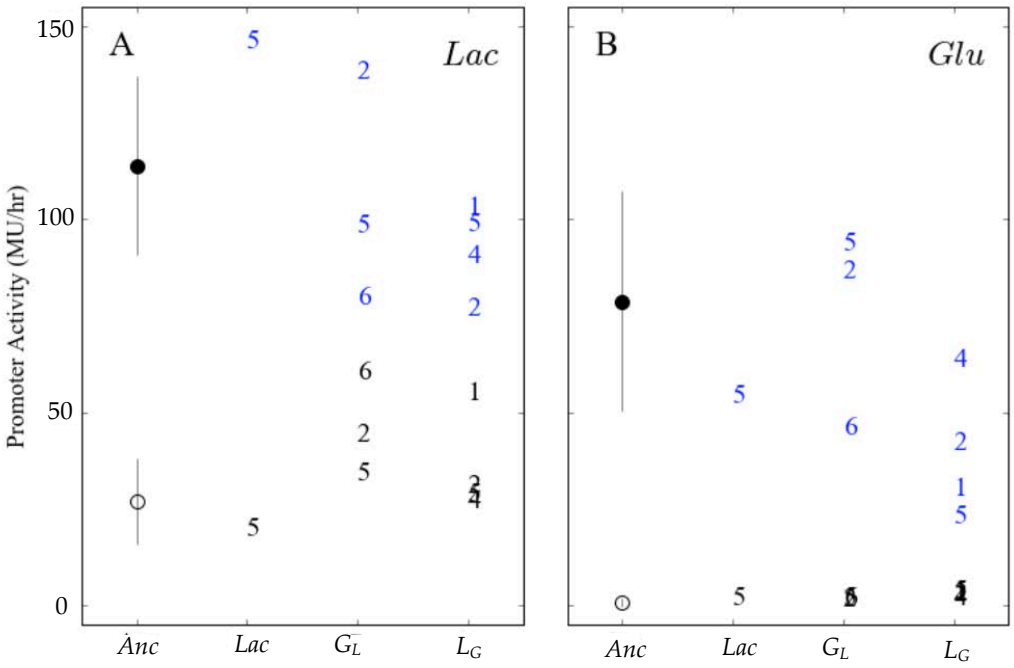

FIGURE 4.6: **Natural *lac* expression of *lacI*+$_{ev}$ populations in *Lac* (A) and *Glu* (B).** The ancestor is shown as an open black circle, with its *lacI*- mutant as a filled in black circle. Error bars are the 95% confidence intervals. *lacI*+ populations are shown, by environment, with number indicating the population number. Black numbers are *lacI*+$_{ev}$ clones and blue numbers are their *lacI*- mutants.

from increases in evolved strain fitness. If the cost of expression is absolute, it may have a smaller proportional effect on higher fitness strains. Alternatively, faster growing strains may actually have more to lose from the expression of unneeded proteins [269]. Costs are lower for evolved strains in comparison to the ancestor (Table. 4.6, Fig. 4.5). However, there is no significant monotonic relationship for relative fitness in *Lac* (Spearman's $\rho = -0.03$, $p = 0.93$) or *Glu* (Spearman's $\rho = -0.17$, $p = 0.67$). Because evolved fitness alone does not explain the change in cost of *lac* expression, I tested a proposed determinant of growth rate and fitness

in bacteria - translational capacity [269].

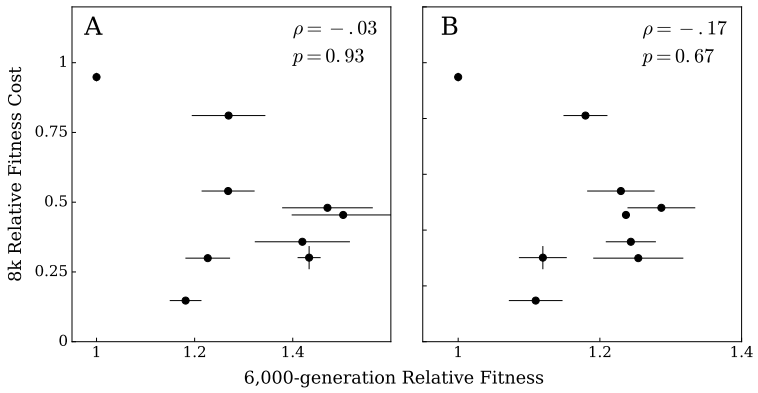

FIGURE 4.7: **Relationship between cost relative fitness in evolution environments.** The relationship was non-significant for both lactose (A) and glucose (B), based on a Spearman's rank correlation test.

4.3.5 Evolved cells have a higher translational capacity

This growth rate of bacterial cells is directly related to protein synthesis, as proteins are necessary for growth. The rate of protein synthesis, which depends on ribosome content, can be captured using the RNA/protein ratio (R). Scott et al. (2010) found that the RNA/protein ratio is linearly correlated with growth rate. This is because faster growing cells require more ribosomes which themselves have a high RNA/protein ratio. They propose a phenomenological parameter — translational capacity (K_t), calculated as

$$K_t = \frac{\lambda}{R - r_0} \tag{4.13}$$

where R is the RNA/protein ratio, λ is the growth rate ($\ln(2)/d_t$), r_0 is the vertical intercept, K_t is the translational capacity.

I compared the selected *lacI*+$_{\text{ev}}$ population, L_G2, to the ancestor, as an indication of evolved translational strain capacity (Fig. 4.8). The range of R is similar between L_G2 and the ancestor, indicating that they have similar ribosome availability. However, R increases with λ more slowly in L_G2 than in the ancestor. This means that the *lacI*+$_{\text{ev}}$ clone has a greater translational capacity ($K_t = 0.20$, 95% CI = 0.05) than the ancestor (Fig. 4.8) ($K_t = 0.12$, 95% CI = 0.02, 2-tailed t-test: $p = 0.03$). In other words, cells improve their rate of protein synthesis as they evolve.

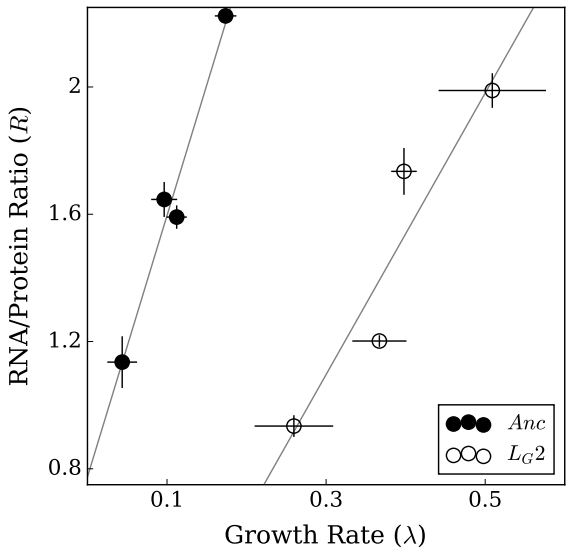

FIGURE 4.8: **Translational capacity measurements in the ancestor and L_G2.** RNA, protein, and growth rate were measured in lactose with increasing concentration from 70 to 210 μM. K_t is calculated as the inverse of the slope for each linear regression. Error bars represent 95% confidence intervals.

Given this finding, I examined whole-genome sequences of *lacI*+$_{ev}$ populations to identify the genetic basis of this increase in K_t. Ribosome synthesis is regulated by multiple mechanisms in response to external (environmental) and internal (cellular) conditions [40]. One of these mechanisms is the alarmone ppGpp (guanosine 5'-diphosphate 3'-diphosphate), which activates the "stringent response" [236]. Under stressful conditions, ppGpp down-regulates ribosome synthesis and increases the transcription of biosynthetic genes [284,300]. In *E. coli*, the RelA and SpoT proteins regulate ppGpp concentration in response to a variety of stresses, including temperature [90, 109], growth cycle phase [170], nutrient availability [22, 100, 283, 307], and amino acid levels [133].

Population	*spoT*
*Lac*5	M330I
G_L2	G207D
G_L5	R701Q
G_L6	G207V
L_G1	-
L_G2	V593E
L_G4	I446M
L_G5	*R*209*L**

TABLE 4.7: **Mutations in *spoT* in *lacI*+$_{ev}$ populations.**

Seven out of eight *lacI*+$_{ev}$ populations have a mutation in *spoT* (Table. 4.7). The lone population without a mutation to *spoT* is L_G1, which is a hypermutator and may have other ribosome-affecting mutations. These mutations are thought to cause a decrease in ppGpp concentration [54], which in turn increases the transcription rate of tRNA and rRNA genes [12]. Higher levels of ribosome synthesis

could then drive an increase in translation rate [280] and growth rate [255]. In fact, 19 of 25 evolved populations (both *lacI*+$_{\text{ev}}$ and *lacI*-$_{\text{ev}}$), in environments used here, have a mutation in *spoT*, suggesting that increasing ribosome synthesis (i.e., K_t) may be a key mechanism for fitness improvements in this experiment [54]. Future work will test if *spoT* mutations are the cause of this increase in K_t and decrease in expression cost.

4.3.6 *lacI*+$_{\text{ev}}$ appear to have substituted *lacI*- alternatives

Expression of the *lac* operon confers lower expression costs *lacI*+$_{\text{ev}}$ strains (Fig. 4.5, Fig 4.5). As such, the cause of decreased fitness effect (Chapter 3) must be a decrease in the benefit conferred in *Lac*. This may be because *lacI*+$_{\text{ev}}$ populations have substituted alternative mutations that provide an equivalent growth advantage. This appears to be the case for the effect of *lacI*- on the growth curve (Fig. 4.2). However, it is difficult to address the basis of this effect directly because of the large number of other mutations present in these 8,000-generation evolved clones ($\geq$ 15). If *lacI*+$_{\text{ev}}$ populations have substituted mutations with equivalent demographic effects to *lacI*-, I expect them to have similar evolved fitness (in *Lac*) to *lacI*-$_{\text{ev}}$ strains.

There is no significant difference between the mean evolved fitness of *lacI*+$_{\text{ev}}$ populations ($W = 1.35$) and *lacI*-$_{\text{ev}}$ populations ($W = 1.37$, two-tailed t-test: $p = 0.60$) (Fig. 4.9). This holds within evolution environments as well. In the *Lac* environment, the only *lacI*+$_{\text{ev}}$ population has a fitness of 1.43 while the mean fitness of

lacI-$_{ev}$ populations is 1.42 ($p = 0.77$). In the 2,000-generation fluctuating environments, *lac*+$_{ev}$ have a mean fitness of 1.33, which is not significantly different from *lacI*-$_{ev}$ populations (1.32, $p = 0.85$).

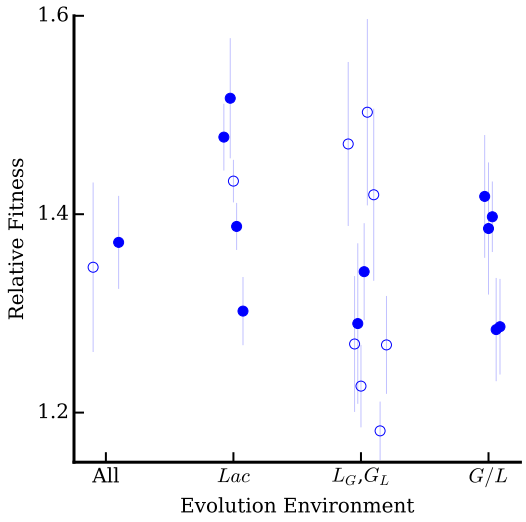

FIGURE 4.9: ***lacI*+$_{ev}$ and *lacI*-$_{ev}$ populations have similar fitness in *Lac* at 6,000-generations.** Filled circles indicate *lacI*-$_{ev}$ and open circles indicate *lacI*+$_{ev}$. The mean for all populations is shown on the left, followed by evolved population fitness each environmental treatment. Error bars are 95% confidence intervals. This data was collected by Rebecca Satterwhite, a previous student in the Cooper lab [257].

4.3.7 *lac* induction is more sensitive in *lacI*+$_{ev}$

To determine the basis of the effect of alternative substitutions in *lacI*+$_{ev}$ strains, I tested the induction-response of the *lac* operon (Fig. 4.10). If *lacI*+$_{ev}$ strains are more sensitive to induction, this would indicate that they are able to induce the

lac operon more quickly in *Lac*. Faster induction in *Lac* may result in the shorter observed lag time.

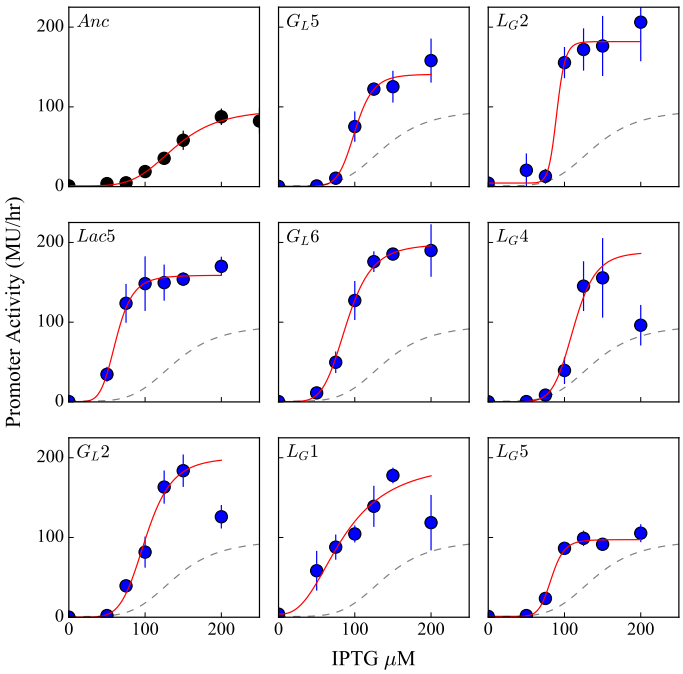

FIGURE 4.10: **Induction-response curves for the ancestor and *lacI+*$_{ev}$ populations.** Blue points represent experimental measurements, with standard deviations shown. Model fits are shown as red lines in each panel. For comparison, ancestor induction-response curve is shown as a grey dashed line in panels of evolved clones.

With glycerol as the sole carbon source and in the absence of IPTG, the ancestor still produces $b = 0.90\ MU/hr$ (Fig. 4.11. This is similar to the level of expression seen in glucose (Fig. 4.6B). In the ancestor, fold change in *lac* expression when IPTG is added ($f = 120$) is significantly lower than in other studies [86, 165, 213]. This is likely due to $b > 0$. Even a small increase in b may in fact be a multiple-fold change in the denominator of the fold-change equation (maximum/basal). The

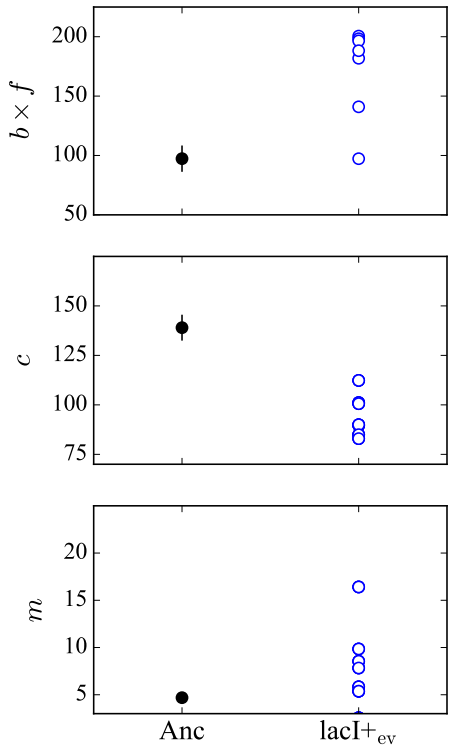

FIGURE 4.11: **Model parameters of induction-response curves for the ancestor and *lacI*+$_{ev}$ populations.** Shown are three parameters of interest: maximum expression ($b \times f$), dissociation constant (c), and sensitivity (m).

Hill Coefficient (m), which describes the cooperativity of ligand-binding, and can be visualized as the rate of increase during the transition region of the sigmoidal repsonse curve, is comparable to previous findings ($m = 4.4$) [165]. The high sensitivity is a result of positive feedback with *lacY*, which codes for the permease that imports lactose (here IPTG) into the cell [165].

In populations that maintained the functional ancestral gene (*lacI*+), the basal

expression rate of the *lac* operon is not significantly different than that of the ancestor (two-tailed *t*-test: $p = 0.71$). Mean fold change is much higher than the ancestor ($f = 532$ vs $f = 120$), however this is driven by a few outliers with very low basal expression. LacI proteins are inferred to dissociate less frequently from IPTG in *lacI*+$_{\text{ev}}$ clones ($c = 90.5$ μM) in comparison to the ancestor ($c = 146$ μM, 2-tailed *t-test*: $p < 0.001$). During lactose evolution there was likely selective pressure for less repression by LacI. Lower c results in less repression by LacI (i.e., more *lac* expression) because LacI dissociates less frequently from IPTG. The mean sensitivity of response (m) is higher in *lacI*+$_{\text{ev}}$ clones than the ancestor ($m = 7.8$ vs $m = 4.4$). This more sensitive response to induction may cause metabolism to occur sooner after exposure to lactose, and could potentially explain the shorter lag phase in *lacI*+$_{\text{ev}}$ strains (Fig. 4.2).

4.4 Discussion

In Chapter 3, I showed that fitness effect of *lacI-* mutations is neutral or deleterious in all 8,000-generation evolved *lacI*+$_{ev}$ populations. I interpreted this to be negative epistasis with the preexisting genotype. This negative epistasis could be a result of multiple mechanisms. First, it could be due to local interactions with other mutations in the *lac* system (1.5). This is likely the case for the *Lac*5 population, where the decrease in *lacI-* fitness occurs within the first 500 generations of evolution (Fig. 3.6). Alternatively, mutation interactions may be mediated globally [164], perhaps through competition for a common resource pool necessary for expression [142]. I hypothesized that this is the case for most *lacI*+$_{ev}$ populations.

To investigate the basis of changes in *lacI–* fitness effect, I measured various phenotypes affected by *lac* expression. Constitutive expression provides a growth benefit in the ancestor by decreasing the length of lag phase [238]. This benefit no longer occurs in *lacI*+$_{ev}$ strains (Fig. 4.2). One possible explanation for this is that lactose transport has changed during evolution, such that expression can occur quickly after lactose exposure without *lacI–*. Cells growing in a very low nutrient medium are predicted to have up-regulated nutrient uptake [302]. For yeast evolving in a glucose limited environment, multiple glycolysis enzymes and proteins, and a hexose transporter were significantly up-regulated [161]. One way to investigate if another lactose transporter exists is to delete *lac* permease (LacY). If *lac* induction still occurs, this would support an alternative mechanism of lactose transport. If *lac* induction does not occur, a regulatory change is likely driving the

observed growth benefit.

Regulatory changes are a common mechanism of evolution [59, 197, 238]. A study by Dekel and Alon (2005) found that *lac* operon expression can be optimized over just a few hundred generations of evolution [74]. Interestingly, *lacI*+$_{ev}$ strains here do not evolve different levels of *lac* expression in the evolution environments (Fig. 4.6). They do, however, evolve a more sensitive induction-response to IPTG (Figure 4.10). This change likely causes sooner metabolism following lactose exposure, and may explain why the lag phase benefit of *lacI*- mutations is nonexistent in *lacI*+$_{ev}$ strains; the lag phase phenotype is already near its fitness optimum. To check if this is the case, I plan to compare the length of lag phase in these 8,000-generation evolved strains to 50,000-generation glucose evolved strains from a similar experiment [174]. If the length of lag phase is similar, this would indicate that *lacI*+$_{ev}$ strains used here are indeed near the lag phase fitness optimum.

In addition to greater sensitivity, *lacI*+$_{ev}$ strains have higher maximum *lac* expression levels under IPTG induction. One explanation for these regulatory changes may be changes in DNA toplogy. DNA supercoiling modulates both transcription and translation. Greater negative supercoiling increases the binding affinity between LacI and the *lac* operator [107], and has been shown to improve the sensitivity of genetic switches [79]. In a similar long-term evolution experiment, there was parallel evolution for greater negative DNA supercoiling [60, 61]. None of the *lacI*+$_{ev}$ populations have mutations to the genes affecting supercoiling identified by Crozat et al. (2010) [61], however it may have increased via an alternative mechanism in this experiment.

In spite of higher expression potential, *lacI*+$_{ev}$ strains have lower costs of *lac* expression. This is in contrast to a prediction that faster growing strains have more to lose from the expression of unnecessary proteins [83, 269]. Two studies have found a higher cost of protein synthesis for cells with higher growth rates [83, 269]. These studies manipulated growth rate using nutrient quality, as opposed to evolved strains with different growth rates in the same medium. It's possible that expression is more costly in those studies because cells are not previously adapted to the environments used. In contrast, cells that are well-adapted to a minimal sugar environment may have optimized gene expression during their evolution, and thus suffer lower costs. This hypothesis is supported by the finding that highly expressed genes in natural bacteria are optimized to minimize protein production cost [105].

The basis for expression costs may be that unnecessary expression diverts cellular resources from necessary gene expression that contributes to growth [117]. Ribosomes are a necessary resource for translation and have been shown to be growth-limiting in both slow and fast growing *E. coli* [269]. If evolved costs have decreased due to greater ribosome synthesis, this would be evident by higher a RNA/protein ratio (R) in evolved cells. However, I do not find higher R in a *lacI*+$_{ev}$ strain. Instead, I find that this evolved strain can grow faster than the ancestor at similar R (i.e., they have a higher translational capacity, Fig. 4.8). This higher translational capacity is potentially a result of improved translation efficiency, which could occur at the multiple levels of translation, including initiation, elongation, or protein folding [244].

Improvements in translation efficiency may occur at the level of mRNA [244]. In *E. coli*, there are $\sim$ 500 times as many proteins as mRNA [180, 266]. As such, costs of expression may occur from mRNA scarcity. Resources may be allocated to transcription and translation, but protein synthesis delayed due to limited mRNA availability. An increase in mRNA would alleviate this issue, however its synthesis is costly [308]. Alternatively, mRNA half life may have increased. The typical mRNA half life is $\sim$ 5 minutes in *E. coli*, while protein half-lives are 180 minutes on average [244]. Even a small increase in half-life would create a significant improvement in the proteins produced per mRNA. This hypothesis is also consistent with the finding of higher maximum inducible expression levels for $lacI+_{\mathrm{ev}}$ (Fig. 4.10).

Beyond changes in the magnitude of cost, the shape of the expression-cost relationship is a departure from the exponential cost curve predicted by Dekel and Alon (2005) [74]. They model *lac* expression cost based on the intuition that cost is a result of constrained cellular resources. They predicted that cost increases exponentially as those resources become rarer. A more recent study found that, in genetically engineered strains, the cost of *lac* expression was due to the toxicity of the *lac* permease (*lacY*) [85]. They found that cost increases quickly with LacZ concentration and then slows as the cell reaches maximum *lac* expression. My findings are consistent with this cost function, suggesting that costs of expression are a result of protein toxicity.

If cost is due to protein toxicity, there may be a simple explanation for lower costs in evolved strains. In a separate, but similar, long-term evolution experiment

with *E. coli*, cell size increased significantly in evolved strains [173]. If costs are indeed due to protein-toxicity, it is plausible that dilution effects may cause costs to decrease as cell size increases. Because we do not have cell size data for the experiment used here, I used the Lenski long-term experiment for a brief analysis [174]. In that experiment, cells increased from the ancestral size of 0.37 fL (10^{-15} L) to an average size of 0.82 fL (SD: 0.13) after 8,000-generations of evolution [173]. In this Chapter, I found that the relative fitness cost of *lac* expression decreased from 0.95 in the ancestor to an average of 0.42 in 8,000-generation *lacI*+$_{\text{ev}}$ strains (Table 4.6). Remarkably, this is a very similar fold-change (2.24x) to the Lenski experiment increase cell size (2.21x). If cells in this experiment evolved similar increases in cell size to those in the Lenski experiment, then the dilution-effect on protein toxicity seems a likely candidate to explain decreases in cost of expression. Future work will determine if *lacY* protein toxicity is indeed the cause of expression costs in this experiment, and if the evolution of cell size explains decreases in *lac* expression cost.

In total, I found that *lacI*+$_{\text{ev}}$ populations have likely substituted alternative mutations to *lacI*– that provide an equivalent (or similar) growth benefit in lactose. I found changes in *lac* regulation, cost of expression, and translational capacity — all of which merit further work to elucidate the underlying causes.

Chapter 5

The Imperfections of Evolution Experiments

Perhaps the first laboratory evolution experiment was done by W.H. Dallinger in the nineteenth century [64]. He subjected unidentified protists to progressively increasing temperatures over the course of seven years. The ancestral population was sensitive to temperatures above 140 °F, yet adapted individuals were able to survive at 158 °F. Over the past 100+ years, laboratory experimental evolution has improved our understanding of mutation characteristics [18, 94, 194], genotype × environment effects [314], social evolution [220], the evolution of sex [8, 118, 130, 152, 227, 249], and many other concepts [110]. In Chapters 2 and 3, I used experimental evolution to investigate the influence of historical contingency on divergent evolution, and the cause of changes in mutation fitness effect. One complication to generalizing my findings is the applicability of evolution experiments to natural environments.

Experimental evolution provides a unique balance between strength of inference and technical feasibility. Experiments are relatively easy to maintain over many months or years. Population size, environment, and replication can be easily manipulated. For example, the Lenski evolution experiment is at $\sim 70,000$ generations [174]. However, despite its appeal, laboratory experimental evolution does have some limitations. The most obvious, perhaps, is the difference between laboratory and natural environment.

Laboratory environments tend to be much simpler than those in nature. Benign environments likely impose selection on many fewer traits than natural environments, and the strength of selection is likely weaker as well. For example, I find that genetic divergence in *E. coli* is a result of multiple genotypic solutions to the same phenotypic problem (Chapter 4). This may not be possible in harsher, natural environments. Natural environments tend to be more complex and the fitness landscapes are more rugged [192]. If there are fewer accessible paths to higher fitness, I expect negative epistasis, due to benefit redundancies, to drive less genetic divergence than in the laboratory. Of course, divergence could still occur for other reasons, such as adaptation to alternate peaks. Some studies have found that genome architecture is quite different between natural and laboratory *E. coli* strains [80, 106]. Even among natural isolates, there can be significant variation in genome size [25, 91, 230]. Such discrepancies should caution biologists from applying inferences from laboratory experimental evolution to natural populations. Of course, one solution to this problem is to make laboratory environments more similar to natural environments. For example, Bradshaw and Holzapfel (2001)

used the natural plant habitat of a mosquito species as a micro-habitat in the lab, and used natural photo- and thermo-periods to simulate sunlight [33]. A second complication is that inferences based on laboratory-evolved populations cannot be directly applied to natural populations. The way in which laboratory organisms respond to selection can be fundamentally different from those in nature [223,254]. Transferring organisms directly from the field is an ideal solution for this issue. However, such populations must then adapt to both the laboratory environment in general, as well as the specific medium that they are subjected to. For example, microbes that are transferred into the laboratory quickly evolve changes in colony morphology [166]. Starting with natural populations allows for more direct inferences. However, these inferences are confounded by the effects of domestication. On the other hand, using laboratory-adapted populations isolates the effects of selection, but limits the ability to extrapolate findings to natural populations. A solution to both of these issues is to do experimental evolution in the field. This has been successfully carried out in multiple cases [192,289]. However, it tends to be logistically challenging. Furthermore, it's difficult to determine the exact cause of observed changes due to the simultaneously presence of many variables. Despite some drawbacks, laboratory experimental evolution offers one of the most applicable and technically feasible approaches for studying the underlying processes and mechanisms of adaptation.

A separate problem, specifically related to the study of fitness landscapes, is 'the problem of scale' [70]. Experimental landscape constructions to date provide

only a local view of the fitness landscape. The information they provide is dependent on the small set of mutations used. As a result, inferences from such experiments are not necessarily indicative of characteristics of the entire landscape. In order to understand general principles of the fitness landscape, it's ideal to conduct experiments at a large scale. A recent experiment tested $> 45,000$ interactions between 87 mutation-pairs in yeast tRNA [82]. Modern genetic methods are making it increasingly feasible to examine large numbers of genotypes within a given gene. Another study synthesized 4^{10} DNA oligomers and tested for affinity to one protein [248]. It is technically more difficult to study interactions between genes. Nonetheless, its important to continue analysis of the inter-gene fitness landscape on a case-study basis, as presented in Chapters 3 and 4. Beyond the academic pursuit of evolutionary principles, studying the fitness landscape has the potential to solve 'real-world' problems. For example, epistasis plays a critical role in the evolution of the H5N1 influenza virus [119] and evolution of antibiotic resistance [224].

Because fitness landscapes are difficult to study at large-scale, it's important to combine experiments with modeling approaches. Models play an integral role in the study of evolutionary biology. However, their utility is often questioned [65]. Models are useful for a few reasons. First, they can be used to generate empirically testable, quantitative predictions [147]. Second, they can be used to improve upon empirically observed patterns. Lastly, as Servedio et al.(2014) eloquently explain, models have significant utility even as "proof-of-concepts" [272]. These models test verbal arguments by specifying them mathematically and testing their

validity. Some models have an obvious connection to empirical work. For example, models of DNA substitution can take into account known biochemistry, GC content variation, and the nucleotides themselves [6, 132]. However, the utility of models is often questioned when they are of qualitative nature, as opposed to quantitative. Evolutionary mechanisms, and the resulting biological patterns, are complex and verbal models are nearly always flawed in some regard. I posit that qualitative mathematical models, such as FGM, are in fact necessary to help develop verbal models to the stage of empirical testing. Take FGM as an example. R.A. Fisher explained his geometric model in $\sim$ 1 page in *The Genetical Theory of Natural Selection* [99]. Yet, over the past 90 years, the model has proven useful to study the effects of beneficial mutations during adaptation [217], genetic incompatibilities and speciation [102], epistatic interactions [194], the DFE [20, 193], and the core adaptive processes of mutation and selection [193] (Chapter 2). For adaptive landscapes in particular, we should continue to develop methods for comparison between models and experiments [29, 295].

My hope is that the work presented in this thesis, using both modeling (FGM) and experiments (*E. coli*), improves our understanding of the processes and mechanisms underlying evolution. I have employed a combined approach of modeling and experiments in an effort to better understand evolution on the fitness landscape.

Bibliography

[1] T Aita and Y Husimi. Fitness spectrum among random mutants on Mt. Fuji-type fitness landscape. *J. Theor. Biol*, 182(4):469–85, 1996.

[2] Arianne Y K Albert, Sterling Sawaya, Timothy H. Vines, Anne K. Knecht, Craig T. Miller, Brian R. Summers, Sarita Balabhadra, David M. Kingsley, and Dolph Schluter. The genetics of adaptive shape shift in stickleback: Pleiotropy and effect size. *Evolution*, 62(1):76–85, 2008.

[3] H. Allen Orr. The rate of adaptation in asexuals. *Genetics*, 155(2):961–968, 2000.

[4] Ken J. Andrews and George D. Hegeman. Selective disadvantage of non-functional protein synthesis in *Escherichia coli*. *Journal of Molecular Evolution*, 8(4):317–328, 1976.

[5] Maia Angelova and Asma Ben-Halim. Dynamic model of gene regulation for the lac operon. *Journal of Physics: Conference Series*, 286:012007, 2011.

[6] Miguel Arenas. Trends in substitution models of molecular evolution. *Frontiers in Genetics*, 6(Oct), 2015.

[7] K.C. Atwood, Lillian K. Schneider, and Francis J Ryan. Periodic Selection in Escherichia Coli. *Sciences-New York*, 37(3):146–155, 1951.

[8] Ricardo B R Azevedo, Rolf Lohaus, Suraj Srinivasan, Kristen K Dang, and Christina L Burch. Sexual reproduction selects for robustness and negative epistasis in artificial gene networks. *Nature*, 440(7080):87–90, Mar 2006.

[9] Homayoun C. Bagheri and Günter P. Wagner. Evolution of dominance in metabolic pathways. *Genetics*, 168(3):1713–1735, 2004.

[10] J Baranyi. Simple is good as long as it is enough. *Food Microbiology*, 14(2):189–192, 1997.

[11] József Baranyi and Terry A. Roberts. A dynamic approach to predicting bacterial growth in food. *International Journal of Food Microbiology*, 23(3-4):277–294, 1994.

[12] Melanie M. Barker, Tamas Gaal, Cathleen A. Josaitis, and Richard L. Gourse. Mechanism of regulation of transcription initiation by ppGpp. I. Effects of ppGpp on transcription initiation in vivo and in vitro. *Journal of Molecular Biology*, 305(4):673–688, 2001.

[13] Jeffrey E. Barrick, Mark R. Kauth, Christopher C. Strelioff, and Richard E. Lenski. *Escherichia coli* rpoB mutants have increased evolvability in proportion to their fitness defects. *Mol. Biol. Evol.*, 27(6):1338–1347, 2010.

[14] Jeffrey E Barrick, Dong Su Yu, Sung Ho Yoon, Haeyoung Jeong, Tae Kwang Oh, Dominique Schneider, Richard E Lenski, and Jihyun F Kim. Genome

evolution and adaptation in a long-term experiment with *Escherichia coli*. *Nature*, 461(7268):1243–1247, 2009.

[15] N. H. Barton. The role of hybridization in evolution. *Mol. Ecol.*, 10(3):551–568, 2001.

[16] Nick Barton and Linda Partridge. Limits to natural selection. *BioEssays*, 22(12):1075–1084, 2000.

[17] Aditya Barve, Sayed-Rzgar Hosseini, Olivier C Martin, and Andreas Wagner. Historical contingency and the gradual evolution of metabolic properties in central carbon and genome-scale metabolisms. *BMC systems biology*, 8(1):48, 2014.

[18] Thomas Bataillon. Estimation of spontaneous genome-wide mutation rate parameters: Whither beneficial mutations? *Heredity*, 84(5):497–501, 2000.

[19] Thomas Bataillon and Susan F Bailey. Effects of new mutations on fitness: insights from models and data. *Ann. N.Y. Acad. Sci*, 1320:76–92, Jul 2014.

[20] Thomas Bataillon, Tianyi Zhang, and Rees Kassen. Cost of adaptation and fitness effects of beneficial mutations in Pseudomonas fluorescens. *Genetics*, 189(3):939–49, Nov 2011.

[21] William Bateson. *Mendels Principles of Heredity*. 1909.

[22] Aurélia Battesti and Emmanuelle Bouveret. Acyl carrier protein/SpoT interaction, the switch linking SpoT-dependent stress response to fatty acid metabolism. *Molecular Microbiology*, 62(4):1048–1063, 2006.

[23] Stéphanie Bedhomme, Guillaume Lafforgue, and Santiago F Elena. Genotypic but not phenotypic historical contingency revealed by viral experimental evolution. *BMC evolutionary biology*, 13:46, 2013.

[24] Graham Bell. *Phil. Trans. R. Soc. B*.

[25] Ulfar Bergthorsson and Howard Ochman. Chromosomal Changes during Experimental Evolution in Laboratory Populations of. *Society*, 181(4):1360–1363, 1999.

[26] Joan L. Betz, Henri M. Sasmor, Fritz Buck, Maggie Y. Insley, and Marvin H. Caruthers. Base substitution mutants of the lac operator: in vivo and in vitro affinities for lac repressor. *Gene*, 50(1-3):123–132, 1986.

[27] Mikhail V. Blagosklonny. Aging and immortality: Quasi-programmed senescence and its pharmacologic inhibition. *Cell Cycle*, 5(18):2087–2102, 2006.

[28] Mikhail V. Blagosklonny. Revisiting the antagonistic pleiotropy theory of aging: TOR-driven program and quasi-program. *Cell Cycle*, 9(16):3151–3156, 2010.

[29] François Blanquart, Guillaume Achaz, Thomas Bataillon, and Olivier Tenaillon. Properties of selected mutations and genotypic landscapes under Fisher's Geometric Model. *Evolution*, pages 1–51, Oct 2014.

[30] Zachary D. Blount, Jeffrey E. Barrick, Carla J. Davidson, and Richard E. Lenski. Genomic analysis of a key innovation in an experimental *Escherichia coli* population. *Nature*, 489(7417):513–518, 2012.

[31] Zachary D Blount, Christina Z Borland, and Richard E Lenski. Historical contingency and the evolution of a key innovation in an experimental population of *Escherichia coli*. *Proc. Natl. Acad. Sci. U.S.A*, 105(23):7899–906, Jun 2008.

[32] Daniel I. Bolnick and On Lee Lau. Predictable Patterns of Disruptive Selection in Stickleback in Postglacial Lakes. *The American Naturalist*, 172(1):1–11, 2008.

[33] W E Bradshaw, W E Bradshaw, C M Holzapfel, and C M Holzapfel. Phenotypic evolution and the genetic architecture underlying photoperiodic time measurement. *Journal of Insect Physiology*, 47(8):809–820, 2001.

[34] Michael S Breen, Carsten Kemena, Peter K Vlasov, Cedric Notredame, and Fyodor A Kondrashov. Epistasis as the primary factor in molecular evolution. *Nature*, 490(7421):535–538, 2012.

[35] Hans Bremer and Patrick P Dennis. Modulation of Chemical Composition and Other Parameters of the Cell at Different Exponential Growth Rates. *EcoSal Plus*, 1(2), 2008.

[36] Jamie T. Bridgham, Sean M. Carroll, and Joseph W. Thornton. Evolution of hormone-receptor complexity by molecular exploitation. *Science*, 312(5770):97–101, 2006.

[37] Jamie T Bridgham, Eric a Ortlund, and Joseph W Thornton. An epistatic ratchet constrains the direction of glucocorticoid receptor evolution. *Nature*, 461(7263):515–519, 2009.

[38] Kyle M. Brown, Marna S. Costanzo, Wenxin Xu, Scott Roy, Elena R. Lozovsky, and Daniel L. Hartl. Compensatory mutations restore fitness during the evolution of dihydrofolate reductase. *Mol. Biol. Evol.*, 27(12):2682–2690, 2010.

[39] Christina L Burch and Lin Chao. Evolution by small steps and rugged landscapes in the RNA virus ϕ6. *Genetics*, 151(3):921–927, 1999.

[40] Hector L. Burgos, Kevin O'Connor, Patricia Sanchez-Vazquez, and Richard L. Gourse. Roles of Transcriptional and Translational Control Mechanisms in Regulation of Ribosomal Protein Synthesis in *Escherichia coli*. *Journal of Bacteriology*, 199(21):JB.00407–17, 2017.

[41] D. Butcher. Muller's ratchet, epistasis and mutation effects. *Genetics*, 141(1):431–437, 1995.

[42] Sean B. Carroll. Evo-Devo and an Expanding Evolutionary Synthesis: A Genetic Theory of Morphological Evolution. *Cell*, 134(1):25–36, 2008.

[43] L I N Chao and Edward C Cox. Competition Between High and Low Mutating Strains of *Escherichia coli*. *Evolution*, 37(1):125–134, 1983.

[44] D Charlesworth and B Charlesworth. The pattern of neutral molecular variation under the background selection model. *Genetics*, 141:1619–1632, 1995.

[45] Peiqiu Chen and Eugene I. Shakhnovich. Lethal mutagenesis in viruses and bacteria. *Genetics*, 183(2):639–650, 2009.

[46] James M Cheverud. Developmental Integration and the Evolution of Pleiotropy. *Integrative and Comparative Biology*, 36(1):44–50, 1996.

[47] Luis-Miguel Chevin, Guillaume Martin, and Thomas Lenormand. Fisher's model and the genomics of adaptation: restricted pleiotropy, heterogenous mutation, and parallel evolution. *Evolution*, 64(11):3213–31, Nov 2010.

[48] H.-C. Chiu, C. J. Marx, and D. Segre. Epistasis from functional dependence of fitness on underlying traits. *Proceedings of the Royal Society B: Biological Sciences*, 279(1745):4156–4164, 2012.

[49] Hsin-Hung Chou, Hsuan-Chao Chiu, Nigel F Delaney, Daniel Segrè, and Christopher J Marx. Diminishing returns epistasis among beneficial mutations decelerates adaptation. *Science (New York, N.Y.)*, 332(6034):1190–2, 2011.

[50] Bryan Clarke and Wallace Arthur. What constitutes a 'large' mutational change in phenotype. *Evolution and Development*, 2:238–240, 2000.

[51] Tim Connallon and Andrew G. Clark. The distribution of fitness effects in an uncertain world. *Evolution*, 69(6):1610–1618, 2015.

[52] TF Cooper, EA Ostrowski, and Michael Travisano. A negative relationship between mutation pleiotropy and fitness effect in yeast. *Evolution*, 61(6):1495–9, Jun 2007.

[53] Tim F Cooper and Richard E Lenski. Experimental evolution with E. coli in diverse resource environments. I. Fluctuating environments promote divergence of replicate populations. *BMC evolutionary biology*, 10:11, Jan 2010.

[54] Tim F Cooper, Daniel E Rozen, and Richard E Lenski. Parallel changes in gene expression after 20 , 000 generations of evolution in *Escherichia coli*. *Proc. Natl. Acad. Sci. U.S.A*, 100(3):1072–1077, 2003.

[55] V. S. Cooper, D. Schneider, M. Blot, and R. E. Lenski. Mechanisms causing rapid and parallel losses of ribose catabolism in evolving populations of *Escherichia coli* B. *Journal of Bacteriology*, 183(9):2834–2841, 2001.

[56] Vaughn S. Cooper and Richard E. Lenski. The population genetics of ecological specialization in evolving *Escherichia coli* populations. *Nature*, 407(6805):736–739, 2000.

[57] Marna S. Costanzo, Kyle M. Brown, and Daniel L. Hartl. Fitness trade-offs in the evolution of Dihydrofolate reductase and drug resistance in plasmodium falciparum. *PLoS ONE*, 6(5), 2011.

[58] Matthew C Cowperthwaite and Lauren Ancel Meyers. How Mutational Networks Shape Evolution: Lessons from RNA Models. *Annu. Rev. Ecol. Evol. Syst.*, 38:203–230, 2007.

[59] Anton Crombach and Paulien Hogeweg. Evolution of evolvability in gene regulatory networks. *PLoS Computational Biology*, 4(7), 2008.

[60] Estelle Crozat, Nadège Philippe, Richard E. Lenski, Johannes Geiselmann, and Dominique Schneider. Long-term experimental evolution in *Escherichia coli*. XII. DNA topology as a key target of selection. *Genetics*, 169(2):523–532, 2005.

[61] Estelle Crozat, Cynthia Winkworth, Joel Gaffe, Peter F. Hallin, Margaret A. Riley, Richard E. Lenski, and Dominique Schneider. Parallel genetic and phenotypic evolution of DNA superhelicity in experimental populations of escherichia coli. *Mol. Biol. Evol.*, 27(9):2113–2128, 2010.

[62] Y. Cui, W. H. Wong, E. Bornberg-Bauer, and H. S. Chan. Recombinatoric exploration of novel folded structures: A heteropolymer-based model of protein evolutionary landscapes. *Proceedings of the National Academy of Sciences*, 99(2):809–814, 2002.

[63] Jack Da Silva, Mia Coetzer, Rebecca Nedellec, Cristina Pastore, and Donald E. Mosier. Fitness epistasis and constraints on adaptation in a human immunodeficiency virus type 1 protein region. *Genetics*, 185(1):293–303, 2010.

[64] W H Dallinger. On the life-history of a minute septic organism: with an account of experiments made to determine its thermal death point. *Proceedings of the Royal Society of London*, 27:332–350, 1878.

[65] W. Daniel Hillis. Why physicists like models and why biologists should. *Current Biology*, 3(2):79–81, 1993.

[66] Charles Darwin. *On the Origin of Species by Means of Natural Selection*. 1859.

[67] Alexandre Dawid, Daniel J. Kiviet, Manjunatha Kogenaru, Marjon de Vos, and Sander J. Tans. Multiple peaks and reciprocal sign epistasis in an empirically determined genotype-phenotype landscape. *Chaos*, 20(2), 2010.

[68] J Arjan G M de Visser, Tim F Cooper, and Santiago F Elena. The causes of epistasis. *Proceedings of the Royal Society B: Biological Sciences*, 278(1725):3617–3624, Dec 2011.

[69] J Arjan G. M. de Visser, Joachim Hermisson, Günter P. Wagner, Lauren Ancel Meyers, Homayoun Bagheri-Chaichian, Jeffrey L. Blanchard, Lin Chao, James M. Cheverud, Santiago F Elena, Walter Fontana, Greg Gibson, Thomas F. Hansen, David Krakauer, Richard C. Lewontin, Charles Ofria, Sean H Rice, George von Dassow, Andreas Wagner, and Michael C. Whitlock. Perspective: Evolution and detection of genetic robustness. *Evolution*, 57(9):1959–72, 2003.

[70] J. Arjan G.M. M de Visser and Joachim Krug. Empirical fitness landscapes and the predictability of evolution. *Nature Reviews Genetics*, 15(7):480–490, 2014.

[71] J. Arjan G.M. M de Visser, Clifford Zeyl, Philip J Gerrish, Jeffrey L Blanchard, and Richard E. Lenski. Diminishing Returns from Mutation Supply Rate in Asexual Populations. *Science*, 283(5568):404–406, 1999.

[72] J. Arjan G. M. de Visser, Su-Chan Park, and Joachim Krug. Exploring the Effect of Sex on Empirical Fitness Landscapes. *The American Naturalist*, 174(S1):S15–S30, 2009.

[73] Daniel E. Deatherage and Jeffrey E. Barrick. Identification of mutations in laboratory evolved microbes from next-generation sequencing data using breseq. *Methods in Molecular Biology*, 1151:1–22, 2014.

[74] Erez Dekel and Uri Alon. Optimality and evolutionary tuning of the expression level of a protein. *Nature*, 436(7050):588–92, 2005.

[75] Patrick P Dennis, Mans Ehrenberg, and Hans Bremer. Control of rRNA synthesis in *Escherichia coli*: a systems biology approach. *Microbiol Mol Biol Rev*, 68(4):639–668, 2004.

[76] Jeremy R Dettman, Caroline Sirjusingh, Linda M Kohn, and James B Anderson. Incipient speciation by divergent adaptation and antagonistic epistasis in yeast. *Nature*, 447(7144):585–588, 2007.

[77] Luis Díaz-Martínez, Isabel Brichette-Mieg, Axier Pineño-Ramos, Guillermo Domínguez-Huerta, and Ana Grande-Pérez. Lethal mutagenesis of an RNA plant virus via lethal defection. *Scientific Reports*, 8(1):1–13, 2018.

[78] B. C. Dickinson, A. M. Leconte, B. Allen, K. M. Esvelt, and D. R. Liu. Experimental interrogation of the path dependence and stochasticity of protein evolution using phage-assisted continuous evolution. *Proceedings of the National Academy of Sciences*, 110(22):9007–9012, 2013.

[79] Y. Ding, C. Manzo, G. Fulcrand, F. Leng, D. Dunlap, and L. Finzi. DNA supercoiling: A regulatory signal for the lambda repressor. *Proceedings of the National Academy of Sciences*, 111(43):15402–15407, 2014.

[80] Ulrich Dobrindt, Franziska Agerer, Kai Michaelis, Andreas Janka, Carmen Buchrieser, Martin Samuelson, Catharina Svanborg, Gerhard Gottschalk, and Helge Karch. Analysis of Genome Plasticity in Pathogenic and Commensal. *Society*, 185(6):1831–1840, 2003.

[81] Theodosius Dobzhansky. Genetics and the Origin of Species. *Columbia University Press, New York*, 1941.

[82] Júlia Domingo, Guillaume Diss, and Ben Lehner. Pairwise and higher-order genetic interactions during the evolution of a tRNA. *Nature*, 2018.

[83] H Dong, L Nilsson, C G Kurland, Hengjiang Dong, Lars Nilsson, and Charles G Kurland. Gratuitous overexpression of genes in *Escherichia coli*

leads to growth inhibition and ribosome destruction. *Journal of Bacteriology*, 177(6):1497–1504, 1995.

[84] D. E. Dykhuizen, A. M. Dean, and D. L. Hartl. Metabolic flux and fitness. *Genetics*, 115(1):25–31, 1987.

[85] Matt Eames and Tanja Kortemme. Cost-Benefit Tradeoffs in Engineered lac Operons. *Science*, 336:911–915, 2012.

[86] Elis Eismann, Brigitte V.Wilcken-Bergmann, and Benno Müller-Hill. Specific destruction of the second lac operator decreases repression of the lac operon in *Escherichia coli* fivefold. *Journal of Molecular Biology*, 195(4):949–952, 1987.

[87] Santiago F Elena, Lynette Ekunwe, Neerja Hajela, Shenandoah A Oden, and Richard E Lenski. Distribution of fitness effects caused by random insertion mutations in *Escherichia coli*. *Genetica*, 102-103:349–358, 1998.

[88] Santiago F Elena and Richard E Lenski. Test of synergistic interactions among deleterious mutations in bacteria. *Nature*, 390(6658):395–398, 1997.

[89] Valur Emilsson and Charles G Kurland. Growth rate dependence of transfer RNA abundance in *Escherichia coli*. *Embo J*, 9(13):4359–4366, 1990.

[90] B. P. English, V. Hauryliuk, A. Sanamrad, S. Tankov, N. H. Dekker, and J. Elf. Single-molecule investigations of the stringent response machinery in living bacterial cells. *Proceedings of the National Academy of Sciences*, 108(31):E365–E373, 2011.

[91] Patricia Escobar-Páramo, Arnaud Le Menac'h, Tony Le Gall, Christine Amorin, Stéphanie Gouriou, Bertrand Picard, David Skurnik, and Erick Denamur. Identification of forces shaping the commensal *Escherichia coli* genetic structure by comparing animal and human isolates. *Environmental Microbiology*, 8(11):1975–1984, 2006.

[92] Suzanne Estes, Beverly C. Ajie, Michael Lynch, and Patrick C. Phillips. Spontaneous mutational correlations for life-history, morphological and behavioral characters in *Caenorhabditis elegans*. *Genetics*, 170(2):645–653, 2005.

[93] Adam Eyre-Walker and Peter D. Keightley. The distribution of fitness effects of new mutations. *Nature Reviews Genetics*, 8(8):610–618, 2007.

[94] Adam Eyre-Walker, Megan Woolfit, and Ted Phelps. The distribution of fitness effects of new deleterious amino acid mutations in humans. *Genetics*, 173(2):891–900, 2006.

[95] C. M. Falcon and Kathleen S. Matthews. Operator DNA sequence variation enhances high affinity binding by hinge helix mutants of lactose repressor protein. *Biochemistry*, 39(36):11074–11083, 2000.

[96] Philip J. Farabaugh. Sequence of the lacI gene. *Nature*, 274(5673):765–769, 1978.

[97] J. M. Fernandez, S. Chu, and A F Oberhauser. RNA structure. Pulling on hair(pins). *Science*, 292(5517):653–654, 2001.

[98] R. a. Fisher. The Possible Modification of the Response of the Wild Type to Recurrent Mutations. *The American Naturalist*, 62(679):115, 1928.

[99] R a Fisher. The Genetical Theory of Natural Selection. *Genetics*, 154:272, 1930.

[100] K Flärdh, T Axberg, N H Albertson, and S Kjelleberg. Stringent control during carbon starvation of marine Vibrio sp. strain S14: molecular cloning, nucleotide sequence, and deletion of the relA gene. *Journal of bacteriology*, 176(19):5949–57, 1994.

[101] Kenneth M Flynn, Tim F Cooper, Francisco B-G Moore, and Vaughn S Cooper. The environment affects epistatic interactions to alter the topology of an empirical fitness landscape. *PLoS Genet.*, 9(4):e1003426, Apr 2013.

[102] Christelle Fraïsse, P Alexander Gunnarsson, Denis Roze, Nicolas Bierne, and John J Welch. The genetics of speciation : insights from Fisher's Geometric Model. *Evolution*, 70(7):1450–1464, 2016.

[103] Jasper Franke, Alexander Klözer, J. Arjan G. M. de Visser, and Joachim Krug. Evolutionary accessibility of mutational pathways. *PLoS Computational Biology*, 7:p.e1002134, Mar 2011.

[104] Bonnie A. Fraser, Axel Künstner, David N. Reznick, Christine Dreyer, and Detlef Weigel. Population genomics of natural and experimental populations of guppies (Poecilia reticulata). *Mol. Ecol.*, 24(2):389–408, 2015.

[105] Idan Frumkin, Dvir Schirman, Aviv Rotman, Fangfei Li, Liron Zahavi, Ernest Mordret, Omer Asraf, Song Wu, Sasha F. Levy, and Yitzhak Pilpel. Gene Architectures that Minimize Cost of Gene Expression. *Molecular Cell*, 65(1):142–153, 2017.

[106] Satoru Fukiya, Satoru Fukiya, Hiroshi Mizoguchi, Hiroshi Mizoguchi, Toru Tobe, Toru Tobe, Hideo Mori, and Hideo Mori. Extensive Genomic Diversity in Pathogenic. *Society*, 186(12):3911–3921, 2004.

[107] Geraldine Fulcrand, Samantha Dages, Xiaoduo Zhi, Prem Chapagain, Bernard S. Gerstman, David Dunlap, and Fenfei Leng. DNA supercoiling, a critical signal regulating the basal expression of the lac operon in *Escherichia coli*. *Scientific Reports*, 6(October 2015):1–12, 2016.

[108] W Gabriel, M Lynch, and R Bürger. Muller's ratchet and mutational meltdowns. *Evolution*, 47(6):1744–1757, 1993.

[109] Jonathan Gallant, Linda Palmer, and Chia Chu Pao. Anomalous synthesis of ppGpp in growing cells. *Cell*, 11(1):181–185, 1977.

[110] Theodore Garland and Michael Rose. *Experimental Evolution*, volume 53. 2009.

[111] S Gavrilets. A dynamical theory of speciation on holey adaptive landscapes. *Am. Nat.*, 154(1):1–22, 1999.

[112] Sergey Gavrilets. Evolution and speciation on holey adaptive landscapes, 1997.

[113] Sergey Gavrilets. *Fitness Landscapes and the Origin of Species*. 2004.

[114] P J Gerrish and R E Lenski. The fate of competing beneficial mutations in an asexual population. *Genetica*, 102-103(1-6):127–144, 1998.

[115] G Gibson. Epistasis and pleiotropy as natural properties of transcriptional regulation. *Theor. Pop. Biol.*, 49(0003):58–89, 1996.

[116] Alexandre Gillet-Markowska, Guillaume Louvel, and Gilles Fischer. bz-rates: A Web Tool to Estimate Mutation Rates from Fluctuation Analysis. *G3*, 5(11):2323–7, 2015.

[117] Bernard R Glick. Metabolic load and heterogenous gene expression. *Biotechnology Advances*, 13(2):247–261, 1995.

[118] Matthew R Goddard, Charles JH Godfray, and Austin Burt. Sex increases the efficacy of natural selection in experimental yeast populations. *Journal of Geophysical Research*, 107(B11):636–640, 2002.

[119] Lizhi Ian Gong, Marc A. Suchard, and Jesse D. Bloom. Stability-mediated epistasis constrains the evolution of an influenza protein. *eLife*, 2013(2):1–19, 2013.

[120] Benjamin H Good and Michael M Desai. The impact of macroscopic epistasis on long-term evolutionary dynamics. *Genetics*, 199(1):177–90, Jan 2015.

[121] Isabel Gordo and P R Campos. Evolution of clonal populations approaching a fitness peak. *Biol Lett*, 9(1):20120239, 2013.

[122] Isabel Gordo and Paulo R A Campos. Sex and deleterious mutations. *Genetics*, 179(1):621–626, 2008.

[123] Isabel Gordo and Brian Charlesworth. The degeneration of asexual haploid populations and the speed of Muller's ratchet. *Genetics*, 154(3):1379–1387, 2000.

[124] S.J. Gould. *Wonderful Life: The Burgess Shale and the Nature of History*. 1989.

[125] B R Grant and P R Grant. The University of Chicago Natural Selection in a Population of Darwin ' s Finches. *The American Naturalist*, 133(3):377–393, 1989.

[126] Pierre Alexis Gros, Hervé L. Nagard, and Olivier Tenaillon. The evolution of epistasis and its links with genetic robustness, complexity and drift in a phenotypic model of adaptation. *Genetics*, 182(1):277–293, 2009.

[127] J.B.S Haldane. *A mathematical theory of natural and artificial selection. V. Selection and mutation.* 1927.

[128] David W. Hall and Sarah B. Joseph. A high frequency of beneficial mutations across multiple fitness components in *Saccharomyces cerevisiae*. *Genetics*, 185(4):1397–1409, 2010.

[129] G. H. Hardy. Mendelian Proportions in a Mixed Population. *Science*, 28(706):49–50, 1908.

[130] E. Harrison, R. C. Maclean, V. Koufopanou, and A. Burt. Sex drives intracellular conflict in yeast. *Journal of Evolutionary Biology*, 27(8):1757–1763, 2014.

[131] Matthew Hartfield, Sarah P. Otto, and Peter D. Keightley. The role of advantageous mutations in enhancing the evolution of a recombination modifier. *Genetics*, 184(4):1153–1164, 2010.

[132] Masami Hasegawa, Hirohisa Kishino, and Taka aki Yano. Dating of the human-ape splitting by a molecular clock of mitochondrial DNA. *Journal of Molecular Evolution*, 22(2):160–174, 1985.

[133] W. A. Haseltine and R. Block. Synthesis of Guanosine Tetra- and Pentaphosphate Requires the Presence of a Codon-Specific, Uncharged Transfer Ribonucleic Acid in the Acceptor Site of Ribosomes. *Proceedings of the National Academy of Sciences*, 70(5):1564–1568, 1973.

[134] Matthew Hegreness, Noam Shoresh, Daniel Hartl, and Roy Kishony. An Equivalence Principle for the Incorporation of Favorable Mutations in Asexual Populations. *Science*, 311(5767):1613–1615, 2006.

[135] W. G. Hill. Understanding and using quantitative genetic variation. *Phil. Trans. R. Soc. B*, 365(1537):73–85, 2010.

[136] Jonathan Hodgkin. Seven types of pleiotropy. *International Journal of Developmental Biology*, 42(3):501–505, 1998.

[137] Bengt v. Hofsten. The inhibitory effect of galactosides on the growth of *Escherichia coli*. *BBA - Biochimica et Biophysica Acta*, 48(1):164–171, 1961.

[138] Tadao Horiuchi, Jun-Ichi Tomizawa, and Aaron Novick. Isolation and properties of bacteria capable of high rates of β-galactosidase synthesis. *Biochimica et Biophysica Acta*, 55(1-2):152–163, 1962.

[139] David Houle, Kimberly A Hughes, D K Hoffmaster, J Ihara, S Assimacopoulos, D Canada, and Brian Charlesworth. The Effects of Spontaneous Mutation on Quantitative Traits. I. Variances and Covariances of Life History Traits. *Evolution*, 138(3):773–785, 1994.

[140] Marianne Imhof and C. Schlotterer. Fitness effects of advantageous mutations in evolving *Escherichia coli* populations. *Proceedings of the National Academy of Sciences*, 98(3):1113–1117, 2001.

[141] Toby Johnson and Nick Barton. *Phil. Trans. R. Soc. B*.

[142] H. Kacser and J. A. Burns. The molecular basis of dominance. *Genetics*, 97(3-4):639–666, 1981.

[143] Moshe Kafri, Eyal Metzl-Raz, Ghil Jona, and Naama Barkai. The Cost of Protein Production. *Cell Reports*, 14(1):22–31, 2016.

[144] Ata Kalirad and Ricardo B.R. Azevedo. Spiraling complexity: A test of the snowball effect in a computational model of RNA folding. *Genetics*, 206(1):377–388, 2017.

[145] Mary N. Karn and L. S. Penrose. Birth Weight and Gestation Time in Relation to Maternal Age, Parity, and Infant Survival. *Annals of Eugenics*, 16(1):147–164, 1951.

[146] Stuart Kauffman and Simon Levin. Towards a general theory of adaptive walks on rugged landscapes. *J. Theor. Biol*, 128(1):11–45, 1987.

[147] Stuart A. Kauffman and Edward D. Weinberger. The NK model of rugged fitness landscapes and its application to maturation of the immune response. *J. Theor. Biol*, 141(2):211–245, 1989.

[148] Tadeusz J. Kawecki, Richard E. Lenski, Dieter Ebert, Brian Hollis, Isabelle Olivieri, and Michael C. Whitlock. Experimental evolution. *Trends in Ecology and Evolution*, 27(10):547–560, 2012.

[149] P. D. Keightley. Models of quantitative variation of flux in metabolic pathways. *Genetics*, 121(4):869–876, 1989.

[150] P. D. Keightley. The distribution of mutation effects on viability in Drosophila melanogaster. *Genetics*, 138(4):1315–1322, 1994.

[151] P. D. Keightley and H. Kacser. Dominance, pleiotropy and metabolic structure. *Genetics*, 117(2):319–329, 1987.

[152] Peter D Keightley and Sarah P Otto. Interference among deleterious mutations favours sex and recombination in finite populations. *Nature*, 443(7107):89–92, Sep 2006.

[153] Jane P. Kenney-Hunt, Bing Wang, Elizabeth a. Norgard, Gloria Fawcett, Doug Falk, L. Susan Pletscher, Joseph P. Jarvis, Charles Roseman, Jason Wolf, and James M. Cheverud. Pleiotropic patterns of quantitative trait loci for 70 murine skeletal traits. *Genetics*, 178(4):2275–2288, 2008.

[154] Aisha I Khan, Duy M Dinh, Dominique Schneider, Richard E Lenski, and Tim F Cooper. Negative epistasis between beneficial mutations in an evolving bacterial population. *Science*, 332(6034):1193–6, Jun 2011.

[155] Travis T Kibota and Michael Lynch. Estimate of the genomic mutation rate deleterious to overall fitness in *E. coli*. *Nature*, 381(6584):694–696, Jun 1996.

[156] Motoo Kimura. *The Neutral Theory of Molecular Evolution*. 1983.

[157] Joel G Kingsolver, Hopi E Hoekstra, J M Hoekstra, David Berrigan, S N Vignieri, C E Hill, A Hoang, Patricia Gibert, and Peter Beerli. The strength of phenotypic selection in natural populations. *Am. Nat.*, 157(3):245–261, 2001.

[158] S. Klumpp, M. Scott, S. Pedersen, and T. Hwa. Molecular crowding limits translation and cell growth. *Proceedings of the National Academy of Sciences*, 110(42):16754–16759, 2013.

[159] Stefan Klumpp, Zhongge Zhang, and Terence Hwa. Growth Rate-Dependent Global Effects on Gene Expression in Bacteria. *Cell*, 139(7):1366–1375, 2009.

[160] a L Koch. The protein burden of lac operon products. *Journal of molecular evolution*, 19(6):455–62, 1983.

[161] Annemieke Kolkman, Pascale Daran-Lapujade, Asier Fullaondo, Maurien M.A. Olsthoorn, Jack T. Pronk, Monique Slijper, and Albert J.R. Heck. Proteome analysis of yeast response to various nutrient limitations. *Molecular Systems Biology*, 2, 2006.

[162] R. Korona, C. H. Nakatsu, L. J. Forney, and R. E. Lenski. Evidence for multiple adaptive peaks from populations of bacteria evolving in a structured habitat. *Proceedings of the National Academy of Sciences*, 91(19):9037–9041, 1994.

[163] Athanasios Kousathanas and Peter D. Keightley. A comparison of models to infer the distribution of fitness effects of new mutations. *Genetics*, 193(4):1197–1208, 2013.

[164] Sergey Kryazhimskiy, D. P. Rice, E. Jerison, and Michael M Desai. Global Epistasis Makes Adaptation Predictable Despite Sequence-Level Stochasticity. *Science*, 344(6191):1519–1522, 2014.

[165] Thomas Kuhlman, Zhongge Zhang, Milton H Saier, and Terence Hwa. Combinatorial transcriptional control of the lactose operon of *Escherichia coli*. *Proc. Natl. Acad. Sci. U.S.A*, 104(14):6043–8, 2007.

[166] Martin Kuthan, Frédéric Devaux, Blanka Janderová, Iva Slaninová, Claude Jacq, and Zdena Palková. Domestication of wild Saccharomyces cerevisiae is accompanied by changes in gene expression and colony morphology. *Molecular Microbiology*, 47(3):745–754, 2003.

[167] Daniel J. Kvitek and Gavin Sherlock. Reciprocal sign epistasis between frequently experimentally evolved adaptive mutations causes a rugged fitness landscape. *PLoS Genet.*, 7(4), 2011.

[168] Matthew J. Larcombe, Barbara Holland, Dorothy A. Steane, Rebecca C. Jones, Dean Nicolle, René E. Vaillancourt, and Brad M. Potts. Patterns of

reproductive isolation in eucalyptus - A phylogenetic perspective. *Mol. Biol. Evol.*, 32(7):1833–1846, 2015.

[169] Kit Fun Lau and Ken A. Dill. A Lattice Statistical Mechanics Model of the Conformational and Sequence Spaces of Proteins. *Macromolecules*, 22(10):3986–3997, 1989.

[170] Robert a Lazzarini, Michael Cashel, and Jonathan Gallant. On the Regulation of Guanosine Tetraphosphate Levels in Stringent and Relaxed Strains of *Escherichia coli* On the Regulation of Guanosine Tetraphosphate Levels in Stringent and Relaxed Strains of Escherichia co. *The Journal of Biological Chemistry*, 246(14):4381–4385, 1971.

[171] Heewook Lee, Ellen Popodi, Haixu Tang, and Patricia L Foster. Rate and molecular spectrum of spontaneous mutations in the bacterium *Escherichia coli* as determined by whole-genome sequencing. *Proceedings of the National Academy of Sciences*, 109(41):E2774–E2783, 2012.

[172] Ben Lehner. Genotype to phenotype: Lessons from model organisms for human genetics. *Nature Reviews Genetics*, 14(3):168–178, 2013.

[173] R. E. Lenski and M. Travisano. Dynamics of adaptation and diversification: a 10,000-generation experiment with bacterial populations. *Proceedings of the National Academy of Sciences*, 91(15):6808–6814, 1994.

[174] Richard E Lenski, Michael R Rose, Suzanne C Simpson, and Scott C Tadler. Long-Term Experimental Evolution in *Escherichia coli*. I . Adaptation and Divergence During, 1991.

[175] D. J. Lipman and W. J. Wilbur. Modelling Neutral and Selective Evolution of Protein Folding. *Proceedings of the Royal Society B: Biological Sciences*, 245(1312):7–11, 1991.

[176] Predrag Ljubuncic and Abraham Z. Reznick. The evolutionary theories of aging revisited - A mini-review. *Gerontology*, 55(2):205–216, 2009.

[177] Laurence Loewe, Volker Textor, and Siegfried Scherer. High Deleterious Genomic Mutation Rate in Stationary Phase of *Escherichia coli*. *Science*, 302(5650):1558–1560, 2003.

[178] João Lourenço, Nicolas Galtier, and Sylvain Glémin. Complexity, Pleiotropy, and the Fitness Effect of Mutations. *Evolution*, 65(6):1559–1571, Jun 2011.

[179] E. R. Lozovsky, T. Chookajorn, K. M. Brown, M. Imwong, P. J. Shaw, S. Kamchonwongpaisan, D. E. Neafsey, D. M. Weinreich, and D. L. Hartl. Stepwise acquisition of pyrimethamine resistance in the malaria parasite. *Proceedings of the National Academy of Sciences*, 106(29):12025–12030, 2009.

[180] Peng Lu, Christine Vogel, Rong Wang, Xin Yao, and Edward M. Marcotte. Absolute protein expression profiling estimates the relative contributions of transcriptional and translational regulation. *Nature Biotechnology*, 25(1):117–124, 2007.

[181] Mark Lunzer, G. Brian Golding, and Antony M. Dean. Pervasive cryptic epistasis in molecular evolution. *PLoS Genet.*, 6(10):1–10, 2010.

[182] Mark Lunzer, Stephen P Miller, Roderick Felsheim, and Antony M Dean. The biochemical architecture of an ancient adaptive landscape. *Science (New York, N.Y.)*, 310(5747):499–501, 2005.

[183] Salvador Luria and Max Delbrück. Mutations of Bacteria from Virus Sensitivity to Virus Resistance. *Genetics*, 28(6):491–511, Nov 1943.

[184] Michael Lynch, Matthew S. Ackerman, Jean-Francois Gout, Hongan Long, Way Sung, W. Kelley Thomas, and Patricia L. Foster. Genetic drift, selection and the evolution of the mutation rate. *Nature Reviews Genetics*, 17(11):704–714, 2016.

[185] Michael Lynch and Wilfried Gabriel. Mutation Load and the Survival of Small Populations. *Evolution*, 44(7):1725–1737, 1990.

[186] Thomas MacCarthy and Aviv Bergman. Coevolution of robustness, epistasis, and recombination favors asexual reproduction. *Proc. Natl. Acad. Sci. U.S.A*, 104(31):12801–12806, 2007.

[187] Javier Macia, Ricard V. Sole, and Santiago F. Elena. The causes of epistasis in genetic networks. *Evolution*, 66(2):586–596, 2012.

[188] Trudy F C Mackay. Epistasis and quantitative traits: using model organisms to study gene-gene interactions. *Nature reviews. Genetics*, 15(1):22–33, 2014.

[189] Bruce A. Malcolm, Keith P. Wilson, Brian W. Matthews, Jack F. Kirsch, and Allan C. Wilson. Ancestral lysozymes reconstructed, neutrality tested and thermostability linked to hydrocarbon packing. *Nature*, 345(6270):86–89, 1990.

[190] Lynne E. Maquat, Kathleen Thornton, and William S. Reznikoff. lac Promoter mutations located downstream from the transcription start site. *Journal of Molecular Biology*, 139(3):537–549, 1980.

[191] A. G. Marr. Growth rate of *Escherichia coli*. *Microbiology and Molecular Biology Reviews reviews*, 55(2):316–333, 1991.

[192] C. H. Martin and P. C. Wainwright. Multiple Fitness Peaks on the Adaptive Landscape Drive Adaptive Radiation in the Wild. *Science*, 339(6116):208–211, 2013.

[193] G Martin and T Lenormand. A General Multivariate Extension of Fisher's Geometrical Model and the Distribution of Mutation Fitness Effects across Species. *Evolution*, 60(5):893–907, 2006.

[194] Guillaume Martin, Santiago F Elena, and Thomas Lenormand. Distributions of epistasis in microbes fit predictions from a fitness landscape model. *Nat. Genet.*, 39(4):555–60, Apr 2007.

[195] Guillaume Martin and Thomas Lenormand. The fitness effect of mutations across environments: Fisher's geometrical model with multiple optima. *Evolution*, pages 1–36, 2015.

[196] Sebastian Matuszewski, Joachim Hermisson, and Michael Kopp. Fisher's geometric model with a moving optimum. *Evolution*, 68(9):2571–88, Sep 2014.

[197] Avraham E. Mayo, Yaakov Setty, Seagull Shavit, Alon Zaslaver, and Uri Alon. Plasticity of the cis-regulatory input function of a gene. *PLoS Biol.*, 4(4):555–561, 2006.

[198] D M McCandlish, E Rajon, P Shah, Y Ding, and J B Plotkin. The role of epistasis in protein evolution. *Nature*, 497(7451):E1–E2, 2013.

[199] David M McCandlish. Visualizing fitness landscapes. *Evolution*, 65(6):1544–58, Jun 2011.

[200] Katrina McGuigan, Julie M. Collet, Elizabeth A. McGraw, Yixin H. Ye, Scott L. Allen, Stephen F. Chenoweth, and Mark W. Blows. The nature and extent of mutational pleiotropy in gene expression of male *Drosophila serrata*. *Genetics*, 196(3):911–921, 2014.

[201] Justin R. Meyer, Anurag A. Agrawal, Ryan T. Quick, Devin T. Dobias, Dominique Schneider, and Richard E. Lenski. Parallel changes in host resistance to viral infection during 45,000 generations of relaxed selection. *Evolution*, 64(10):3024–3034, 2010.

[202] Stephen P. Miller, Mark Lunzer, and Antony M. Dean. Direct demonstration of an adaptive constraint. *Science*, 314(5798):458–461, 2006.

[203] Simon Conway Morris. *Life's Solution*. 1968.

[204] Michael C. Mossing and M. Thomas Record. Thermodynamic origins of specificity in the lac repressor-operator interaction. Adaptability in the recognition of mutant operator sites. *Journal of Molecular Biology*, 186(2):295–305, 1985.

[205] Leonie C Moyle and Takuya Nakazato. Hybrid incompatibility "snowballs" between Solanum species. *Science (New York, N.Y.)*, 329(5998):1521–3, 2010.

[206] H.J. Muller. Isolating mechanisms, evolution, and temperature. 1942.

[207] H.J. Muller, G.L. Jepsen, G.G. Simpson, and E. Mayr. *Genetics, Paleontology, and Evolution*. Princeton University Press, Princeton, NJ, 1949.

[208] Andre H. Nguyen, Ian J. Molineux, Rachael Springman, and James J. Bull. Multiple genetic pathways to similar fitness limits during viral adaptation to a new host. *Evolution*, 66(2):363–374, 2012.

[209] TN N Nguyen, QG G Phan, LP P Duong, KP P Bertrand, and RE E Lenski. Effects of carriage and expression of the Tn10 tetracycline-resistance operon on the fitness of *Escherichia coli* K12. *Mol. Biol. Evol.*, 6(3):213–225, 1989.

[210] D.-E. Nilsson and Susanne Pelger. A Pessimistic Estimate of the Time Required for an Eye to Evolve. *Proceedings of the Royal Society B: Biological Sciences*, 256(1345):53–58, 1994.

[211] Dan E. Nilsson and Detlev Arendt. Eye Evolution: The Blurry Beginning. *Current Biology*, 18(23):1096–1098, 2008.

[212] Aaron Novick and Milton Weiner. Enzyme Induction as an All-or-None Phenomenon. *PNAS*, 43(7):553–566, 1957.

[213] S Oehler, M Amouyal, P Kolkhof, B von Wilcken-Bergmann, and B Müller-Hill. Quality and position of the three lac operators of E. coli define efficiency of repression. *The EMBO journal*, 13(14):3348–3355, 1994.

[214] Paul E. O'Maille, Arthur Malone, Nikki Dellas, B. Andes Hess, Lidia Smentek, Iseult Sheehan, Bryan T. Greenhagen, Joe Chappell, Gerard Manning, and Joseph P. Noel. Quantitative exploration of the catalytic landscape separating divergent plant sesquiterpene synthases. *Nature Chemical Biology*, 4(10):617–623, 2008.

[215] H a Orr. The "sizes" of mutations fixed in phenotypic evolution: a response to Clarke and Arthur. *Evolution & development*, 3(3):121–3; discussion 124, 2001.

[216] H Allen Orr. The Population Genetics of Adaptation: The Distribution of Factors Fixed during Adaptive Evolution. *Evolution*, 52(4):935–949, 1998.

[217] H Allen Orr. The distribution of fitness effects among beneficial mutations in Fisher's geometric model of adaptation. *J. Theor. Biol*, 238(2):279–85, Jan 2006.

[218] HA Orr. Adaptation and the cost of complexity. *Evolution*, 54(1):13–20, 2000.

[219] Bjørn Østman, Arend Hintze, and Christoph Adami. Impact of epistasis and pleiotropy on evolutionary adaptation. *Proc. R. Soc. B*, 279:247–256, 2012.

[220] Elizabeth A. Ostrowski, Yufeng Shen, Xiangjun Tian, Richard Sucgang, Huaiyang Jiang, Jiaxin Qu, Mariko Katoh-Kurasawa, Debra A. Brock, Christopher Dinh, Fremiet Lara-Garduno, Sandra L. Lee, Christie L. Kovar, Huyen H. Dinh, Viktoriya Korchina, LaRonda Jackson, Shobha Patil, Yi Han, Lesley Chaboub, Gad Shaulsky, Donna M. Muzny, Kim C. Worley, Richard A. Gibbs, Stephen Richards, Adam Kuspa, Joan E. Strassmann, and David C. Queller. Genomic Signatures of Cooperation and Conflict in the Social Amoeba. *Current Biology*, 25(12):1661–1665, 2015.

[221] Sarah P. Otto. Two steps forward, one step back: the pleiotropic effects of favoured alleles. *Proceedings of the Royal Society of London B: Biological Sciences*, 271(1540):705–714, 2004.

[222] Annalise B. Paaby and Matthew V. Rockman. The many faces of pleiotropy. *Tr. Genet.*, 29(2):66–73, 2013.

[223] Zdena Palkova. Multicellular microorganisms: Laboratory versus nature. *EMBO Reports*, 5(5):470–476, 2004.

[224] Michael E. Palmer and Marcus W. Feldman. Dynamics of hybrid incompatibility in gene networks in a constant environment. *Evolution*, 63(2):418–431, 2009.

[225] Mihaela Pavlicev, Elizabeth A. Norgard, Gloria L. Fawcett, and James M. Cheverud. Evolution of pleiotropy: Epistatic interaction pattern supports a

mechanistic model underlying variation in genotype-phenotype map. *J. Exp. Zool. B*, 316 B(5):371–385, 2011.

[226] J. R. Peck. A ruby in the rubbish: Beneficial mutations, deleterious mutations and the evolution of sex. *Genetics*, 137(2):597–606, 1994.

[227] Joel R Peck, Guillaume Barreau, and Simon C Heath. Imperfect genes, Fisherian mutation and the evolution of sex. *Genetics*, 145(4):1171–1199, 1997.

[228] L Perfeito, L Fernandes, C Mota, and I Gordo. Adaptive mutations in bacteria: high rate and small effects. *Science*, 327(August):2005–2008, 2007.

[229] L Perfeito, a Sousa, T Bataillon, and I Gordo. Rates of fitness decline and rebound suggest pervasive epistasis. *Evolution*, 68(1):150–62, Jan 2014.

[230] Nicole T Perna, Guy Plunkett, Valerie Burland, Bob Mau, Jeremy D Glasner, Rose J Debra, George F Mayhew, Peter S Evans, Jason Gregor, Heather A Kirkpatrick, György Pósfai, Jeremiah Hackett, Sara Klink, Adam Boutin, Ying Shao, Leslie Miller, Erik J Grotbeck, N Wayne Davis, A Limk, Eileen T Dimalanta, Konstantinos D Potamousis, Jennifer Apodaca, Thomas S Anantharaman, J Y Lin, Galex Yen, David C Schwartz, R A Welch, and Frederick R Blattner. Genome sequence of enterohaemorrhagic *Escherichia coli* O157 : H7. *Nature*, 409(6819):529–533, 2001.

[231] Nadège Philippe, Jean Pierre Alcaraz, Evelyne Coursange, Johannes Geiselmann, and Dominique Schneider. Improvement of pCVD442, a suicide plasmid for gene allele exchange in bacteria. *Plasmid*, 51(3):246–255, 2004.

[232] Patrick C. Phillips. Epistasis - The essential role of gene interactions in the structure and evolution of genetic systems. *Nature Reviews Genetics*, 9(11):855–867, 2008.

[233] Gwenaël Piganeau and Adam Eyre-Walker. Estimating the Distribution of Fitness Effects from DNA Sequence Data: Implications for the Molecular Clock. *Proceedings of the National Academy of Sciences*, 100(18):10335–10340, 2003.

[234] M. Pigliucci. Genotype-phenotype mapping and the end of the 'genes as blueprint' metaphor. *Phil. Trans. R. Soc. B*, 365(1540):557–566, 2010.

[235] Jessica Plucain, Antonia Suau, Stéphane Cruveiller, Claudine Médigue, Dominique Schneider, and Mickaël Le Gac. Contrasting effects of historical contingency on phenotypic and genomic trajectories during a two-step evolution experiment with bacteria. *BMC evolutionary biology*, 16(1):86, 2016.

[236] Katarzyna Potrykus and Michael Cashel. (p)ppGpp: Still Magical? *Annual Review of Microbiology*, 62(1):35–51, 2008.

[237] Daven C Presgraves. Speciation Genetics: Epistasis, Conflict and the Origin of Species. *Current Biology*, 17(4):125–127, 2007.

[238] Selwyn Quan, J Christian J Ray, Zakari Kwota, Trang Duong, Gábor Balázsi, Tim F Cooper, and Russell D Monds. Adaptive evolution of the lactose utilization network in experimentally evolved populations of *Escherichia coli*. *PLoS Genet.*, 8(1):e1002444, Jan 2012.

[239] Erik M. Quandt, Jimmy Gollihar, Zachary D. Blount, Andrew D. Ellington, George Georgiou, and Jeffrey E. Barrick. Fine-tuning citrate synthase flux potentiates and refines metabolic innovation in the lenski evolution experiment. *eLife*, 4(OCTOBER2015):1–22, 2015.

[240] David C Queller and Joan E. Strassman. Experimental evolution of multicellularity using microbial pseudo-organisms. *Proceedings of the National Academy of Sciences*, 109(5):1595–600, 2012.

[241] Yoav Ram and Lilach Hadany. The probability of improvement in fisher's geometric model: A probabilistic approach. *Theor. Pop. Biol.*, 99:1–6, 2015.

[242] D A Reznick, H Bryga, and J A Ndler. Experimentally induced life-history evolution in a natural population. *Nature*, 346(4):357–359, 1990.

[243] David N. Reznick, Cameron K. Ghalambor, and Kevin Crooks. Experimental studies of evolution in guppies: A model for understanding the evolutionary consequences of predator removal in natural communities. *Mol. Ecol.*, 17(1):97–107, 2008.

[244] Marina V Rodnina. The ribosome in action: Tuning of translational efficiency and protein folding. *Protein Science*, 25:1390–1406, 2016.

[245] Juan Antonio Rodríguez, Urko M. Marigorta, David A. Hughes, Nino Spataro, Elena Bosch, and Arcadi Navarro. Antagonistic pleiotropy and mutation accumulation influence human senescence and disease. *Nature Ecology and Evolution*, 1(3):1–5, 2017.

[246] Darin R Rokyta, Paul Joyce, S Brian Caudle, and Holly a Wichman. An empirical test of the mutational landscape model of adaptation using a single-stranded DNA virus. *Nat. Genet.*, 37(4):441–444, 2005.

[247] Michael R. Rose, Mark D. Drapeau, Puya G. Yazdi, Kandarp H. Shah, Diana B. Moise, Rena R. Thakar, Casandra L. Rauser, and Laurence D. Mueller. Evolution of late-life mortality in Drosophila melanogaster. *Evolution*, 56(10):1982–1991, 2002.

[248] W. Rowe, M. Platt, D. C. Wedge, P. J. Day, D. B. Kell, and J. Knowles. Analysis of a complete DNA-protein affinity landscape. *Journal of The Royal Society Interface*, 7(44):397–408, 2010.

[249] Denis Roze and Alexandre Blanckaert. Epistasis, pleiotropy, and the mutation load in sexual and asexual populations. *Evolution*, 68(1):137–149, 2014.

[250] Daniel E Rozen, J. Arjan G.M. De Visser, and Philip J Gerrish. Fitness effects of fixed beneficial mutations in microbial populations. *Current Biology*, 12(12):1040–1045, 2002.

[251] Daniel E. Rozen, Michelle G J L Habets, Andreas Handel, and J. Arjan G M de Visser. Heterogeneous adaptive trajectories of small populations on complex fitness landscapes. *PLoS ONE*, 3(3):14–17, 2008.

[252] J B Russell and G M Cook. Energetics of bacterial growth: balance of anabolic and catabolic reactions. *Microbiological reviews*, 59(1):48–62, 1995.

[253] R. Sanjuan, M. R. Nebot, N. Chirico, L. M. Mansky, and R. Belshaw. Viral Mutation Rates. *Journal of Virology*, 84(19):9733–9748, 2010.

[254] J. Santos, M. Pascual, P. Simoes, I. Fragata, M. Lima, B. Kellen, M. Santos, A. Marques, M. R. Rose, and M. Matos. From nature to the laboratory: The impact of founder effects on adaptation. *Journal of Evolutionary Biology*, 25(12):2607–2622, 2012.

[255] Edoardo Sarubbi, Kenneth E. Rudd, and Michael Cashel. Basal ppGpp level adjustment shown by new spoT mutants affect steady state growth rates and rrnA ribosomal promoter regulation in *Escherichia coli*. *MGG Molecular & General Genetics*, 213(2-3):214–222, 1988.

[256] Akie Sato, Herbert Tichy, O Colm, Peter R Grant, B Rosemary Grant, and Jan Klein. On the Origin of Darwin ' s Finches. *Mol. Biol. Evol.*, 18(May):299–311, 2001.

[257] Rebecca S. Satterwhite and Tim F. Cooper. Constraints on adaptation of *Escherichia coli* to mixed-resource environments increase over time. *Evolution*, 69(8):2067–2078, 2015.

[258] Michael A. Savageau. Demand theory of gene regulation. II. Quantitative application to the lactose and maltose operons of Escherichia coli. *Genetics*, 149(4):1677–1691, 1998.

[259] R M Schaaper and R L Dunn. Spontaneous mutation in the *Escherichia coli* lacI gene. *Genetics*, 129(2):317–26, Oct 1991.

[260] Roel M. Schaaper, Bryan N. Danforth, and Barry W. Glickman. Mechanisms of spontaneous mutagenesis: An analysis of the spectrum of spontaneous mutation in the *Escherichia coli* lacI gene. *Journal of Molecular Biology*, 189(2):273–284, 1986.

[261] Martijn F Schenk, Ivan G Szendro, Merijn L M Salverda, Joachim Krug, and J Arjan G M de Visser. Patterns of Epistasis between beneficial mutations in an antibiotic resistance gene. *Mol. Biol. Evol.*, 30(8):1779–87, Aug 2013.

[262] Martijn F. Schenk, Ivan G. Szendro, Merijn L M Salverda, Joachim Krug, and J. Arjan G M De Visser. Patterns of epistasis between beneficial mutations in an antibiotic resistance gene. *Mol. Biol. Evol.*, 30(8):1779–1787, 2013.

[263] Sijmen E Schoustra, Thomas Bataillon, Danna R Gifford, and Rees Kassen. The properties of adaptive walks in evolving populations of fungus. *PLoS Biol.*, 7(11):e1000250, Nov 2009.

[264] S J Schrag and V Perrot. Reducing antibiotic resistance. *Nature*, 381(6578):120–121, 1996.

[265] S J Schrag, V Perrot, and B R Levin. Adaptation to the fitness costs of antibiotic resistance in *Escherichia coli*. *Proceedings. Biological sciences / The Royal Society*, 264(1386):1287–91, 1997.

[266] Björn Schwanhüusser, Dorothea Busse, Na Li, Gunnar Dittmar, Johannes Schuchhardt, Jana Wolf, Wei Chen, and Matthias Selbach. Global quantification of mammalian gene expression control. *Nature*, 473(7347):337–342, 2011.

[267] M. Scott, S. Klumpp, E. M. Mateescu, and T. Hwa. Emergence of robust growth laws from optimal regulation of ribosome synthesis. *Molecular Systems Biology*, 10(8):747–747, 2014.

[268] Matthew Scott and Terence Hwa. Bacterial growth laws and their applications. *Current Opinion in Biotechnology*, 22(4):559–565, 2011.

[269] Matthew Scott, Eduard M Mateescu, Zhongge Zhang, and Terence Hwa. Interdependence of Cell Growth Origins and Consequences. *Science*, 330(November):1099–1102, 2010.

[270] Ole Seehausen, Roger K Butlin, Irene Keller, Catherine E Wagner, Janette W Boughman, Paul a Hohenlohe, Catherine L Peichel, Glenn-Peter Saetre, Claudia Bank, Ake Brännström, Alan Brelsford, Chris S Clarkson, Fabrice Eroukhmanoff, Jeffrey L Feder, Martin C Fischer, Andrew D Foote, Paolo Franchini, Chris D Jiggins, Felicity C Jones, Anna K Lindholm, Kay Lucek, Martine E Maan, David a Marques, Simon H Martin, Blake Matthews, Joana I Meier, Markus Möst, Michael W Nachman, Etsuko Nonaka, Diana J Rennison, Julia Schwarzer, Eric T Watson, Anja M Westram, and Alex Widmer. Genomics and the origin of species. *Nature reviews. Genetics*, 15(3):176–92, 2014.

[271] Daniel Segrè, Alexander Deluna, George M Church, and Roy Kishony. Modular epistasis in yeast metabolism. *Nat. Genet.*, 37(1):77–83, 2005.

[272] Maria R. Servedio, Yaniv Brandvain, Sumit Dhole, Courtney L. Fitzpatrick, Emma E. Goldberg, Caitlin A. Stern, Jeremy Van Cleve, and D. Justin Yeh. Not Just a Theory—The Utility of Mathematical Models in Evolutionary Biology. *PLoS Biol.*, 12(12):1–5, 2014.

[273] Y Setty, A E Mayo, M G Surette, and U Alon. Detailed map of a cis-regulatory input function. *Proc. Natl. Acad. Sci. U.S.A*, 100(13):7702–7, 2003.

[274] Irit Shachrai, Alon Zaslaver, Uri Alon, and Erez Dekel. Cost of Unneeded Proteins in E. coli Is Reduced after Several Generations in Exponential Growth. *Molecular Cell*, 38(5):758–767, 2010.

[275] Premal Shah, David M. McCandlish, and Joshua B. Plotkin. Contingency and entrenchment in protein evolution under purifying selection. *Proceedings of the National Academy of Sciences*, 112(25):E3226–E3235, 2015.

[276] J. Silvertown, C. Servaes, P. Biss, and D. Macleod. Reinforcement of reproductive isolation between adjacent populations in the Park Grass Experiment. *Heredity*, 95(3):198–205, 2005.

[277] Jonathan Silvertown, Paul Poulton, Edward Johnston, Grant Edwards, Matthew Heard, and Pamela M. Biss. The Park Grass Experiment 1856-2006: Its contribution to ecology. *Journal of Ecology*, 94(4):801–814, 2006.

[278] Shanya Sivakumaran, Felix Agakov, Evropi Theodoratou, James G. Prendergast, Lina Zgaga, Teri Manolio, Igor Rudan, Paul McKeigue, James F. Wilson,

and Harry Campbell. Abundant pleiotropy in human complex diseases and traits. *Am. J. Hum. Genet.*, 89(5):607–618, 2011.

[279] Paul Sniegowski, Philip J Gerrish, and Richard E. Lenski. letters to nature Evolution of high mutation rates in experimental populations of E . coli. *Nature*, 606:703–706, 1997.

[280] Michael A. Sørensen, Kaj F. Jensen, and Steen Pedersen. High concentrations of ppGpp decrease the RNA chain growth rate. Implications for protein synthesis and translational fidelity during amino acid starvation in *Escherichia coli*, 1994.

[281] Ana Sousa, Sara Magalhães, and Isabel Gordo. Cost of antibiotic resistance and the geometry of adaptation. *Mol. Biol. Evol.*, 29(5):1417–28, May 2012.

[282] Eliot B. Spiess. *Genes in Populations*. 1977.

[283] B Spira, N Silberstein, E Yagil, and Ezra Yagil. Guanosine 3',5'-Bispyrophosphate (ppGpp) Synthesis in Cells of *Escherichia coli* Starved for Pi. 177(14):4053–4058, 1995.

[284] Anjana Srivatsan and Jue D. Wang. Control of bacterial transcription, translation and replication by (p)ppGpp. *Current Opinion in Microbiology*, 11(2):100–105, 2008.

[285] Peter F Stadler and Robert Happel. Random field models for fitness landscapes. pages 435–478, 1999.

[286] Peter F. Stadler and Christopher R. Stephens. *Landscapes and Effective Fitness*, volume 8. 2003.

[287] Mark T Stanek, Tim F Cooper, and Richard E Lenski. Identification and dynamics of a beneficial mutation in a long-term evolution experiment with *Escherichia coli*. *BMC evolutionary biology*, 9:302, Jan 2009.

[288] Tyler N. Starr and Joseph W. Thornton. Epistasis in protein evolution. *Protein Science*, 25:1204–1218, 2016.

[289] Frank W. Stearns and Charles B. Fenster. Fisher's Geometric Model Predicts the Effects of Random Mutations When Tested in the Wild. *Evolution*, pages n/a–n/a, 2016.

[290] Michael Stich, Carlos Briones, and Susanna C. Manrubia. On the structural repertoire of pools of short, random RNA sequences. *J. Theor. Biol*, 252(4):750–763, 2008.

[291] Daniel M. Stoebel, Antony M. Dean, and Daniel E. Dykhuizen. The cost of expression of *Escherichia coli* lac operon proteins is in the process, not in the products. *Genetics*, 178(3):1653–1660, 2008.

[292] Zhixi Su, Yanwu Zeng, and Xun Gu. A preliminary analysis of gene pleiotropy estimated from protein sequences. *J. Exp. Zool. B*, 314 B(2):115–122, 2010.

[293] Sumedha, Olivier C. Martin, and Andreas Wagner. New structural variation in evolutionary searches of RNA neutral networks. *BioSystems*, 90(2):475–485, 2007.

[294] E. Szathmary. Do deleterious mutations act synergistically? Metabolic control theory provides a partial answer. *Genetics*, 133(1):127–132, 1993.

[295] Ivan G Szendro, Martijn F Schenk, Jasper Franke, Joachim Krug, and J Arjan G M de Visser. Quantitative analyses of empirical fitness landscapes. *J. Stat. Mech.*, 2013(01):P01005, Jan 2013.

[296] Nobuto Takeuchi and Paulien Hogeweg. Evolutionary dynamics of RNA-like replicator systems: A bioinformatic approach to the origin of life. *Physics of Life Reviews*, 9(3):219–263, 2012.

[297] Longzhi Tan, Stephen Serene, Hui Xiao Chao, and Jeff Gore. Hidden randomness between fitness landscapes limits reverse evolution. *Physical Review Letters*, 106(19):1–4, 2011.

[298] O. Tenaillon. The Utility of Fisher's Geometric Model in Evolutionary Genetics. *Annu. Rev. Ecol. Evol. Syst.*, 45(1):179–201, Nov 2014.

[299] Michael Travisano and Richard E. Lenski. Long-term experimental evolution in *Escherichia coli*. IV. Targets of selection and the specificity of adaptation. *Genetics*, 143(1):15–26, 1996.

[300] Matthew F Traxler, Sean M Summers, Huyen-tran Nguyen, Vineetha M Zacharia, Joel T Smith, and Tyrrell Conway. The global, ppGpp-mediated

stringent response to amino acid starvation in *Escherichia coli*. *Molecular Microbiology*, 68(5):1128–1148, 2013.

[301] Sandra Trindade, Lilia Perfeito, and Isabel Gordo. Rate and effects of spontaneous mutations that affect fitness in mutator *Escherichia coli*. *Phil. Trans. R. Soc. B*, 365(1544):1177–86, Apr 2010.

[302] Carl Troein, Dag Ahren, Morten Krogh, and Carsten Peterson. Is transcriptional regulation of metabolic pathways an optimal strategy for fitness? *PLoS ONE*, 2(9), 2007.

[303] Danielle M. Tufts, Chandrasekhar Natarajan, Inge G. Revsbech, Joana Projecto-Garcia, Federico G. Hoffmann, Roy E. Weber, Angela Fago, Hideaki Moriyama, and Jay F. Storz. Epistasis constrains mutational pathways of hemoglobin adaptation in high-altitude pikas. *Mol. Biol. Evol.*, 32(2):287–298, 2015.

[304] Caroline B Turner, Zachary D Blount, Daniel H Mitchell, and Richard E. Lenski. Evolution and coexistence in response to a key innovation in a long-term evolution experiment with *Escherichia coli*. Technical report, 2015.

[305] Anna L. Tyler, Folkert W. Asselbergs, Scott M. Williams, and Jason H. Moore. Shadows of complexity: What biological networks reveal about epistasis and pleiotropy. *BioEssays*, 31(2):220–227, 2009.

[306] Jesper Vind, Michael A. Sørensen, Michael D. Rasmussen, and Steen Pedersen. Synthesis of Proteins in *Escherichia coli* is Limited by the Concentration of Free Ribosomes. *Journal of Molecular Biology*, 231(3):678–688, 1993.

[307] Daniel Vinella, Christian Albrecht, Michael Cashel, and Richard D'Ari. Iron limitation induces SpoT-dependent accumulation of ppGpp in *Escherichia coli*. *Molecular Microbiology*, 56(4):958–970, 2005.

[308] Andreas Wagner. Energy constraints on the evolution of gene expression. *Mol. Biol. Evol.*, 22(6):1365–1374, 2005.

[309] Günter P Wagner. Homologues, Natural Kinds and the Evolution of Modularity. *Am. Zool.*, 36(1):36–43, 1996.

[310] Günter P Wagner, Jane P Kenney-Hunt, Mihaela Pavlicev, Joel R Peck, David Waxman, and James M Cheverud. Pleiotropic scaling of gene effects and the 'cost of complexity'. *Nature*, 452(7186):470–2, Mar 2008.

[311] Günter P Wagner, Mihaela Pavlicev, and James M Cheverud. The road to modularity. *Nature reviews. Genetics*, 8(12):921–31, Dec 2007.

[312] Günter P Wagner and Jianzhi Zhang. The pleiotropic structure of the genotype-phenotype map: the evolvability of complex organisms. *Nature reviews. Genetics*, 12(3):204–13, Mar 2011.

[313] Qian Wang, Can Yang, Joel Gelernter, and Hongyu Zhao. Pervasive pleiotropy between psychiatric disorders and immune disorders revealed

by integrative analysis of multiple GWAS. *Human Genetics*, 134(11-12):1195–1209, 2015.

[314] Yinhua Wang, Carolina Díaz Arenas, Daniel M Stoebel, and Tim F Cooper. Genetic background affects epistatic interactions between two beneficial mutations Subject collections Genetic background affects epistatic interactions between two beneficial mutations. *Biology letters*, (August), 2012.

[315] Zhi Wang, Ben-Yang Liao, and Jianzhi Zhang. Genomic patterns of pleiotropy and the evolution of complexity. *Proc. Natl. Acad. Sci. U.S.A*, 107(42):18034–18039, 2010.

[316] D Waxman. Fisher's geometrical model of evolutionary adaptation–beyond spherical geometry. *J. Theor. Biol*, 241(4):887–95, Aug 2006.

[317] D Waxman and J R Peck. Pleiotropy and the presevation of perfection. *Science*, 279:1210–1213, 1998.

[318] D Waxman and J J Welch. Fisher's microscope and Haldane's ellipse. *The American naturalist*, 166(4):447–57, Oct 2005.

[319] Daniel M Weinreich, Nigel F Delaney, Mark a Depristo, and Daniel L Hartl. Darwinian Evolution Can Follow Only Very Few Mutational Paths to Fitter Proteins. *Science*, 312(April):2004–2007, 2006.

[320] Daniel M Weinreich, Yinghong Lan, C Scott Wylie, and Robert B Heckendorn. Should evolutionary geneticists worry about higher-order epistasis? *Curr. Opin. Genet. Dev.*, 23(6):700–7, Dec 2013.

[321] JJ Welch and D Waxman. Modularity and the cost of complexity. *Evolution*, 57(8):1723–1734, 2003.

[322] Annabel C Whibley, Nicolas B Langlade, Christophe Andalo, Andrew I Hanna, Andrew Bangham, Christophe Thébaud, and Enrico Coen. Evolutionary Paths Underlying Flower Color Variation in *Antirrhinum*. *Science*, 313(5789):963–966, 2006.

[323] Michael C. Whitlock and Denis Bourguet. Factors affecting the genetic load in Drosophila: Synergistic epistasis and correlations among fitness components. *Evolution*, 54(5):1654–1660, 2000.

[324] Georg Wick, Peter Berger, Pidder Jansen-Dürr, and Beatrix Grubeck-Loebenstein. A Darwinian-evolutionary concept of age-related diseases. *Experimental Gerontology*, 38(1-2):13–25, 2003.

[325] Sébastien Wielgoss, Jeffrey E Barrick, Olivier Tenaillon, Stéphane Cruveiller, Béatrice Chane-Woon-Ming, Claudine Médigue, Richard E Lenski, and Dominique Schneider. Mutation Rate Inferred From Synonymous Substitutions in a Long-Term Evolution Experiment With *Escherichia coli*. *G3*, 1(3):183–186, Aug 2011.

[326] George C. Williams. Pleiotropy, Natural Selection, and the Evolution of Senescence. *Evolution*, 11(4):398–411, 1957.

[327] D M Wilson, R M Putzrath, and T H Wilson. Inhibition of growth of *Escherichia coli* by lactose and other galactosides. *Biochim Biophys Acta*, 649(2):377–384, 1981.

[328] Dorothy M. Wilson, Meredith Kusch, Jean L. Flagg-Newton, and T. Hastings Wilson. Control of lactose transport in *Escherichia coli*. *FEBS Letters*, 117(August):K37–K44, 1980.

[329] Ned S. Wingreen, Jonathan Miller, and Edward C. Cox. Scaling of mutational effects in models for pleiotropy. *Genetics*, 164(3):1221–1228, 2003.

[330] Michael J Wiser, Noah Ribeck, and Richard E Lenski. Long-term dynamics of adaptation in asexual populations. *Science*, 342(6164):1364–7, 2013.

[331] Jason B. Wolf, Daniel Pomp, Eugene J. Eisen, James M. Cheverud, and Larry J. Leamy. The contribution of epistatic pleiotropy to the genetic architecture of covariation among polygenic traits in mice. *Evolution and Development*, 8(5):468–476, 2006.

[332] R. Woods, D. Schneider, C. L. Winkworth, M. A. Riley, and R. E. Lenski. Tests of parallel molecular evolution in a long-term experiment with *Escherichia coli*. *Proceedings of the National Academy of Sciences*, 103(24):9107–9112, 2006.

[333] Sewall Wright. The roles of mutation, inbreeding, crossbreeding and selection in evolution, 1932.

[334] Andrea Wuensche, Duy M Dinh, Satterwhite, Rebecca S., and Tim F. Cooper. Diminishing-returns epistasis decreases adaptability along an evolutionary trajectory. *Nature Ecology and Evolution*, 2017.

[335] Y. Xia and M. Levitt. Roles of mutation and recombination in the evolution of protein thermodynamics. *Proceedings of the National Academy of Sciences*, 99(16):10382–10387, 2002.

[336] Hyun Youk and Alexander Van Oudenaarden. Growth landscape formed by perception and import of glucose in yeast. *Nature*, 462(7275):875–879, 2009.

[337] Stephen Zamenhof and Herbert H. Eichhorn. Study of microbial evolution through loss of biosynthetic functions: Establishment of "defective" mutants. *Nature*, 216(5114):456–458, 1967.

[338] Clifford Zeyl. Experimental evolution with yeast. *FEMS Yeast Research*, 6(5):685–691, 2006.

[339] Wei Zhang, Vasudha Sehgal, Duy M Dinh, Ricardo B R Azevedo, Tim F Cooper, and Robert Azencott. Estimation of the rate and effect of new beneficial mutations in asexual populations. *Theor. Pop. Biol.*, 81(2):168–78, Mar 2012.

[340] Lihua Zou, Sira Sriswasdi, Brian Ross, Patrycja V. Missiuro, Jun Liu, and Hui Ge. Systematic analysis of pleiotropy in *C. elegans* early embryogenesis. *PLoS Comput. Biol.*, 4(2):e1000003, 2008.